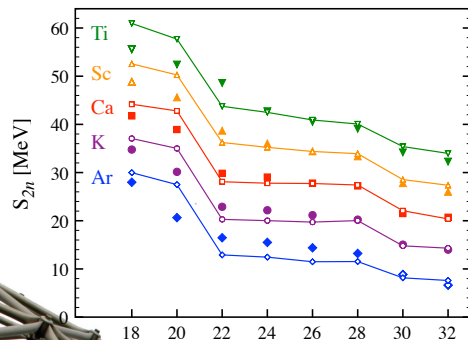


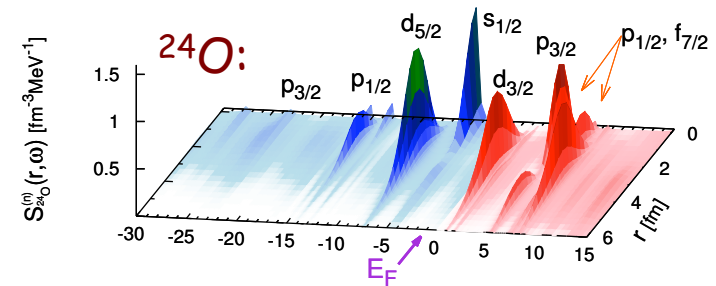
# Medium-mass isotopes from chiral and lattice QCD interactions

Carlo Barbieri — University of Surrey

May 12, 2016



*Phys. Rev. C 89,*  
*061301R (2014)*



*Phys. Rev. Lett. 111, 062501 (2013)*  
*Phys. Rev. C 92, 014306 (2015)*

# Current Status of low-energy nuclear physics

## Composite system of interacting fermions

*Binding and limits of stability*

*Coexistence of individual and collective behaviors*

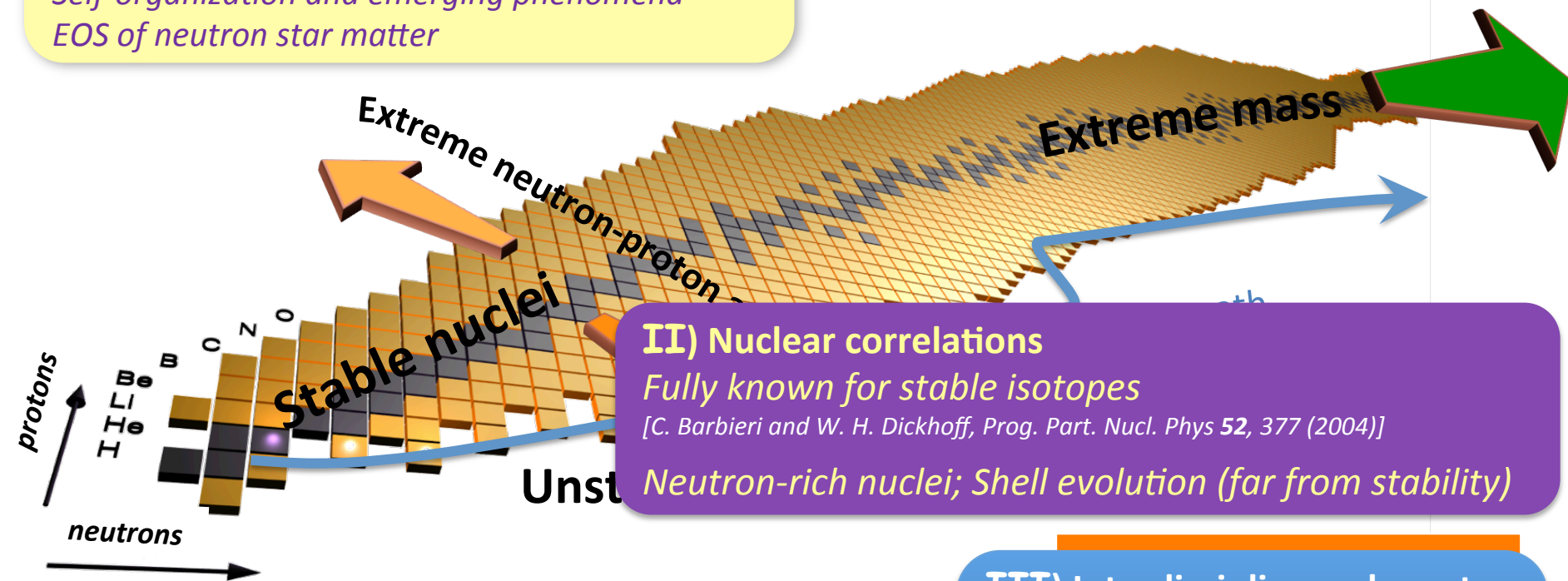
*Self-organization and emerging phenomena*

*EOS of neutron star matter*

Experimental

programs

RIKEN, FAIR, FRIB



## II) Nuclear correlations

*Fully known for stable isotopes*

*[C. Barbieri and W. H. Dickhoff, Prog. Part. Nucl. Phys 52, 377 (2004)]*

*Neutron-rich nuclei; Shell evolution (far from stability)*

## I) Understanding the nuclear force

*QCD-derived; 3-nucleon forces (3NFs)*

*First principle (ab-initio) predictions*

## III) Interdisciplinary character

*Astrophysics*

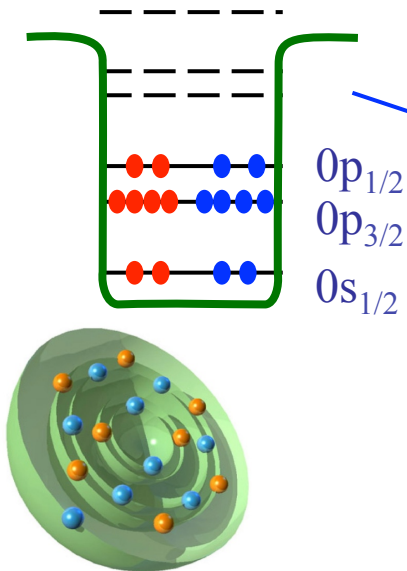
*Tests of the standard model*

*Other fermionic systems:*

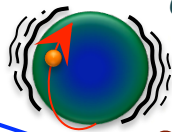
*ultracold gasses; molecules;*

# Concept of correlations

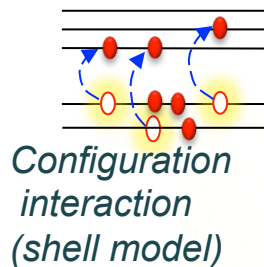
independent particle picture



Particle-vibration coupling (PV)

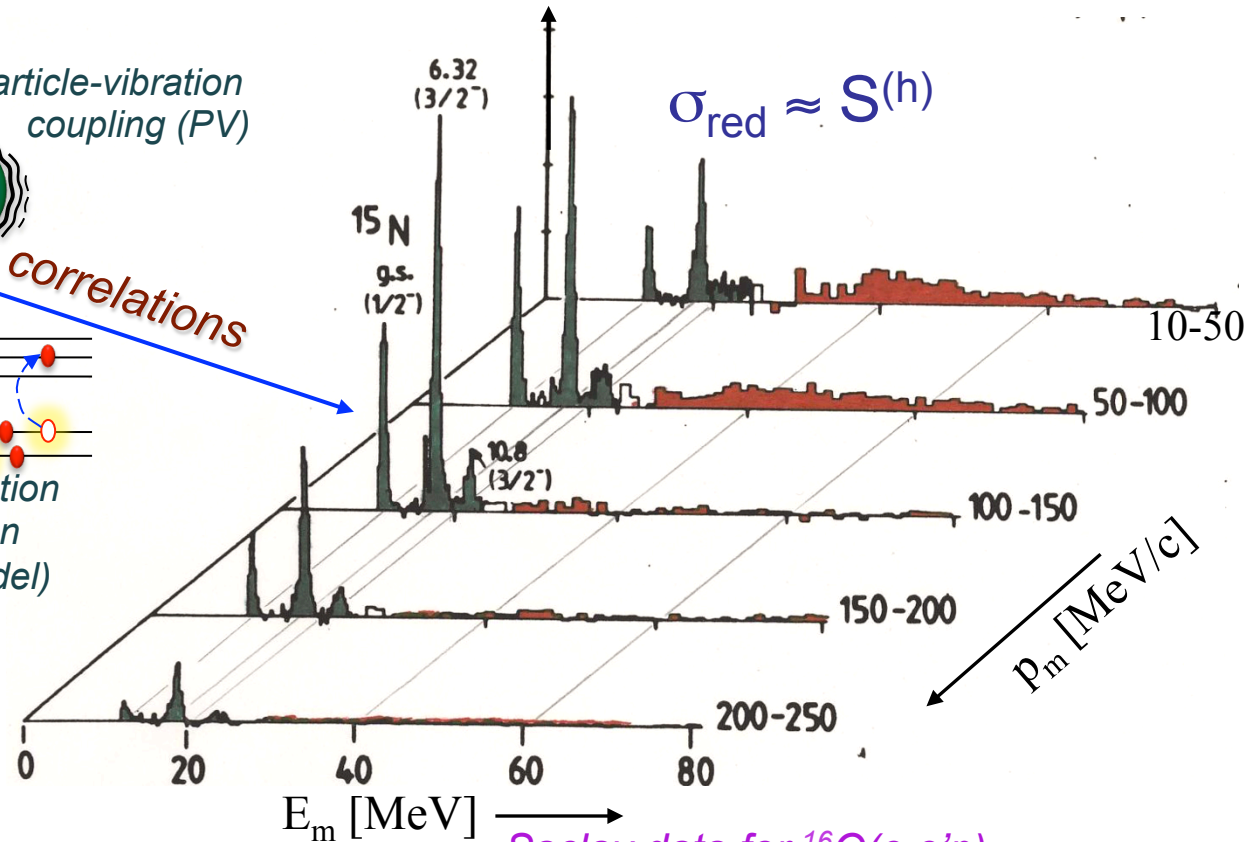


correlations



Configuration interaction (shell model)

Spectral function: distribution of momentum ( $p_m$ ) and energies ( $E_m$ )



Saclay data for  $^{16}O(e,e'p)$

[Mougey et al., Nucl. Phys. A335, 35 (1980)]

Understood for a few stable closed shells:

[CB and W. H. Dickhoff, Prog. Part. Nucl. Phys 52, 377 (2004)]

# Concept of correlations

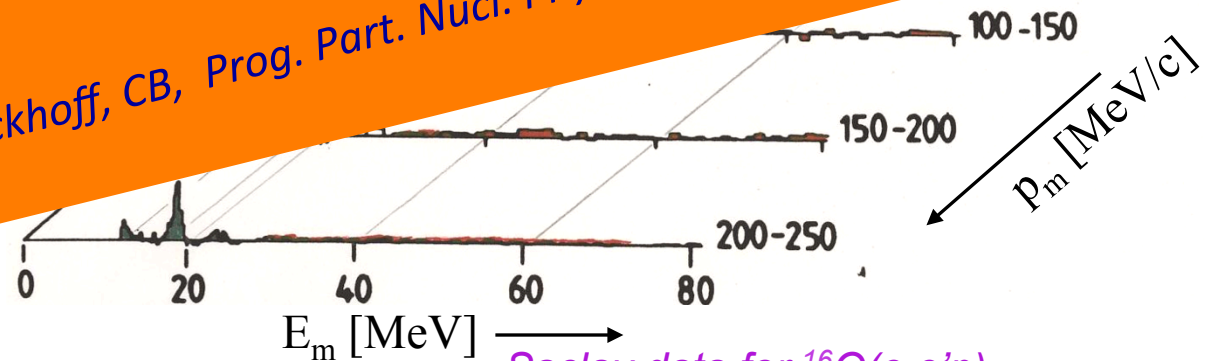
independent  
particle picture

Spectral function: distribution of  
momentum ( $p_m$ ) and energy ( $E_m$ )

Particle-vibration  
coupling

So far, fully characterised only for closed-shell and  
stable isotopes... (!)

[W. Dickhoff, CB, Prog. Part. Nucl. Phys. **52**, 377 (2004)]



Saclay data for  $^{16}\text{O}(e,e'p)$

[Mougey et al., Nucl. Phys. A335, 35 (1980)]

Understood for a few stable closed shells:

[CB and W. H. Dickhoff, Prog. Part. Nucl. Phys **52**, 377 (2004)]

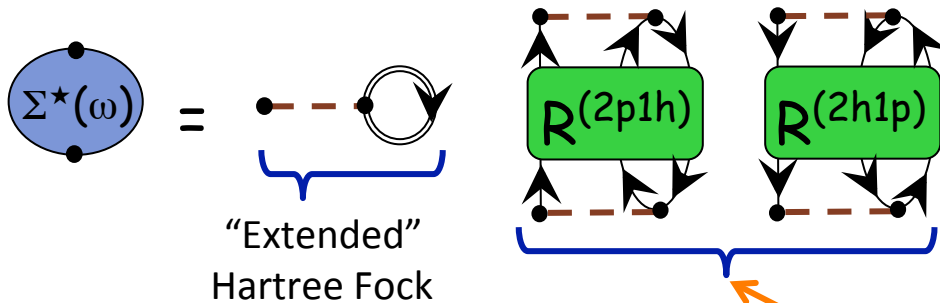


# Ab-Initio SCGF approaches

# The FRPA Method in Two Words

Particle vibration coupling is the main cause driving the distribution of particle strength—on both sides of the Fermi surface...

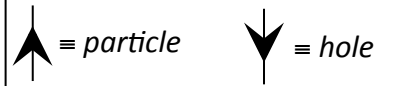
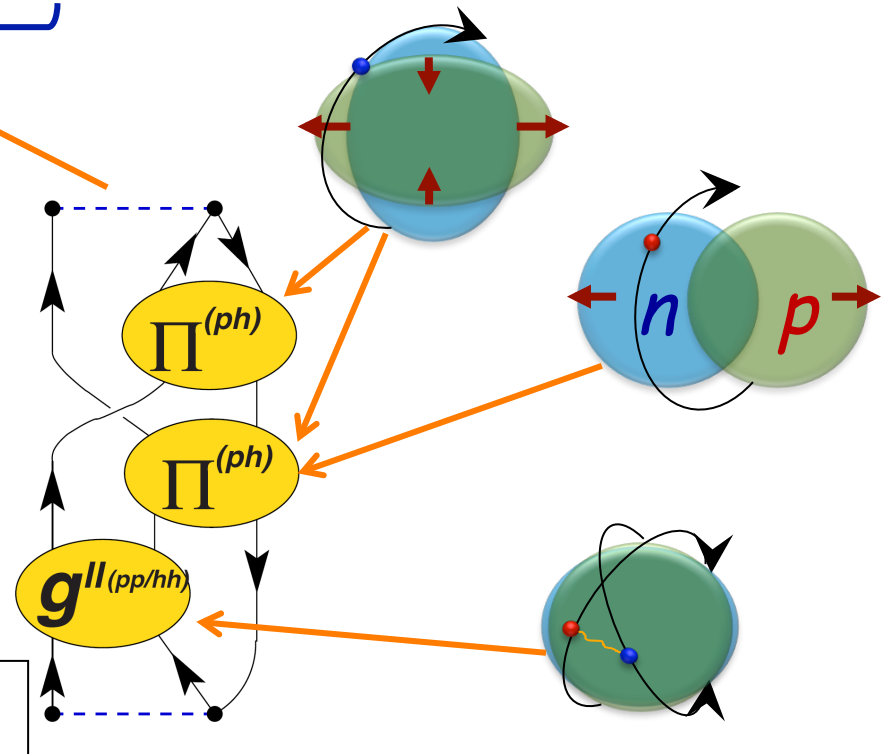
CB et al.,  
 Phys. Rev. C63, 034313 (2001)  
 Phys. Rev. A76, 052503 (2007)  
 Phys. Rev. C79, 064313 (2009)



• A complete expansion requires all types of particle-vibration coupling

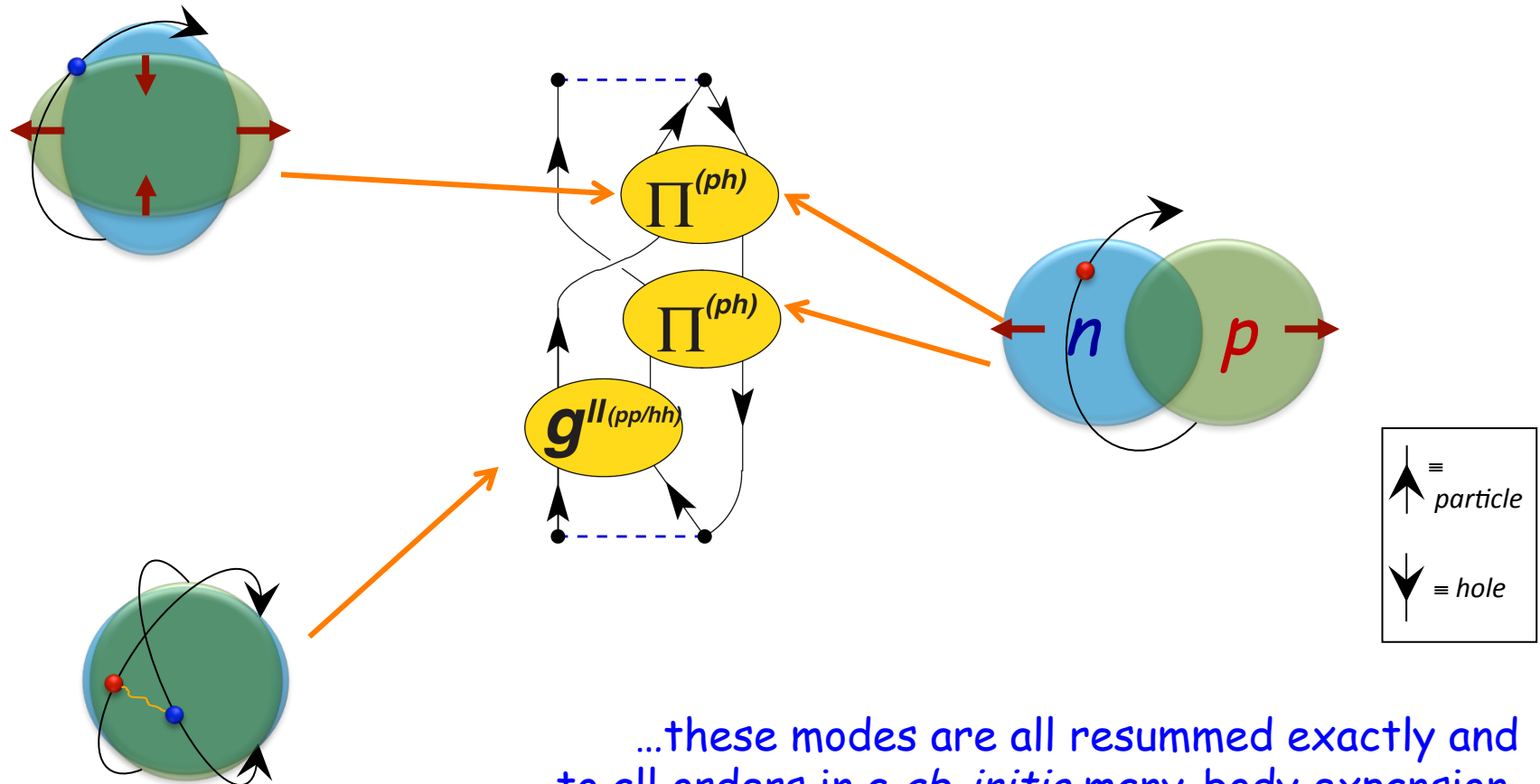
...these modes are all resummed exactly and to all orders in a *ab-initio* many-body expansion.

• The Self-energy  $\Sigma^*(\omega)$  yields both single-particle states and scattering



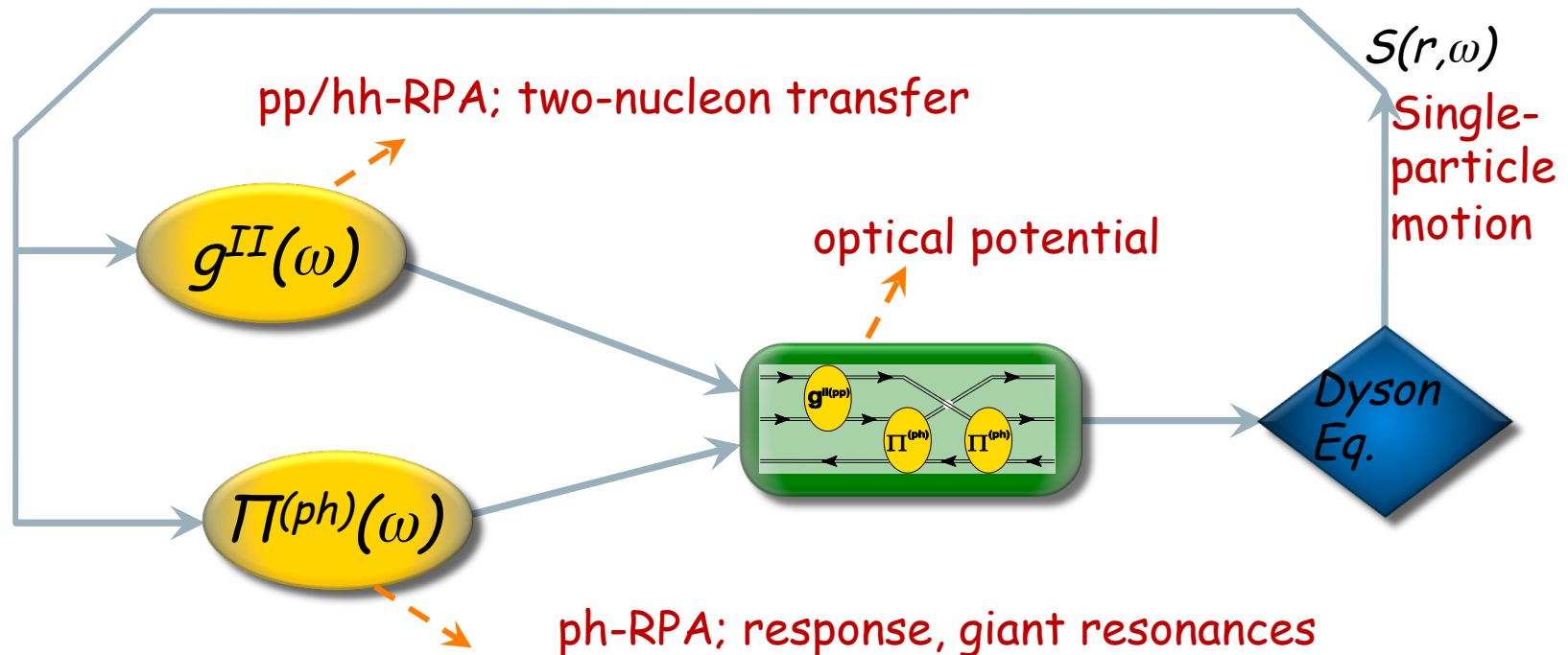
# The FRPA Method in Two Words

Particle vibration coupling is the main cause driving the distribution of particle strength—a least close to the Fermi surface...



...these modes are all resummed exactly and to all orders in a *ab-initio* many-body expansion.

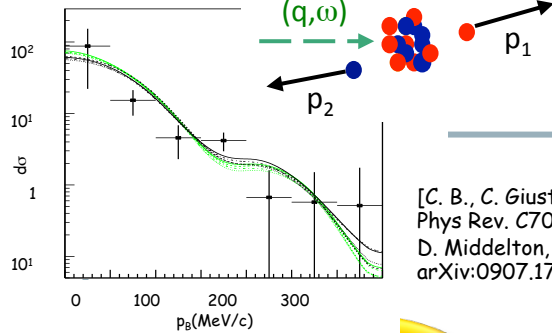
# Self-Consistent Green's Function Approach



- Global picture of nuclear dynamics
- Reciprocal correlations among effective modes
- Guaranties *macroscopic conservation laws*

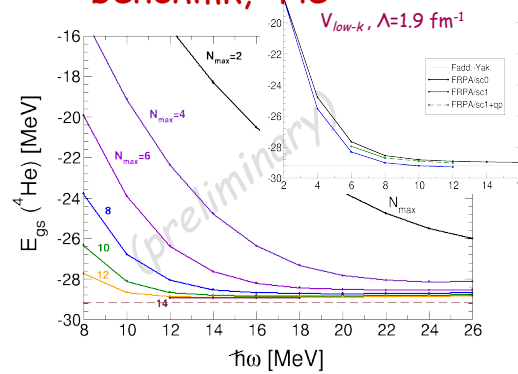
# Self-Consistent Green's Function Approach

$^{16}\text{O}(e,e'pn)^{14}\text{N}$  @ MAINZ



[C. B., C. Giusti, et al. Phys Rev. C70, 014606 (2004)  
D. Middleton, et al. arXiv:0907.1758; EPJA in print]

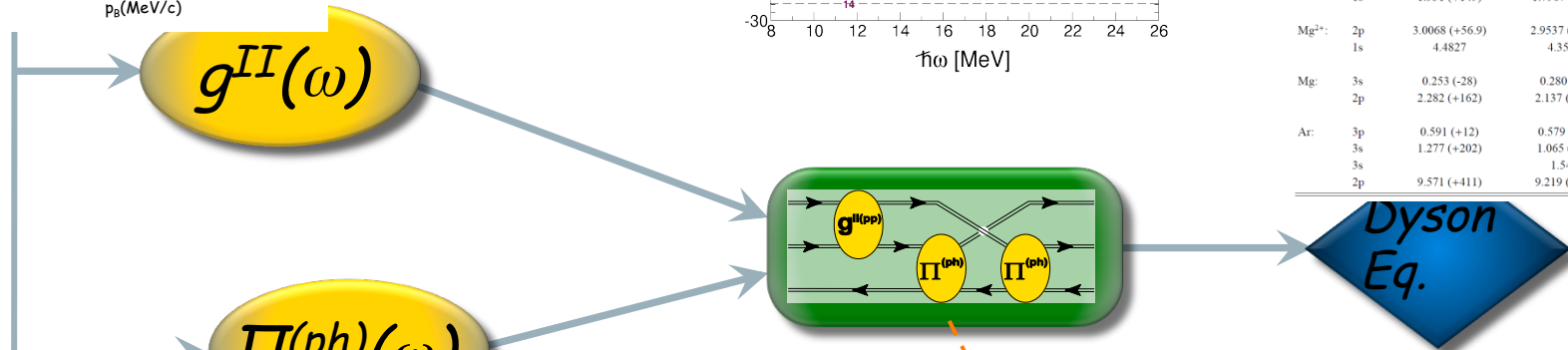
Binding energy benchmk,  $^4\text{He}$  [C. B., arXiv:0909.0336]



Ionization energies/affinities, in atoms

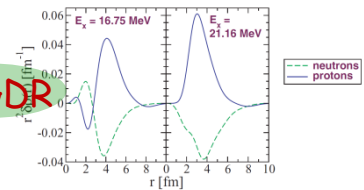
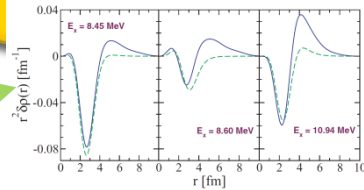
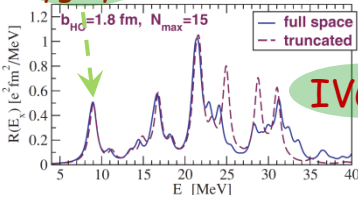
[CB, D. Van Neck, AIP Conf.Proc.1120,104 ('09) & in prep]

	Hartree-Fock	FRPAc	Experiment [16, 17]
He: 1s	0.918 (+14)	0.9008 (-2.9)	0.9037
Be <sup>2+</sup> : 1s	5.6672 (+116)	5.6551 (-0.5)	5.6556
Be: 2s	0.3093 (-34)	0.3224 (-20.2)	0.3426
1s	4.733 (+200)	4.5405 (+8)	4.533
Ne: 2p	0.852 (+57)	0.8037 (+11)	0.793
1s	1.931 (+149)	1.7967 (+15)	1.782
Mg <sup>2+</sup> : 2p	3.0068 (+56.9)	2.9537 (+3.8)	2.9499
1s	4.4827	4.3589	
Mg: 3s	0.253 (-28)	0.280 (-1)	0.281
2p	2.282 (+162)	2.137 (+17)	2.12
Ar: 3p	0.591 (+12)	0.579 (±0)	0.579
3s	1.277 (+202)	1.065 (-10)	1.075
3s		1.544	
2p	9.571 (+411)	9.219 (+59)	9.160



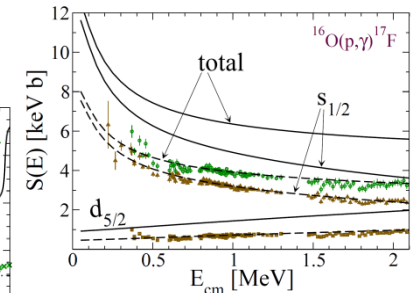
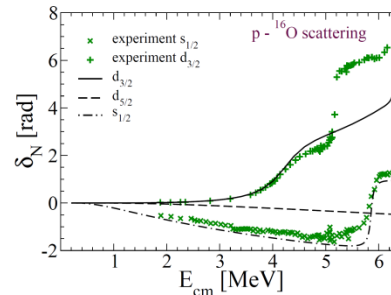
Isovector response for  $^{32}\text{Ar}$ ,  $^{34}\text{Ar}$

Proton Pygmy



IVGDR

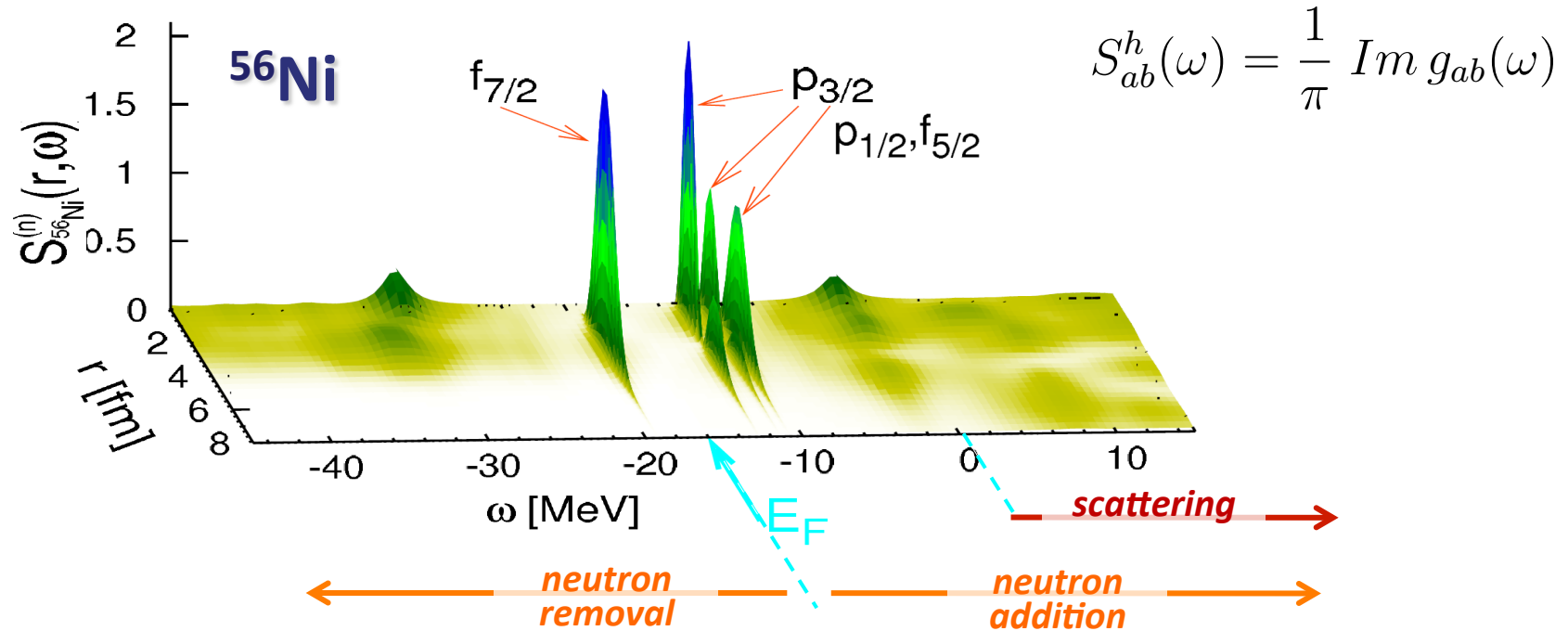
$^{16}\text{O}(p,\gamma)$



[C. B., B. K. Jennings Nucl. Phys A758, 395c (2005)  
Phys Rev. C72, 014613 (2005)]



# $^{56}\text{Ni}$ neutron spectral function



W. Dickhoff, CB, Prog. Part. Nucl. Phys. 53, 377 (2004)  
 CB, M.Hjorth-Jensen, Pys. Rev. C79, 064313 (2009)

# Approaches in GF theory

Truncation  
scheme:

Dyson formulation  
(closed shells)

Gorkov formulation  
(semi-/doubly-magic)

1<sup>st</sup> order:

Hartree-Fock

HF-Bogoliubov

2<sup>nd</sup> order:

2<sup>nd</sup> order

2<sup>nd</sup> order (w/ pairing)

...

...

3<sup>rd</sup> and all-orders  
sums,  
P-V coupling:

ADC(3)  
FRPA  
etc...

G-ADC(3)  
...work in progress



# Approaches in GF theory

Truncation scheme:

Dyson formulation  
(closed shells)

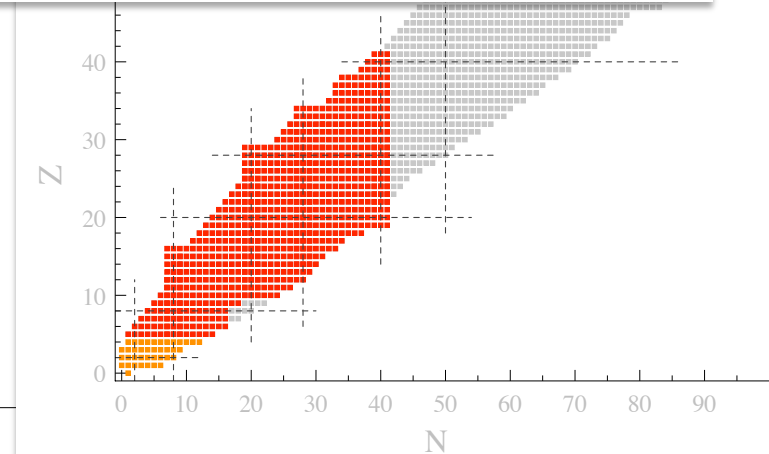
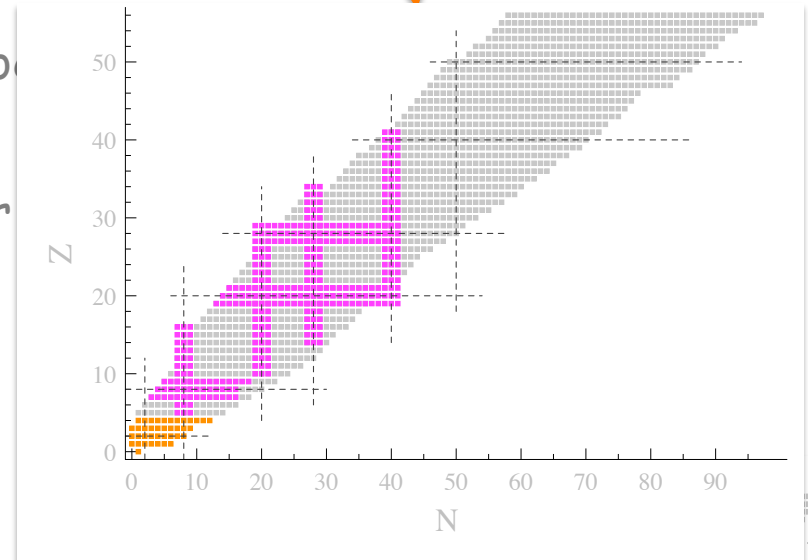
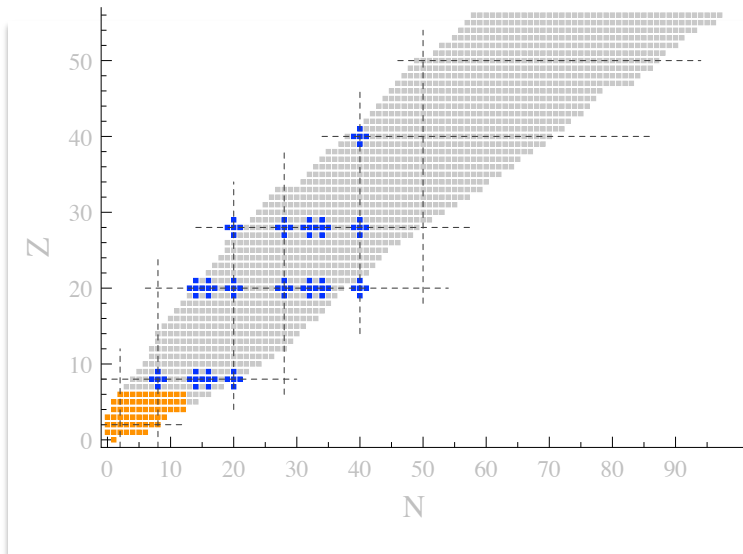
Gorkov formulation  
(semi-/doubly-magic)

1<sup>st</sup> order:

Hartree-Fo

2<sup>nd</sup> order

...  
ADC(3)  
FRPA  
etc...



# Gorkov and symmetry breaking approaches

V. Somà, CB, T. Duguet, , Phys. Rev. C **89**, 024323 (2014)

V. Somà, CB, T. Duguet, Phys. Rev. C **87**, 011303R (2013)

V. Somà, T. Duguet, CB, Phys. Rev. C **84**, 064317 (2011)

➤ Ansatz  $\dots \approx E_0^{N+2} - E_0^N \approx E_0^N - E_0^{N-2} \approx \dots \approx 2\mu$

➤ Auxiliary many-body state  $|\Psi_0\rangle \equiv \sum_N^{\text{even}} c_N |\psi_0^N\rangle$

➤ Mixes various particle numbers

➤ Introduce a “grand-canonical” potential  $\Omega = H - \mu N$

➤  $|\Psi_0\rangle$  minimizes  $\Omega_0 = \langle \Psi_0 | \Omega | \Psi_0 \rangle$  under the constraint  $N = \langle \Psi_0 | N | \Psi_0 \rangle$

➤ This approach leads to the following Feynman diagrams:

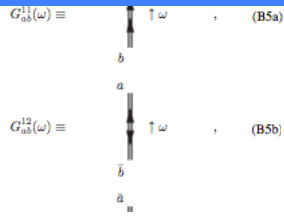
$$\Sigma_{ab}^{11(1)} = \text{Diagram 1}$$

$$\Sigma_{ab}^{12(1)} = \text{Diagram 2}$$

$$\Sigma_{ab}^{11(2)}(\omega) = \text{Diagram 3} + \text{Diagram 4}$$

$$\Sigma_{ab}^{12(2)}(\omega) = \text{Diagram 5} + \text{Diagram 6}$$

# Expressions for 1st & 2nd order diagrams



V. SOMÀ, T. DUGUET, AND C. BARBIERI

It is interesting to note that the first-order  $\alpha$  with a  $J = 0$  many-body state. The other:



$$-i \int_{C_1} \frac{d\omega'}{2\pi} \sum_{cd,k} \tilde{V}_{abcd} \frac{\mathcal{V}_c^*}{\omega' + \omega}$$

$$\Sigma_{ab}^{21(1)} = \frac{1}{2} \sum_{cd,k} \tilde{V}_{cdab} \tilde{U}$$

$$= -\frac{1}{2} \sum_{n_1, n_2, n_3} \sum_{\gamma} \dots$$

$$= \delta_{a\beta} \delta_{m_1 m_2} \frac{1}{2} \dots$$

$$\equiv \delta_{a\beta} \delta_{m_1 m_2} \Sigma_{n_1 n_2}^{21}$$

$$= \delta_{a\beta} \delta_{m_1 m_2} \tilde{F}_{n_1 n_2}^{(a)}$$

Ab INITIO SELF-CONSISTENT GORKOV-GREEN'S ...

## 5. Block-diagonal structure

a. First order

The goal of this subsection is to discuss how the block-diagonals reflects in the various self-energy contributions, starting with the first and (C19) into Eq. (B7), and introducing the factor

$$f_{a\beta\gamma\delta}^{n_1 n_2 n_3 n_4} \equiv \sqrt{1 + \delta_{a\beta} \delta_{n_1 n_2}}$$

one obtains

$$\begin{aligned} \Sigma_{ab}^{11(1)} &= \sum_{cd,k} \tilde{V}_{abcd} \tilde{V}_d^* \tilde{V}_c^* \\ &= \sum_{n_1, n_2, n_3} \sum_{\gamma} \sum_{JM} f_{a\beta\gamma\gamma}^{n_1 n_2 n_3 n_4} C_{JM}^{JM} \\ &= \delta_{a\beta} \delta_{m_1 m_2} \sum_{n_1, n_2} \sum_{\gamma} \sum_{JM} f_{a\beta\gamma\gamma}^{n_1 n_2 n_3 n_4} \frac{1}{2} \\ &\equiv \delta_{a\beta} \delta_{m_1 m_2} \Sigma_{n_1 n_2}^{11(a)(1)} \\ &\equiv \delta_{a\beta} \delta_{m_1 m_2} \Lambda_{n_1 n_2}^{(a)} \end{aligned}$$

where the block-diagonal normal density matrix is introduced through

$$\rho_{n_1 n_2}^{(a)} = \sum_{n_3} \mathcal{V}_{n_3 | a}^{(a)}$$

and properties of Clebsch-Gordan coefficients has been used. The  $\delta_{n_1 n_2}$  and  $\delta_{k_1 k_2}$ , leading to  $\delta_{a\beta} = \delta_{j_1 j_2} \delta_{m_1 m_2} \delta_{k_1 k_2}$ . Similarly, for  $\Sigma^{22(1)}$

$$\begin{aligned} \Sigma_{ab}^{22(1)} &= -\sum_{cd,k} \tilde{V}_{abcd} \tilde{V}_d^* \tilde{V}_c^* \\ &= -\delta_{a\beta} \delta_{m_1 m_2} \sum_{n_1, n_2} \sum_{\gamma} \sum_{JM} f_{a\beta}^{n_1 n_2 n_3 n_4} \\ &\equiv \delta_{a\beta} \delta_{m_1 m_2} \Sigma_{n_1 n_2}^{22(a)(1)} \\ &\equiv -\delta_{a\beta} \delta_{m_1 m_2} \Lambda_{n_1 n_2}^{(a)} \\ &= -\delta_{a\beta} \delta_{m_1 m_2} [\Lambda_{n_1 n_2}^{(a)}]^* \end{aligned}$$

Let us consider the anomalous contributions to the first-order self-energy

$$\begin{aligned} \Sigma_{ab}^{21(1)} &= \frac{1}{2} \sum_{cd,k} \tilde{V}_{abcd} \tilde{V}_d^* \tilde{V}_c^* \\ &= -\frac{1}{2} \sum_{n_1, n_2, n_3} \sum_{\gamma} \sum_{JM} \sum_{M'} f_{a\beta\gamma\gamma}^{n_1 n_2 n_3 n_4} \eta_a \eta_b C_{JM}^{JM'} \\ &= -\frac{1}{2} \sum_{n_1, n_2, n_3} \sum_{\gamma} \sum_{JM} \sum_{M'} f_{a\beta\gamma\gamma}^{n_1 n_2 n_3 n_4} \eta_a \eta_b C_{JM}^{JM'} \\ &= -\frac{1}{2} \sum_{n_1, n_2, n_3} \sum_{\gamma} \sum_{JM} \sum_{M'} f_{a\beta\gamma\gamma}^{n_1 n_2 n_3 n_4} \eta_a \eta_b (-1)^{J-M} C_{JM}^{JM'} \\ &= \delta_{a\beta} \delta_{m_1 m_2} \frac{1}{2} \sum_{n_1, n_2} \sum_{JM} f_{a\beta\gamma\gamma}^{n_1 n_2 n_3 n_4} \pi_a \pi_b (-1)^{J-M} \\ &\equiv \delta_{a\beta} \delta_{m_1 m_2} \Sigma_{n_1 n_2}^{21(a)(1)} \\ &\equiv \delta_{a\beta} \delta_{m_1 m_2} \tilde{F}_{n_1 n_2}^{(a)} \end{aligned}$$

where the block-diagonal anomalous density matrix is introduced through

$$\tilde{\rho}_{n_1 n_2}^{(a)} = \sum_{n_3} \tilde{\mathcal{U}}_{n_3 | a}^{(a)}$$

$$\Sigma_{ab}^{21(1)} = \frac{1}{2} \sum_{cd,k} \tilde{V}_{cdab} \tilde{U}$$

$$= -\frac{1}{2} \sum_{n_1, n_2, n_3} \sum_{\gamma} \dots$$

$$= \delta_{a\beta} \delta_{m_1 m_2} \frac{1}{2} \dots$$

$$\equiv \delta_{a\beta} \delta_{m_1 m_2} \Sigma_{n_1 n_2}^{21}$$

$$= \delta_{a\beta} \delta_{m_1 m_2} \tilde{F}_{n_1 n_2}^{(a)}$$

Block-diagonal forms of second-order angular momentum couplings of the three  $\mathcal{Q}$ ,  $\mathcal{R}$ , and  $\mathcal{S}$ . One proceeds first coupling give  $J_{tot}$ . The recoupled  $\mathcal{M}$  term is computed

$$\begin{aligned} \mathcal{M}_{a(J, J_{tot})}^{b(k_1 k_2)} &= \sum_{m_1, m_2, m_3, M} C_{j_1 m_1 j_2 m_2}^{J M} C_{J M}^{J M} \\ &= \sum_{m_1, m_2, M} C_{j_1 m_1 j_2 m_2}^{J M} C_{J M}^{J M} \\ &= \sum_{m_1, m_2, M} \sum_{J_1, M_1} \delta_{k_1 \beta} \delta_{m_1 \gamma} \\ &\quad \times C_{j_1 m_1 j_2 m_2}^{J_1 M_1} C_{J_1 M_1}^{J M} C_{J M}^{J M} \\ &= \sum_{m_1, m_2, M} \sum_{J_1, M_1} \eta_k f_{a\beta\gamma}^{n_1 n_2 n_3} \\ &= \sum_{m_1, m_2, M} \sum_{J_1, M_1} \eta_k f_{a\beta\gamma}^{n_1 n_2 n_3} \\ &= \sum_{m_1, m_2, M} \sum_{J_1, M_1} \eta_k f_{a\beta\gamma}^{n_1 n_2 n_3} \\ &= \sum_{m_1, m_2, M} \sum_{J_1, M_1} \eta_k f_{a\beta\gamma}^{n_1 n_2 n_3} \\ &= \sum_{m_1, m_2, M} \sum_{J_1, M_1} \eta_k f_{a\beta\gamma}^{n_1 n_2 n_3} \end{aligned}$$

where general properties of Clebsch-Gordan

$$\begin{aligned} \Lambda_{a(J, J_{tot})}^{b(k_1 k_2)} &= \delta_{J_{tot} J_1} \delta_{M_{tot} M_1} \sum_{n_1} \\ &\equiv \delta_{J_{tot} J_1} \delta_{M_{tot} M_1} \mathcal{N}_{n_1} \end{aligned}$$

One can show that the same result is obtained

$$\begin{aligned} \tilde{\mathcal{N}}_{a(J, J_{tot})}^{b(k_1 k_2)} &= \sum_{m_1, m_2, M} C_{j_1 m_1 j_2 m_2}^{J M} C_{J M}^{J M} \\ &= \sum_{m_1, m_2, M} C_{j_1 m_1 j_2 m_2}^{J M} C_{J M}^{J M} \\ &= \sum_{m_1, m_2, M} \sum_{J_1, M_1} \delta_{k_1 \beta} \delta_{m_1 \gamma} \\ &\quad \times C_{j_1 m_1 j_2 m_2}^{J_1 M_1} C_{J_1 M_1}^{J M} C_{J M}^{J M} \\ &= \sum_{m_1, m_2, M} \sum_{J_1, M_1} \delta_{k_1 \beta} \delta_{m_1 \gamma} \\ &\quad \times C_{j_1 m_1 j_2 m_2}^{J_1 M_1} C_{J_1 M_1}^{J M} C_{J M}^{J M} \\ &= \sum_{m_1, m_2, M} \sum_{J_1, M_1} \delta_{k_1 \beta} \delta_{m_1 \gamma} \\ &\quad \times C_{j_1 m_1 j_2 m_2}^{J_1 M_1} C_{J_1 M_1}^{J M} C_{J M}^{J M} \end{aligned}$$

$$C_{n_1 n_2 n_3 n_4}^{n_1 n_2 n_3 n_4} J_c \equiv \frac{1}{\sqrt{6}} [M_{n_1 n_2 n_3 n_4}^{n_1 n_2 n_3 n_4} J_c - \mathcal{P}_{n_1 n_2 n_3 n_4}^{n_1 n_2 n_3 n_4} J_c - \mathcal{R}_{n_1 n_2 n_3 n_4}^{n_1 n_2 n_3 n_4} J_c], \quad (C43a)$$

## [V. Somà, T. Duguet, CB, Pys. Rev. C84, 046317 (2011)]

$$\begin{aligned} &= \sum_{m_1, m_2, n_1, n_2} \eta_a \eta_b f_{a\beta\gamma}^{n_1 n_2 n_3} C_{j_1 m_1}^{J M} \\ &= \sum_{m_1, m_2, n_1, n_2} \eta_a \eta_b f_{a\beta\gamma}^{n_1 n_2 n_3} \frac{\sqrt{2J_1+1}}{\sqrt{2J_2+1}} (-) \\ &= \delta_{J_{tot} J_1} \delta_{M_{tot} - M_1} \sum_{n_1, n_2} \eta_k f_{a\beta\gamma}^{n_1 n_2 n_3} \frac{\sqrt{2J}}{\sqrt{2}} \\ &= -\delta_{J_{tot} J_1} \delta_{M_{tot} - M_1} \eta_a \mathcal{N}_{n_1 n_2 n_3}^{n_1 n_2 n_3} \end{aligned}$$

which recovers relation (72a). The remaining quantum  $\{k_1, k_2, k_3\}$  indices and can be obtained from Eqs. (C43) to  $J_{tot}$  and  $J_c$  as follows:

$$\begin{aligned} \mathcal{P}_{a(J, J_{tot})}^{b(k_1 k_2)} &= \sum_{J_c} (-1)^{J_1+J_2+J_3+J_4} \sqrt{2J_c} \\ &= -\delta_{J_{tot} J_1} \delta_{M_{tot} - M_1} \sum_{n_1, n_2} \sum_{J_c} \pi_k \\ &\quad \times \tilde{V}_{J_c [a(k_1 k_2) J_c]}^{n_1 n_2 n_3} \mathcal{U}_{n_1 [k_1]}^{n_1 n_2} \mathcal{U}_{n_2 [k_2]}^{n_1 n_2} \\ &\equiv \delta_{J_{tot} J_1} \delta_{M_{tot} - M_1} \mathcal{P}_{n_1 n_2 n_3}^{n_1 n_2 n_3} J_c \end{aligned}$$

$$\begin{aligned} \mathcal{Q}_{a(J, J_{tot})}^{b(k_1 k_2)} &= \sum_{J_c} (-1)^{J_1+J_2+J_3+J_4} \sqrt{2J_c} \\ &= \delta_{J_{tot} J_1} \delta_{M_{tot} - M_1} \sum_{n_1, n_2} \sum_{J_c} \pi_k \\ &\quad \times \tilde{V}_{J_c [a(k_1 k_2) J_c]}^{n_1 n_2 n_3} \mathcal{V}_{n_1 [k_1]}^{n_1 n_2} \mathcal{V}_{n_2 [k_2]}^{n_1 n_2} \\ &\equiv \delta_{J_{tot} J_1} \delta_{M_{tot} - M_1} \mathcal{Q}_{n_1 n_2 n_3}^{n_1 n_2 n_3} J_c \end{aligned}$$

$$\begin{aligned} \mathcal{R}_{a(J, J_{tot})}^{b(k_1 k_2)} &= \sum_{J_c} (-1)^{J_1+J_2+J_3+J_4} \sqrt{2J_c} + 1 \\ &= -\delta_{J_{tot} J_1} \delta_{M_{tot} - M_1} \sum_{n_1, n_2} \sum_{J_c} \pi_k \\ &\quad \times \tilde{V}_{J_c [a(k_1 k_2) J_c]}^{n_1 n_2 n_3} \mathcal{U}_{n_1 [k_1]}^{n_1 n_2} \mathcal{U}_{n_2 [k_2]}^{n_1 n_2} \\ &\equiv \delta_{J_{tot} J_1} \delta_{M_{tot} - M_1} \mathcal{R}_{n_1 n_2 n_3}^{n_1 n_2 n_3} J_c \end{aligned}$$

$$\begin{aligned} \mathcal{S}_{a(J, J_{tot})}^{b(k_1 k_2)} &= \sum_{J_c} (-1)^{J_1+J_2+J_3+J_4} \sqrt{2J_c} + 1 \\ &= \delta_{J_{tot} J_1} \delta_{M_{tot} - M_1} \sum_{n_1, n_2} \sum_{J_c} \pi_k \\ &\quad \times \tilde{V}_{J_c [a(k_1 k_2) J_c]}^{n_1 n_2 n_3} \mathcal{V}_{n_1 [k_1]}^{n_1 n_2} \mathcal{V}_{n_2 [k_2]}^{n_1 n_2} \\ &\equiv \delta_{J_{tot} J_1} \delta_{M_{tot} - M_1} \mathcal{S}_{n_1 n_2 n_3}^{n_1 n_2 n_3} J_c \end{aligned}$$

$$\begin{aligned} \mathcal{S}_{a(J, J_{tot})}^{b(k_1 k_2)} &= \sum_{J_c} (-1)^{J_1+J_2+J_3+J_4} \sqrt{2J_c} + 1 \\ &= \delta_{J_{tot} J_1} \delta_{M_{tot} - M_1} \sum_{n_1, n_2} \sum_{J_c} \pi_k \\ &\quad \times \tilde{V}_{J_c [a(k_1 k_2) J_c]}^{n_1 n_2 n_3} \mathcal{V}_{n_1 [k_1]}^{n_1 n_2} \mathcal{V}_{n_2 [k_2]}^{n_1 n_2} \\ &\equiv \delta_{J_{tot} J_1} \delta_{M_{tot} - M_1} \mathcal{S}_{n_1 n_2 n_3}^{n_1 n_2 n_3} J_c \end{aligned}$$

$$\begin{aligned} \mathcal{S}_{a(J, J_{tot})}^{b(k_1 k_2)} &= \sum_{J_c} (-1)^{J_1+J_2+J_3+J_4} \sqrt{2J_c} + 1 \\ &= \delta_{J_{tot} J_1} \delta_{M_{tot} - M_1} \sum_{n_1, n_2} \sum_{J_c} \pi_k \\ &\quad \times \tilde{V}_{J_c [a(k_1 k_2) J_c]}^{n_1 n_2 n_3} \mathcal{V}_{n_1 [k_1]}^{n_1 n_2} \mathcal{V}_{n_2 [k_2]}^{n_1 n_2} \\ &\equiv \delta_{J_{tot} J_1} \delta_{M_{tot} - M_1} \mathcal{S}_{n_1 n_2 n_3}^{n_1 n_2 n_3} J_c \end{aligned}$$

These terms are finally put together to form the different contributions to second-order self-energies. Let us consider  $\Sigma_{ab}^{21}$  as an example (see Eq. (75)). By inserting Eqs. (C35) and (C36) and summing over all possible total and intermediate angular momenta, one has

$$\Sigma_{ab}^{21(2)} = \frac{1}{2} \sum_{J_c} \sum_{k_1 k_2} \left\{ \frac{\mathcal{M}_{a(J, J_{tot})}^{b(k_1 k_2)} (\mathcal{M}_{b(J, J_{tot})}^{a(k_1 k_2)})^*}{\omega - (\omega_k_1 + \omega_k_2 + \omega_k_3) + i\eta} + \frac{\mathcal{M}_{a(J, J_{tot})}^{b(k_1 k_2)} (\mathcal{M}_{b(J, J_{tot})}^{a(k_1 k_2)})^*}{\omega + (\omega_k_1 + \omega_k_2 + \omega_k_3) - i\eta} \right\}$$

064317-29

064317-30



$$\begin{aligned} &\frac{1}{2} \sum_{cdef} \tilde{V}_{cdef} \tilde{V}_{abab} \left\{ \frac{\mathcal{V}_c^* \mathcal{U}_c^* \mathcal{U}_d^* \mathcal{V}_d^* \mathcal{V}_c^* \mathcal{V}_d^*}{\omega - (\omega_k_1 + \omega_k_2 + \omega_k_3) + i\eta} + \frac{\mathcal{U}_c^* \mathcal{V}_c^* \mathcal{U}_d^* \mathcal{V}_d^* \mathcal{V}_c^* \mathcal{U}_d^*}{\omega + (\omega_k_1 + \omega_k_2 + \omega_k_3) - i\eta} \right\} \end{aligned} \quad (B32)$$



# Ab-initio Nuclear Computation & BcDor code

BoccaDorata code:

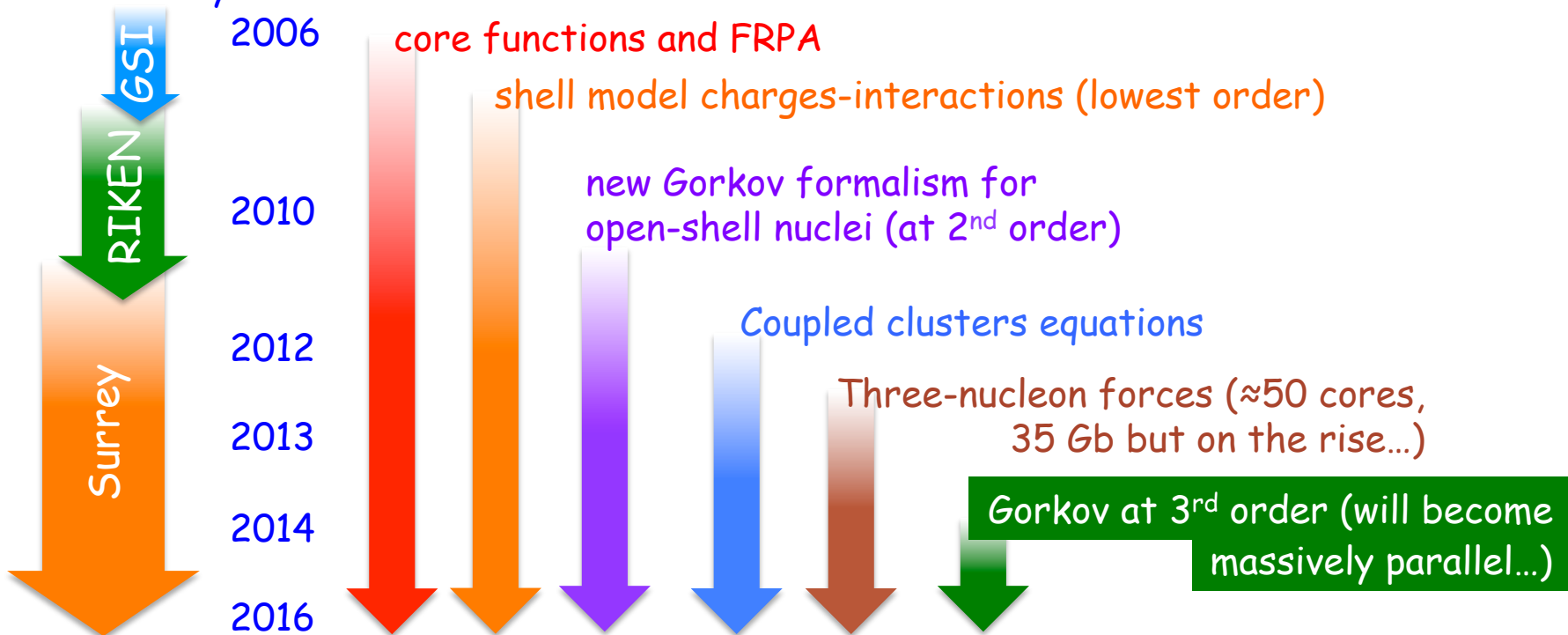
(C. Barbieri 2006-14

V. Somà 2011-14

A. Cipollone 2012-13)

- Provides a *C++ class library* for handling many-body propagators ( $\approx 40,000$  lines, MPI&OpenMP based).
- Allows to solve for nuclear spectral functions, many-body propagators, RPA responses, coupled cluster equations and effective interaction/charges for the shell model.

Code history:

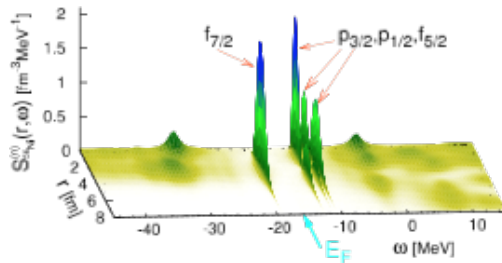


... applications ...

# Ab-initio Nuclear Computation & BcDor code

<http://personal.ph.surrey.ac.uk/~cb0023/bcdor/>

## Computational Many-Body Physics



Download

Documentation

### Welcome

From here you can download a public version of my self-consistent Green's function (SCGF) code for nuclear physics. This is a code in J-coupled scheme that allows the calculation of the single particle propagators (a.k.a. one-body Green's functions) and other many-body properties of spherical nuclei.

This version allows to:

- Perform Hartree-Fock calculations.
- Calculate the correlation energy at second order in perturbation theory (MBPT2).
- Solve the Dyson equation for propagators (self consistently) up to second order in the self-energy.
- Solve coupled cluster CCD (doubles only!) equations.

When using this code you are kindly invited to follow the creative commons license agreement, as detailed at the weblinks below. In particular, we kindly ask you to refer to the publications that led the development of this software.

Relevant references (which can also help in using this code) are:

- Prog. Part. Nucl. Phys. 52, p. 377 (2004),
- Phys. Rev. A76, 052503 (2007),
- Phys. Rev. C79, 064313 (2009),
- Phys. Rev. C89, 024323 (2014)

# Medium-mass isotopes from chiral interactions

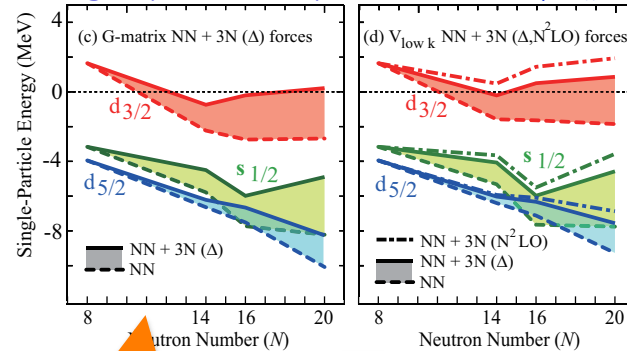
# Modern realistic nuclear forces

## Chiral EFT for nuclear forces:

	2N forces	3N forces	4N forces
LO $\mathcal{O}\left(\frac{Q^0}{\Lambda^0}\right)$			
NLO $\mathcal{O}\left(\frac{Q^2}{\Lambda^2}\right)$			
N <sup>2</sup> LO $\mathcal{O}\left(\frac{Q^3}{\Lambda^3}\right)$			
N <sup>3</sup> LO $\mathcal{O}\left(\frac{Q^4}{\Lambda^4}\right)$			

(3NFs arise naturally at N2LO)

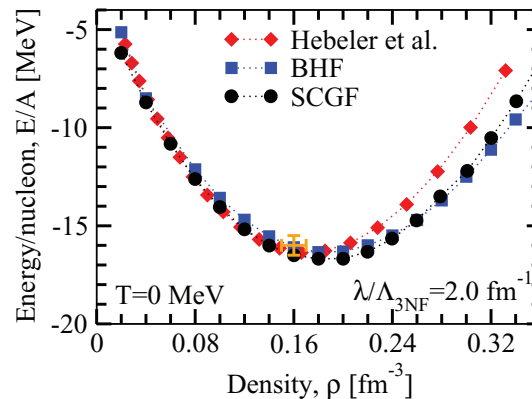
## Single particle spectrum at $E_{\text{fermi}}$ :



[T. Otsuka et al., Phys Rev. Lett **105**, 032501 (2010)]

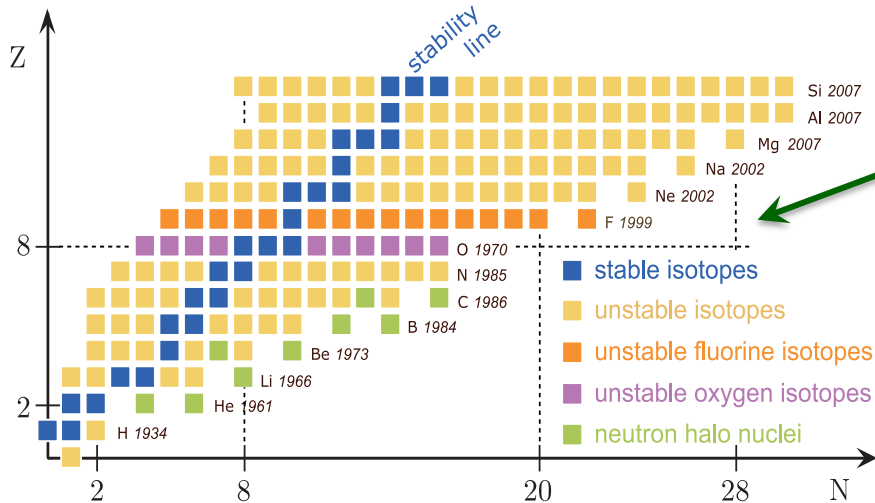
Need at LEAST 3NF!!!  
("cannot" do RNB physics without...)

## Saturation of nuclear matter:



[A. Carbone et al., Phys Rev. C **88**, 044302 (2013)]

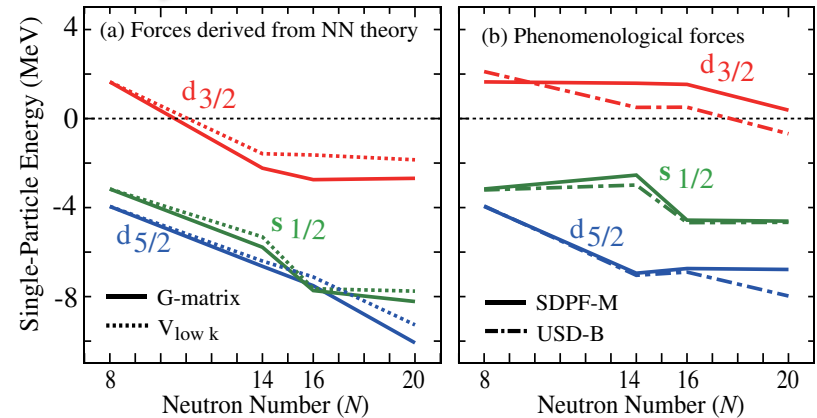
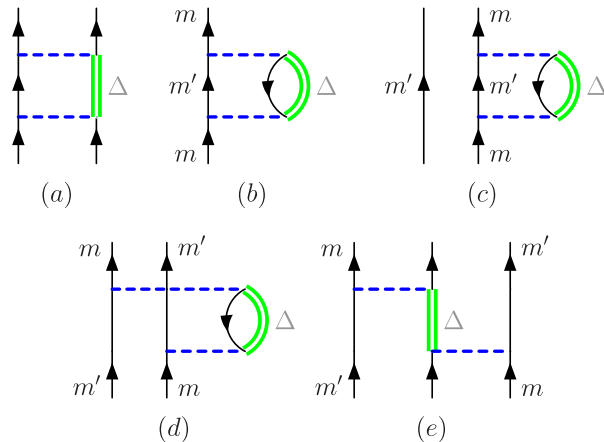
# Oxygen puzzle...



The oxygen dripline is at  $^{24}\text{O}$ , at odds with other neighbor isotope chains.

Phenomenological shell model interaction reflect this in the s.p. energies but no realistic NN interaction alone is capable of reproducing this...

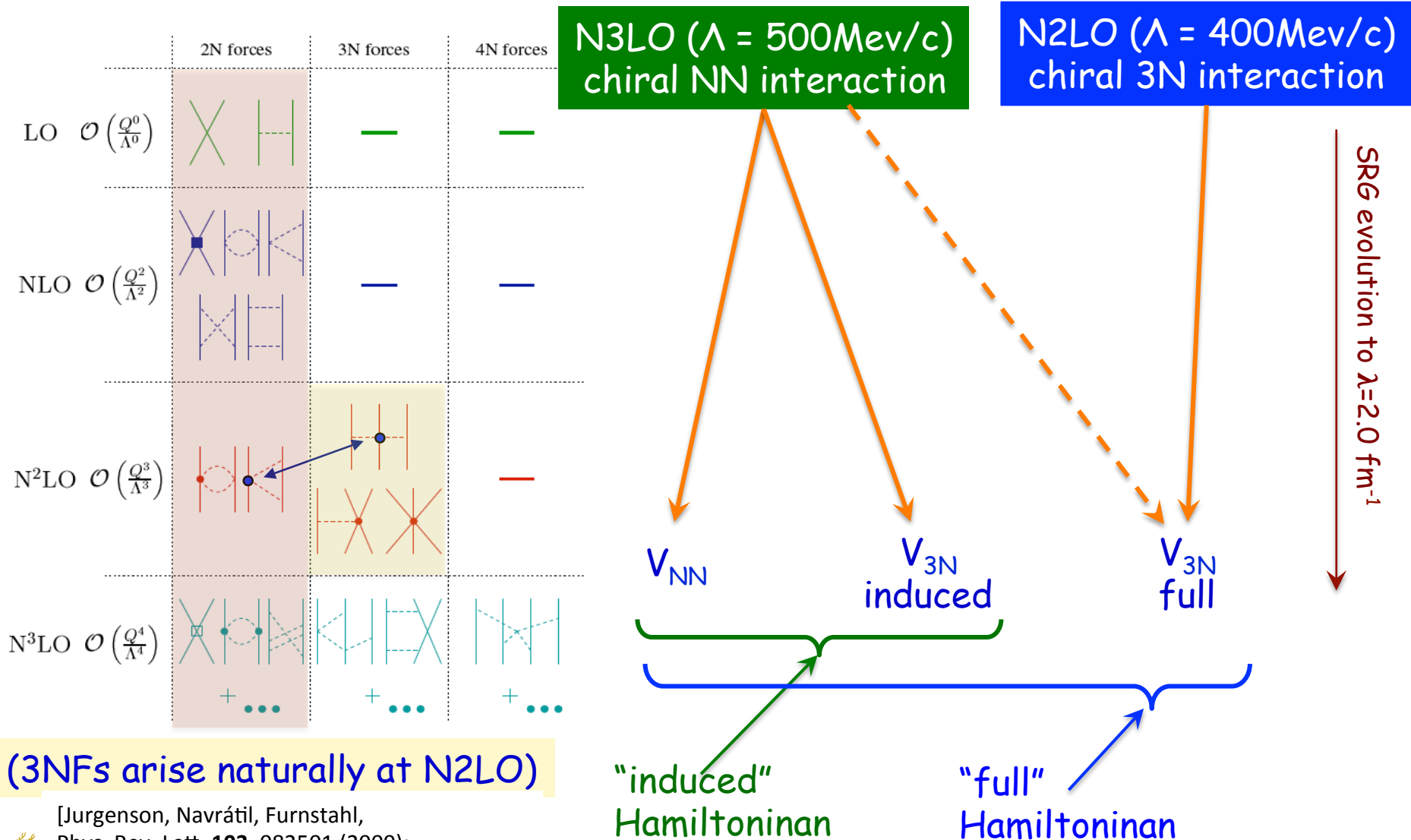
The fujita-Miyazawa 3NF provides repulsion through Pauli screening of other 2NF terms:



[T. Otsuka et al., Phys Rev. Lett **105**, 32501 (2010)]



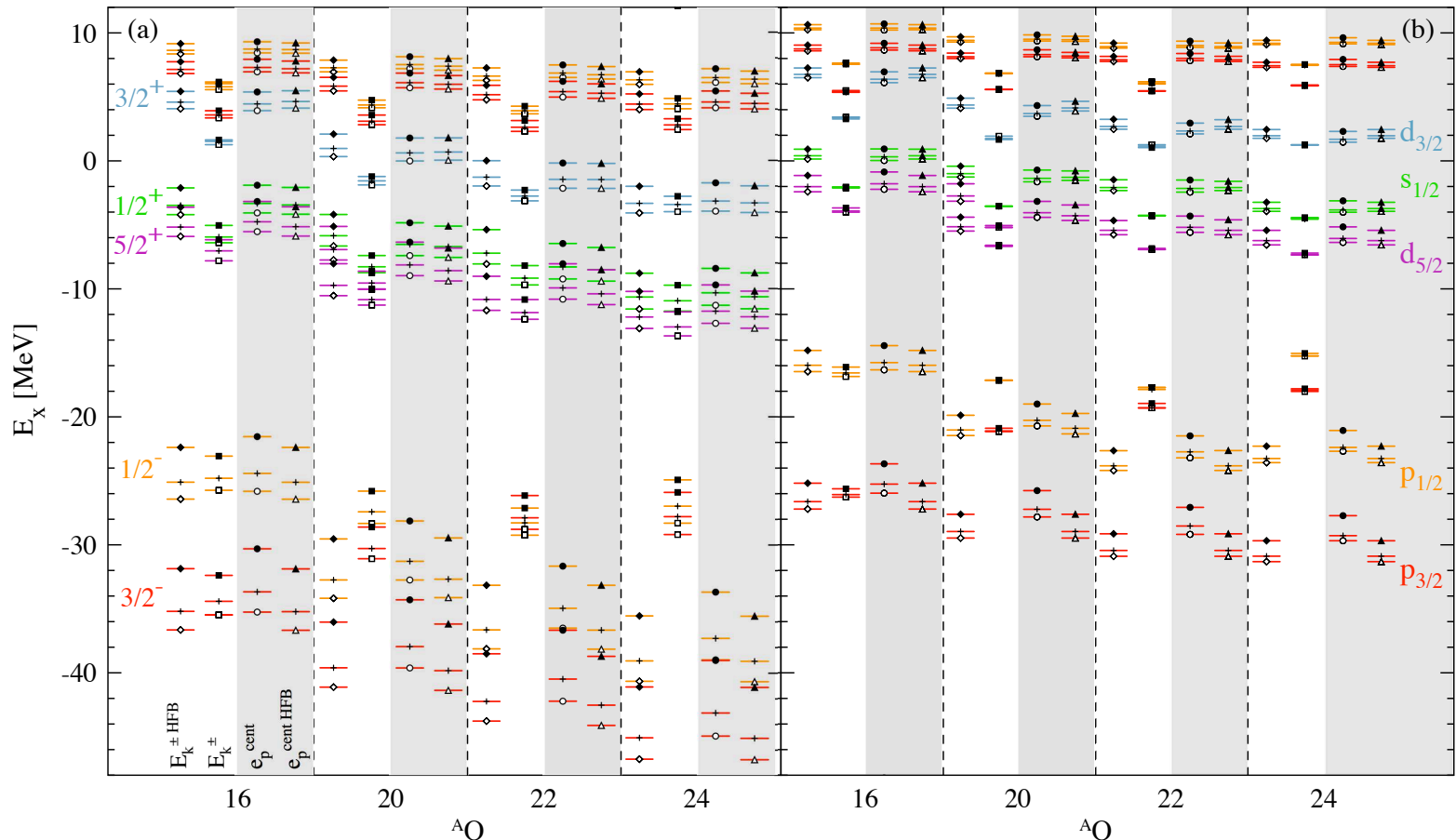
# Chiral Nuclear forces - SRG evolved



# Convergence of s.p. spectra w.r.t. SRG

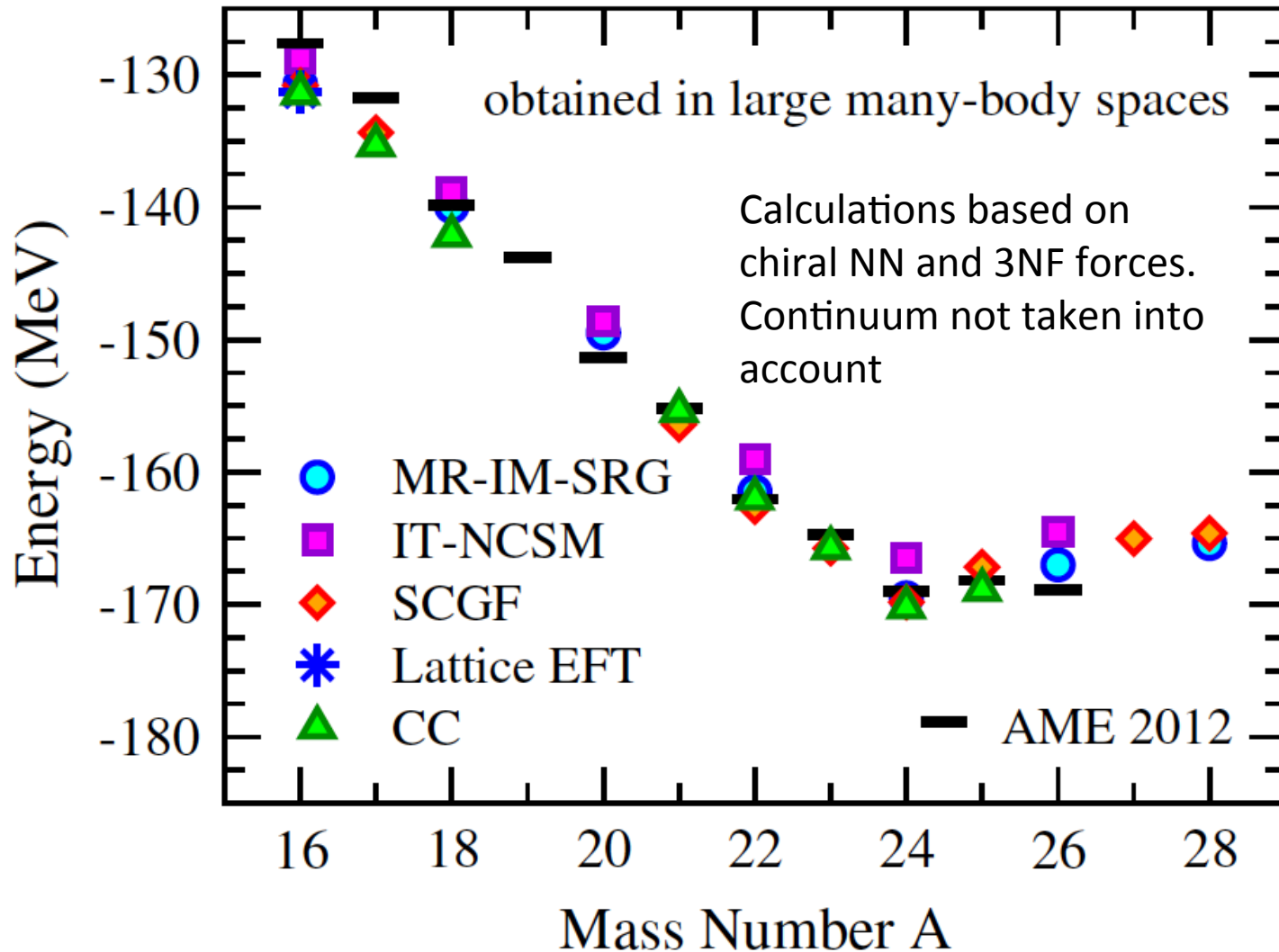
Cutoff dependence is reduced, indicating good convergence of many-body truncation and many-body forces

PhysRevC92, 034313 (2015)  
 ✓ only dominant s.p. peaks shown



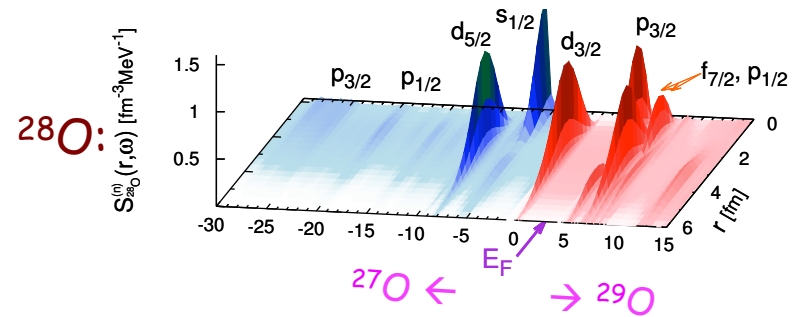
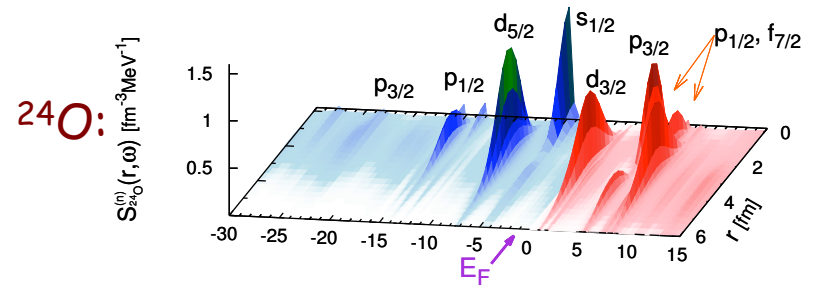
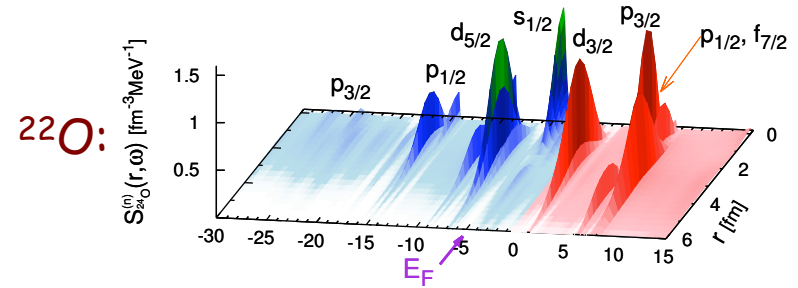
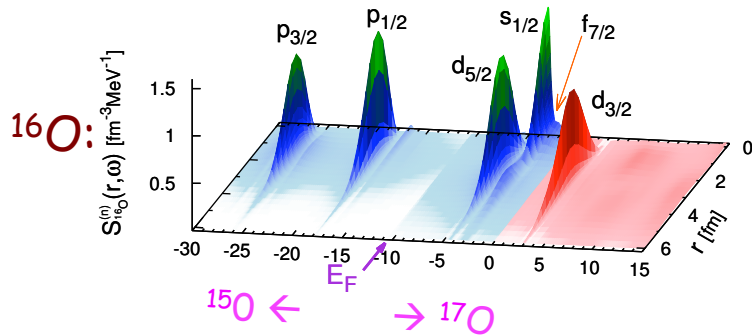
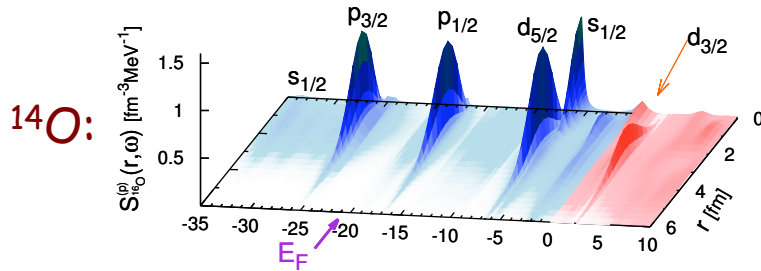
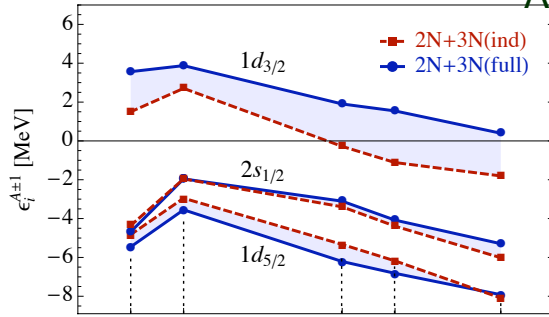
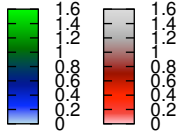
NN terms (no induced 3NF)  $\leftrightarrow$  NN+3NF fully included

# Benchmark of *ab-initio* methods in the oxygen isotopic chain



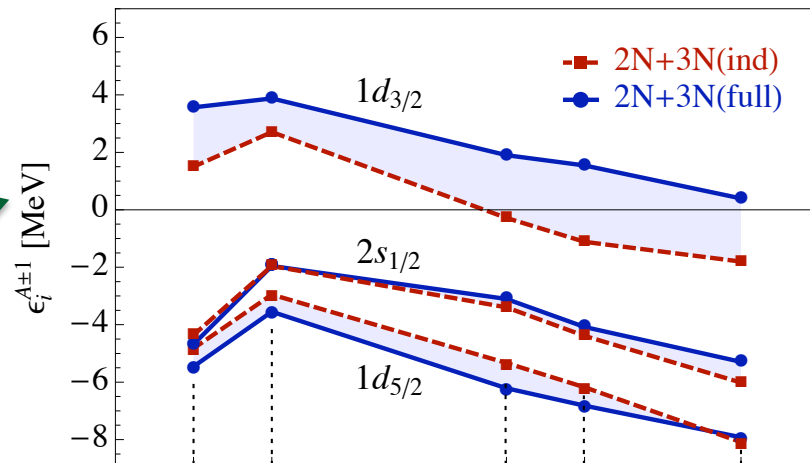
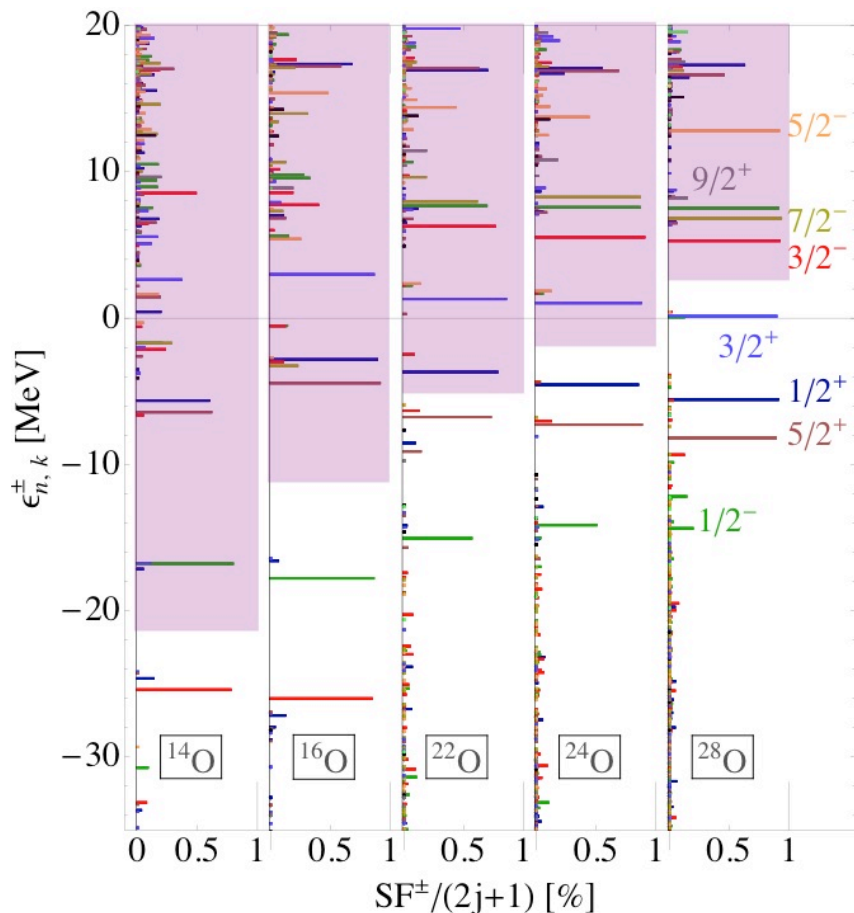
# Neutron spectral function of Oxygens

A. Cipollone, CB, P. Navrátil, *Phys. Rev. C* 92, 014306 (2015)



# Results for the N-O-F chains

A. Cipollone, CB, P. Navrátil, Phys. Rev. Lett. **111**, 062501 (2013)  
and Phys. Rev. C **92**, 014306 (2015)



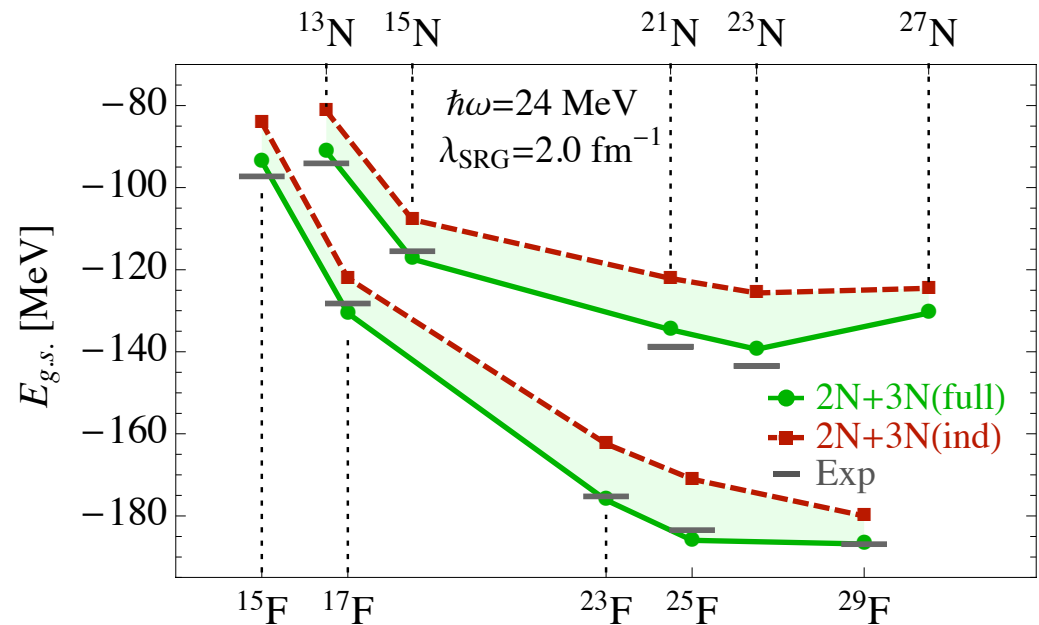
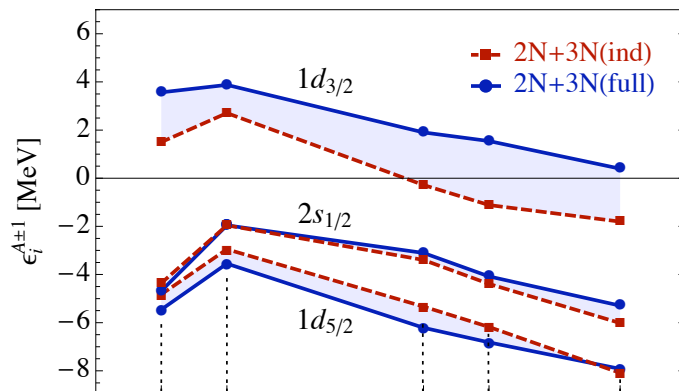
→  $d_{3/2}$  raised by genuine 3NF

→ cf. microscopic shell model [Otsuka et al, PRL**105**, 032501 (2010).]



# Results for the N-O-F chains

A. Cipollone, CB, P. Navrátil, Phys. Rev. Lett. **111**, 062501 (2013)



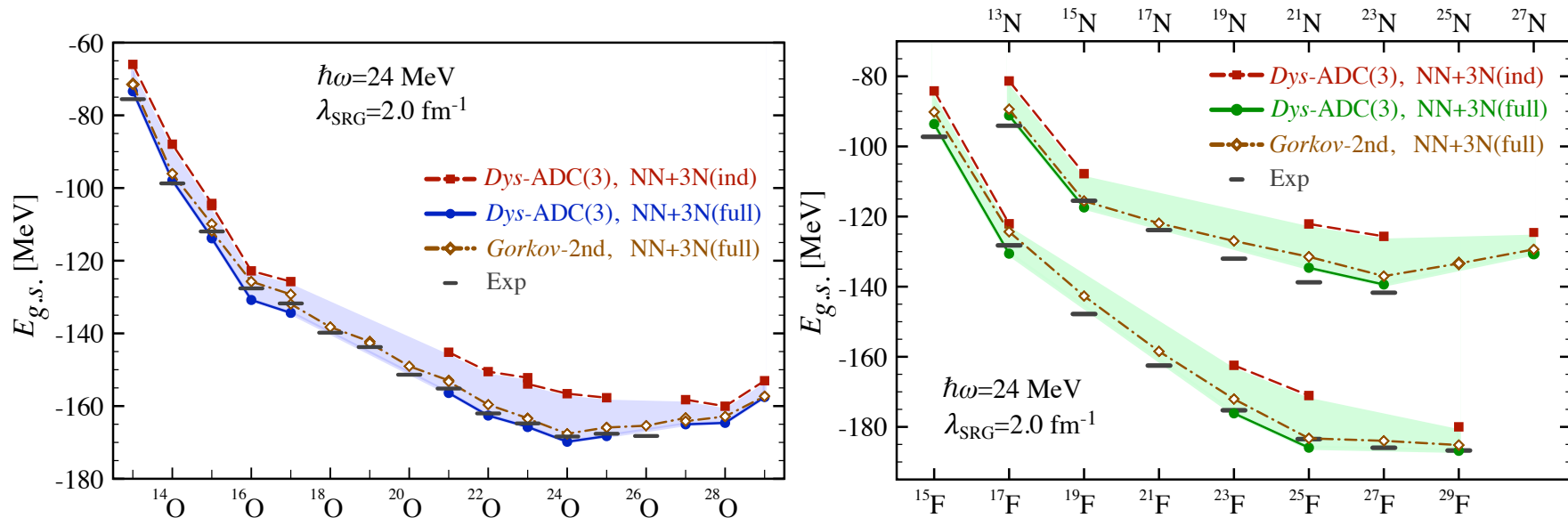
→ 3NF crucial for reproducing binding energies and driplines around oxygen

→  $d_{3/2}$  raised by genuine 3NF

→ cf. microscopic shell model [Otsuka et al, PRL**105**, 032501 (2010).]

# Results for the N-O-F chains

A. Cipollone, CB, P. Navrátil, Phys. Rev. Lett. **111**, 062501 (2013)  
and Phys. Rev. C **92**, 014306 (2015)

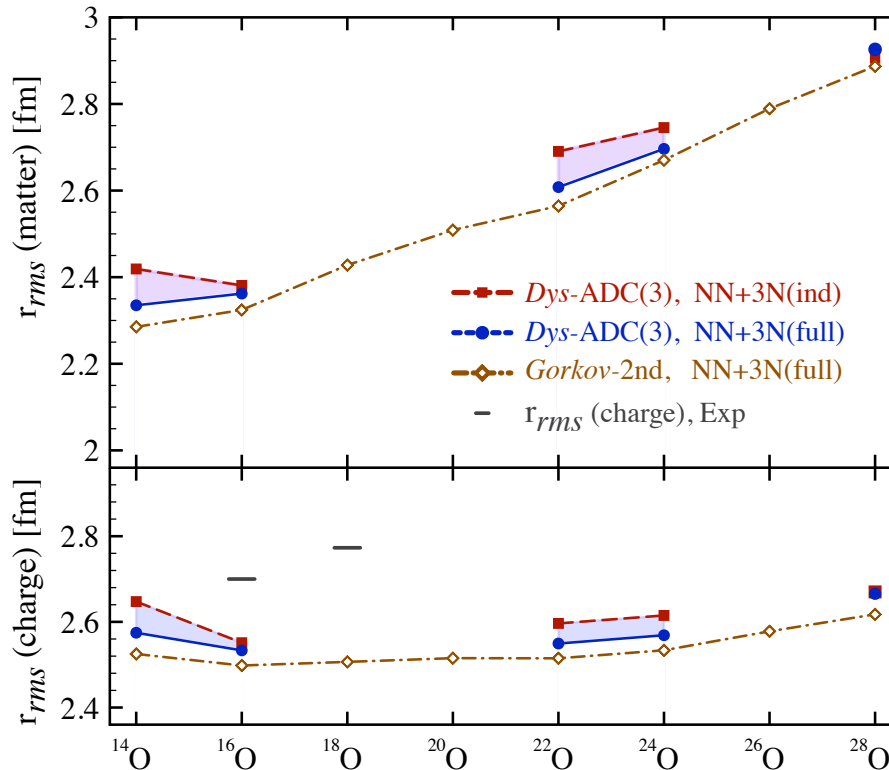


→ 3NF crucial for reproducing binding energies and driplines around oxygen

→ cf. microscopic shell model [Otsuka et al, PRL**105**, 032501 (2010).]

# Results for the oxygen chain

A. Cipollone, CB, P. Navrátil, Phys. Rev. C **92**, 014306 (2015)



→ Single particle spectra slightly to spread and

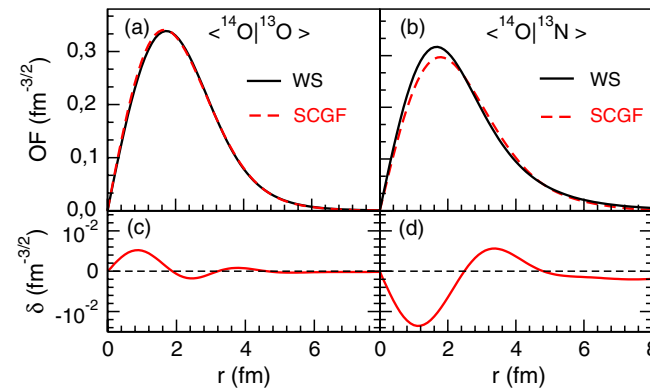
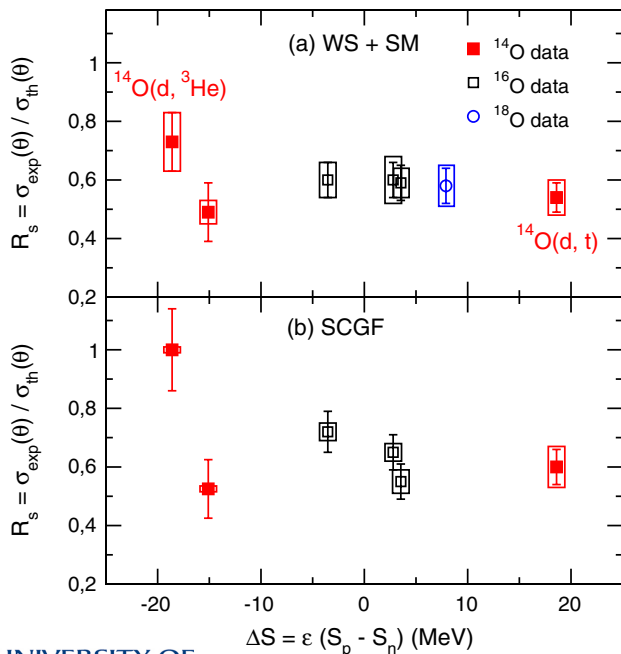
→ systematic underestimation of radii

# Single nucleon transfer in the oxygen chain

[F. Flavigny et al, PRL110, 122503 (2013)]

→ Analysis of  $^{14}\text{O}(d,t)^{13}\text{O}$  and  $^{14}\text{O}(d,^3\text{He})^{13}\text{N}$  transfer reactions @ SPIRAL

Reaction	$E^*$ (MeV)	$J^\pi$	$R_{\text{rms}}^{\text{HFB}}$ (fm)	$r_0$ (fm)	$C^2S_{\text{exp}}$ (WS)	$C^2S_{\text{th}}$ $0p + 2\hbar\omega$	$R_s$ (WS)	$C^2S_{\text{exp}}$ (SCGF)	$C^2S_{\text{th}}$ (SCGF)	$R_s$ (SCGF)
$^{14}\text{O}(d,t)^{13}\text{O}$	0.00	$3/2^-$	2.69	1.40	1.69 (17)(20)	3.15	0.54(5)(6)	1.89(19)(22)	3.17	0.60(6)(7)
$^{14}\text{O}(d,^3\text{He})^{13}\text{N}$	0.00	$1/2^-$	3.03	1.23	1.14(16)(15)	1.55	0.73(10)(10)	1.58(22)(2)	1.58	1.00(14)(1)
	3.50	$3/2^-$	2.77	1.12	0.94(19)(7)	1.90	0.49(10)(4)	1.00(20)(1)	1.90	0.53(10)(1)
$^{16}\text{O}(d,t)^{15}\text{O}$	0.00	$1/2^-$	2.91	1.46	0.91(9)(8)	1.54	0.59(6)(5)	0.96(10)(7)	1.73	0.55(6)(4)
$^{16}\text{O}(d,^3\text{He})^{15}\text{N}$ [19,20]	0.00	$1/2^-$	2.95	1.46	0.93(9)(9)	1.54	0.60(6)(6)	1.25(12)(5)	1.74	0.72(7)(3)
	6.32	$3/2^-$	2.80	1.31	1.83(18)(24)	3.07	0.60(6)(8)	2.24(22)(10)	3.45	0.65(6)(3)
$^{18}\text{O}(d,^3\text{He})^{17}\text{N}$ [21]	0.00	$1/2^-$	2.91	1.46	0.92(9)(12)	1.58	0.58(6)(10)			

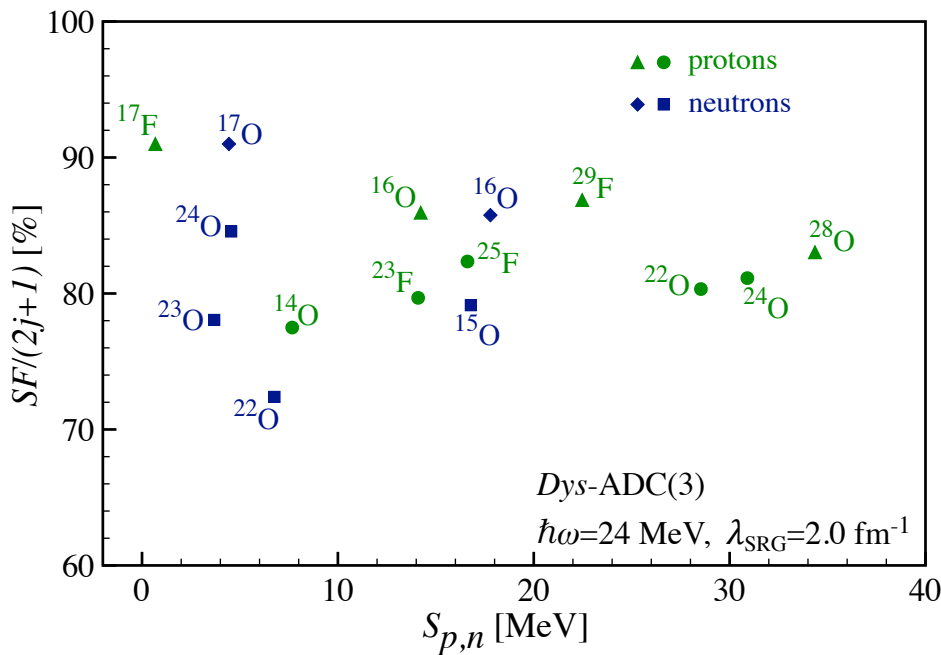


- Overlap functions and strengths from GF
- $R_s$  independent of asymmetry

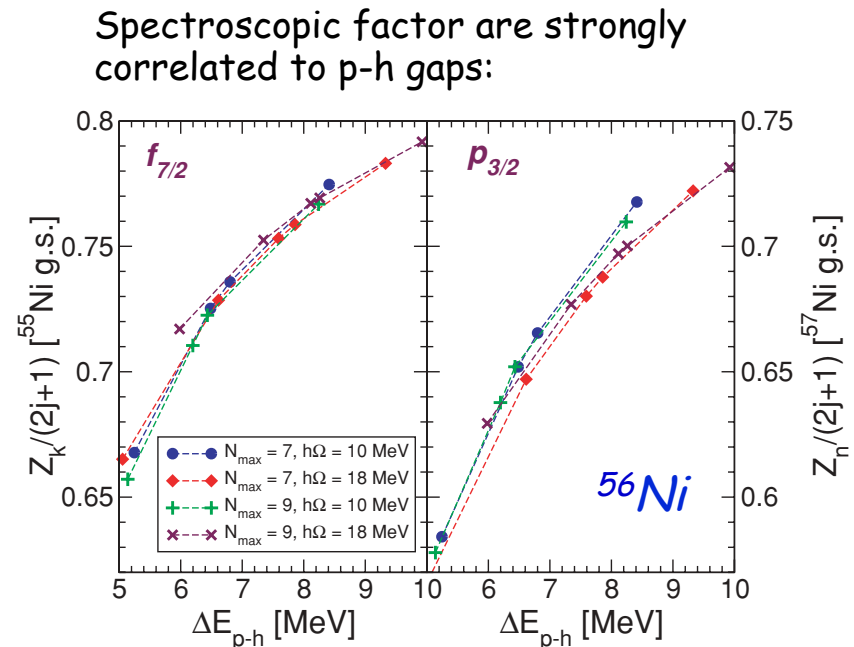
# Z/N asymmetry dependence of SFs - Theory

Ab-initio calculations explain (a very weak) the Z/N dependence but the effect is much lower than suggested by direct knockout

Rather the quenching is high correlated to the gap at the Femi surface.



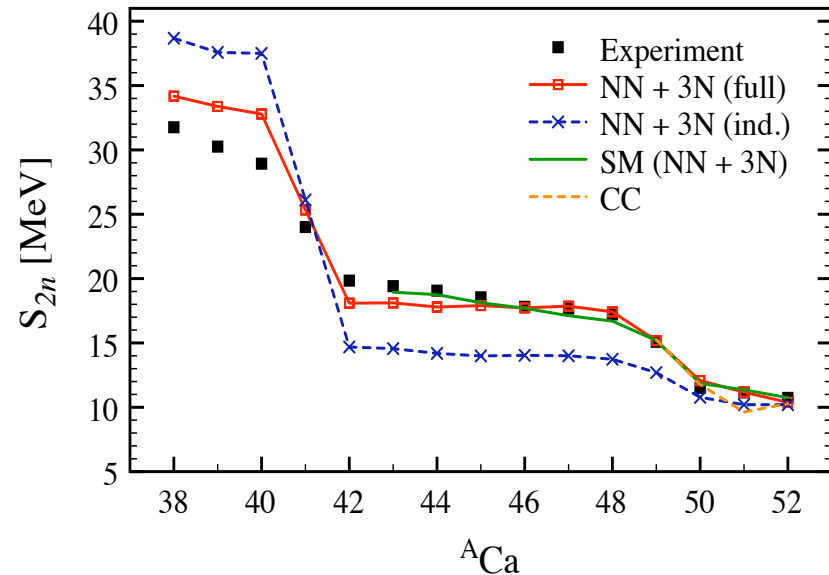
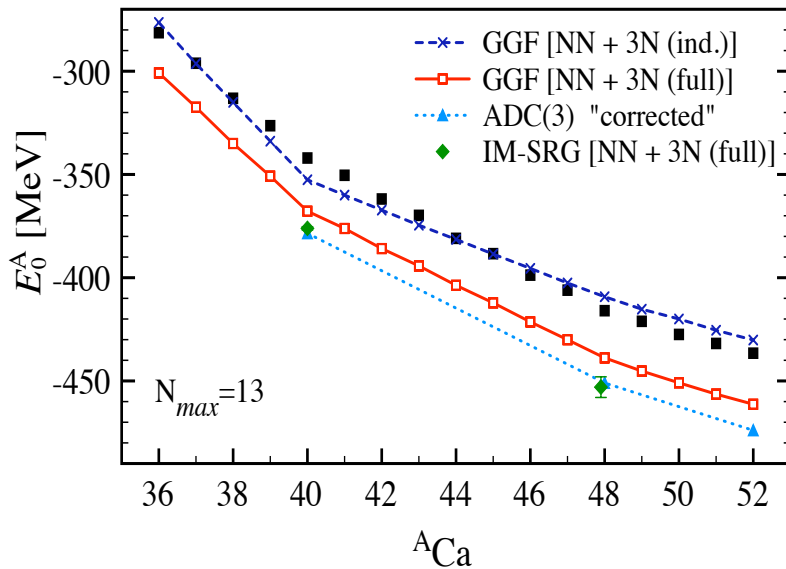
A. Cipollone, CB, P Navrátil  
Phys. Rev. C **92**, 014306 (2015)



CB, M. Hjorth-Jensen,  
Phys. Rev. C **79**, 064313 (2009)

# Calcium isotopic chain

Ab-initio calculation of the whole Ca: *induced* and *full* 3NF investigated



→ *induced* and *full* 3NF investigated

→ *genuine* (N2LO) 3NF needed to reproduce the energy curvature and  $S_{2n}$

→ N=20 and Z=20 gaps *overestimated!*

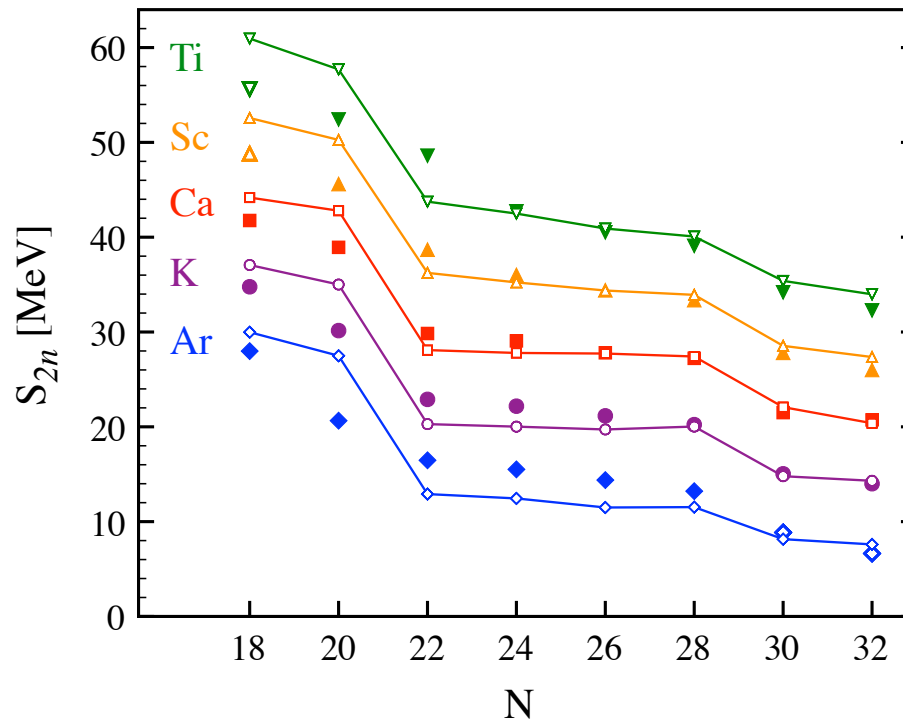
→ Full 3NF give a *correct* trend but *over bind!*



# Neighbouring Ar, K, Ca, Sc, and Ti chains

V. Somà, CB *et al.* Phys. Rev. C89, 061301R (2014)

Two-neutron separation energies predicted by chiral NN+3NF forces:

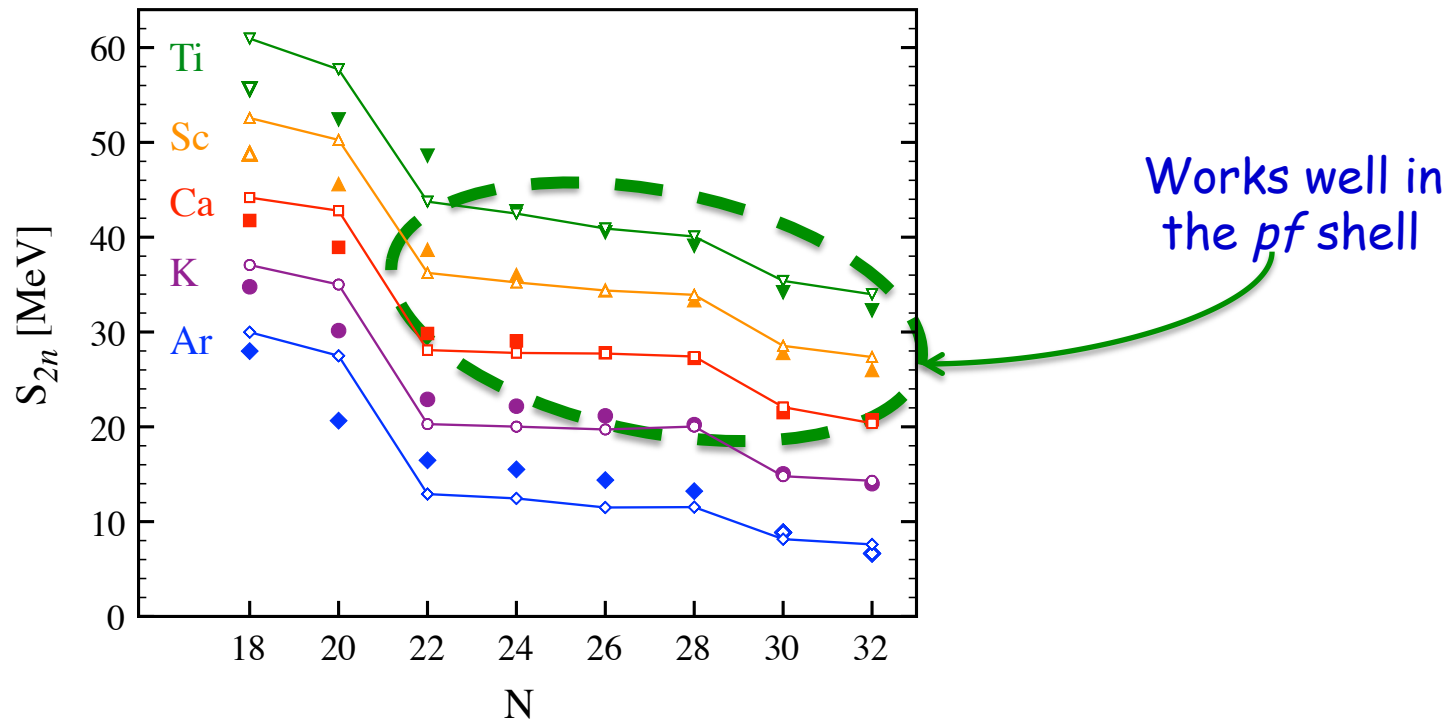


→ First *ab-initio* calculation over a contiguous portion of the nuclear chart—open shells are now possible through the Gorkov-GF formalism

# Neighbouring Ar, K, Ca, Sc, and Ti chains

V. Somà, CB *et al.* Phys. Rev. C89, 061301R (2014)

Two-neutron separation energies predicted by chiral NN+3NF forces:

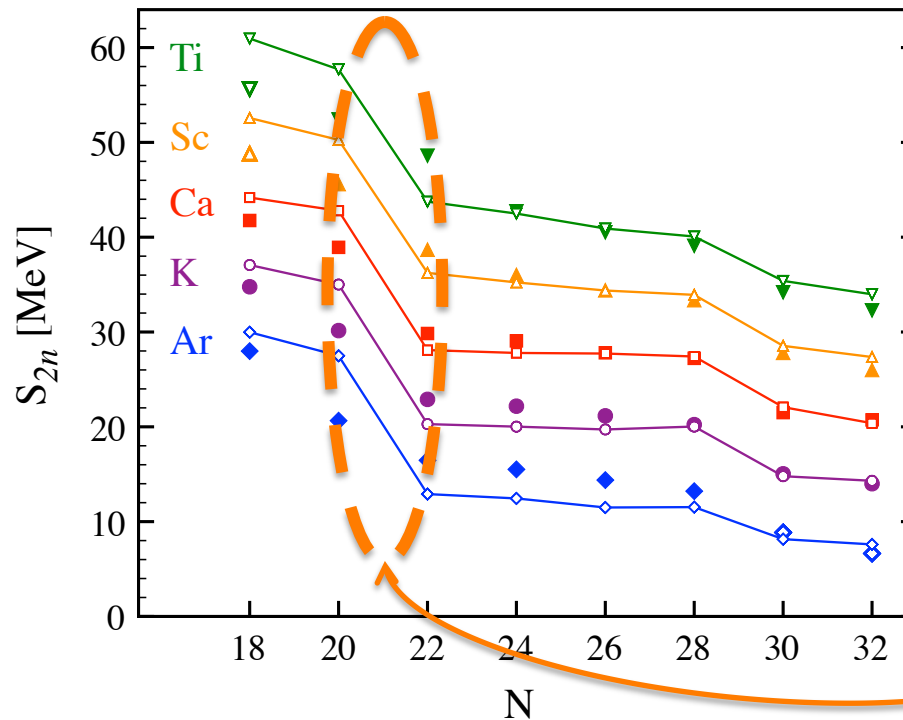


→ First *ab-initio* calculation over a contiguous portion of the nuclear chart—open shells are now possible through the Gorkov-GF formalism

# Neighbouring Ar, K, Ca, Sc, and Ti chains

V. Somà, CB *et al.* Phys. Rev. C89, 061301R (2014)

Two-neutron separation energies predicted by chiral NN+3NF forces:



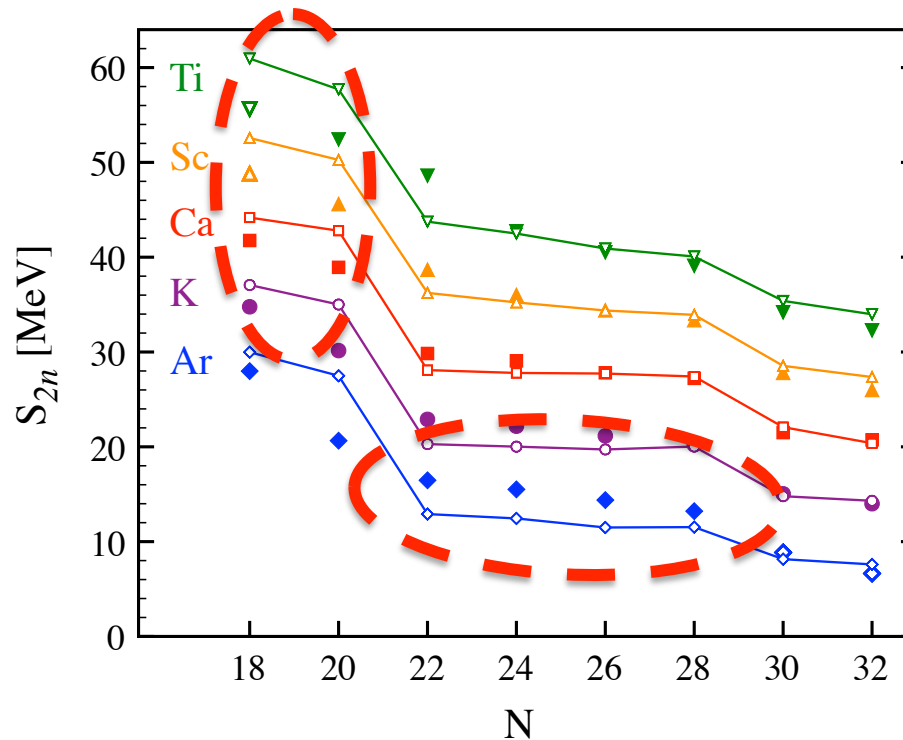
Over estimated  
N=20 and Z=20 gaps

→ First *ab-initio* calculation over a contiguous portion of the nuclear chart—open shells are now possible through the Gorkov-GF formalism

# Neighbouring Ar, K, Ca, Sc, and Ti chains

V. Somà, CB *et al.* Phys. Rev. C89, 061301R (2014)

Two-neutron separation energies predicted by chiral NN+3NF forces:



Lack of deformation due to quenched cross-shell quadrupole excitations

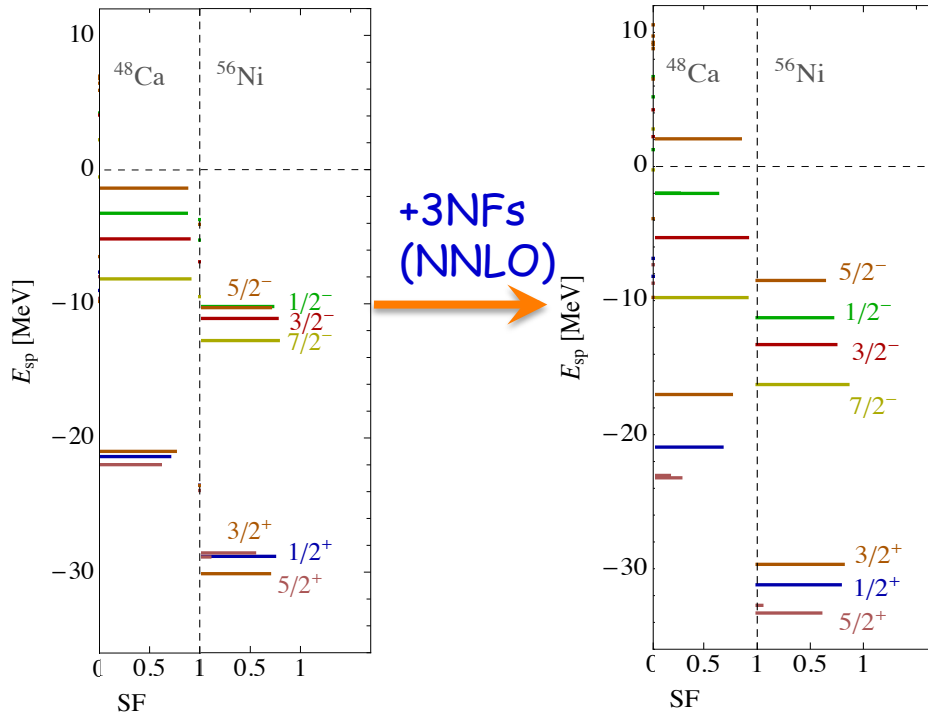
→ First *ab-initio* calculation over a contiguous portion of the nuclear chart—open shells are now possible through the Gorkov-GF formalism

# The *sd*-*pf* shell gap

Neutron spectral distributions for  $^{48}\text{Ca}$  and  $^{56}\text{Ni}$ :

2N + 3NF (induced)

2N + 3NF (FULL)



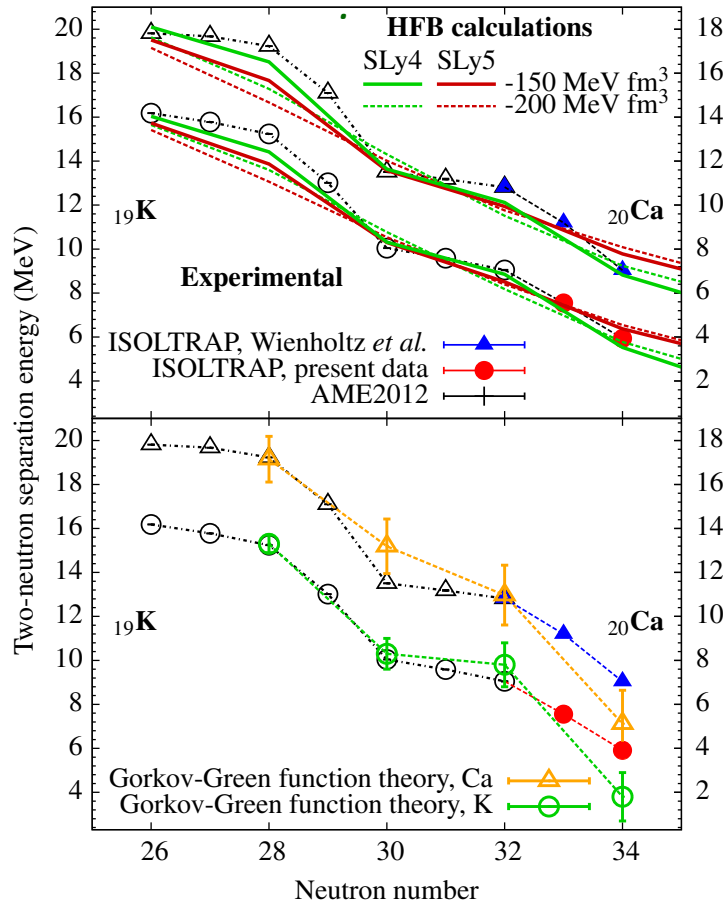
- *sd*-*pf* separation is *overestimated* even with leading order N<sup>2</sup>LO 3NF
- Correct increase of  $p_{3/2}$ - $f_{7/2}$  splitting (see Zuker 2003)

	2NF only	2+3NF(ind.)	2+3NF(full)	Experiment
$^{16}\text{O}$ :	2.10	2.41	2.38	$2.718 \pm 0.210$ [19]
$^{44}\text{Ca}$ :	2.48	2.93	2.94	$3.520 \pm 0.005$ [20]

CB *et al.*, arXiv:1211.3315 [nucl-th]

# Two-neutron separation energies for neutron rich K isotopes

M. Rosenbusch, et al., PRL114, 202501 (2015)



Measurements  
@ ISOLTRAP

Theory tend to overestimate the gap at N=34, but overall good

→ Error bar in predictions are from extrapolating the many-body expansion to convergence of the model space.

# Inversion of $d_{3/2}-s_{1/2}$ at $N=28$

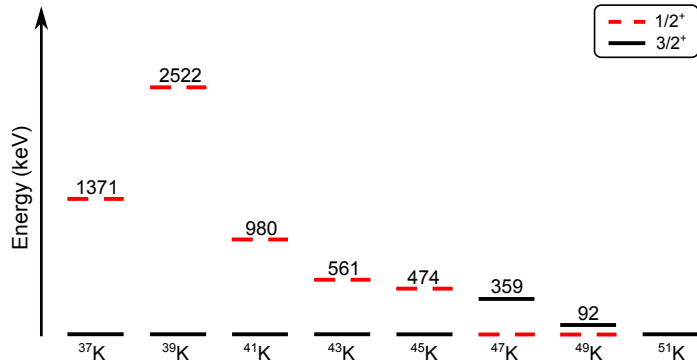


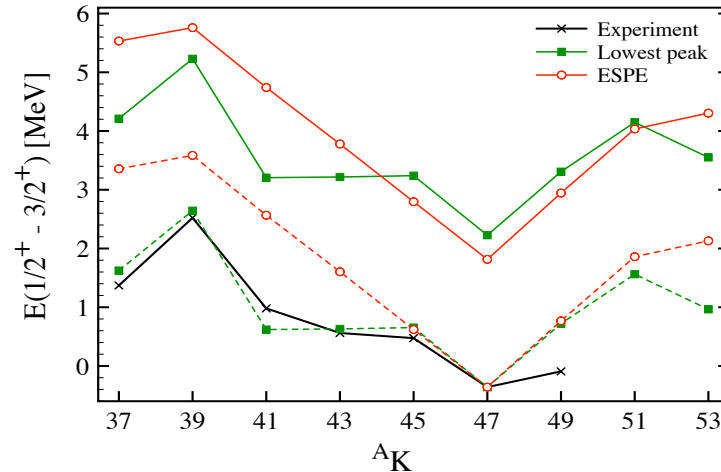
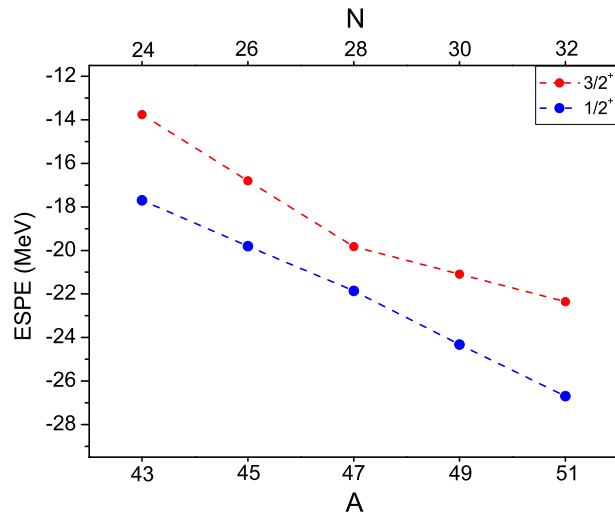
FIG. 1. (color online) Experimental energies for  $1/2^+$  and  $3/2^+$  states in odd-A K isotopes. Inversion of the nuclear spin is obtained in  $^{47,49}\text{K}$  and reinversion back in  $^{51}\text{K}$ . Results are

J. Papuga, et al., Phys. Rev. Lett. **110**, 172503 (2013);  
Phys. Rev. C **90**, 034321 (2014)

$A$ K isotopes

Laser spectroscopy @ ISOLDE

Change in separation described by chiral NN+3NF:



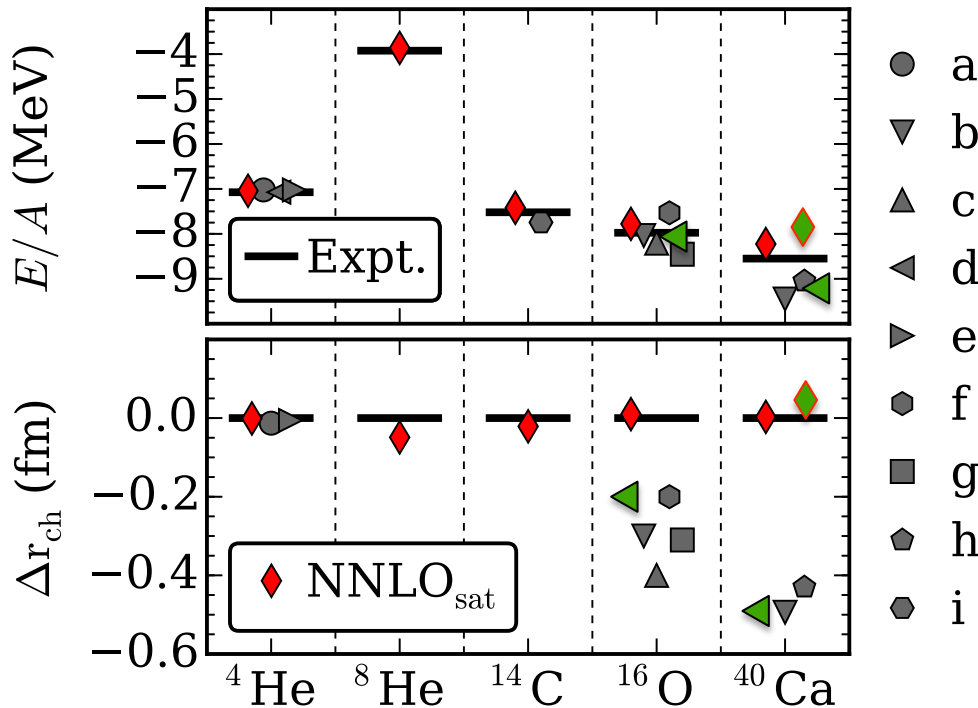
ESPE: "centroid" energies

(Gorkov calculations at 2<sup>nd</sup> order)



# NNLO-sat : a global fit up to $A \approx 24$

A. Ekström *et al.* Phys. Rev. C91, 051301(R) (2015)



- Constrain NN phase shifts

- Constrain radii and energies up to  $A \leq 24$

→ Provides saturation up to large masses!

◆ NNLOsat (V2 + W3) -- Grkv 2nd ord.

From SCGF:

◀

V2-N3LO(500) + W3-NNLO(400MeV/c) w/ SRG at  $2.0 \text{ fm}^{-1}$

A. Cipollone, CB, P. Navrátil, Phys. Rev. Lett. **111**, 062501 (2013)

V. Somà, CB *et al.* Phys. Rev. C**89**, 061301R (2014)

# BE and radii for Oxygens

- New fits of chiral interactions (NNLO<sub>sat</sub>) highly improve comparison to data

- Deficiencies remain for neutron rich isotopes

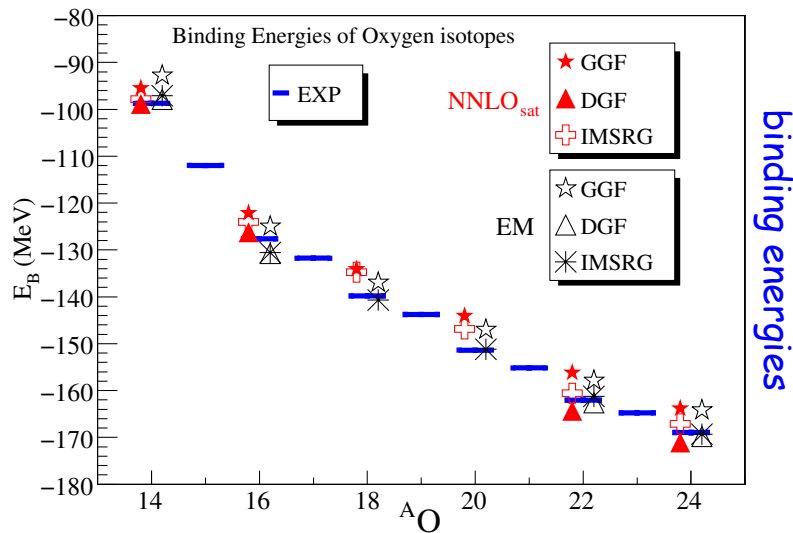
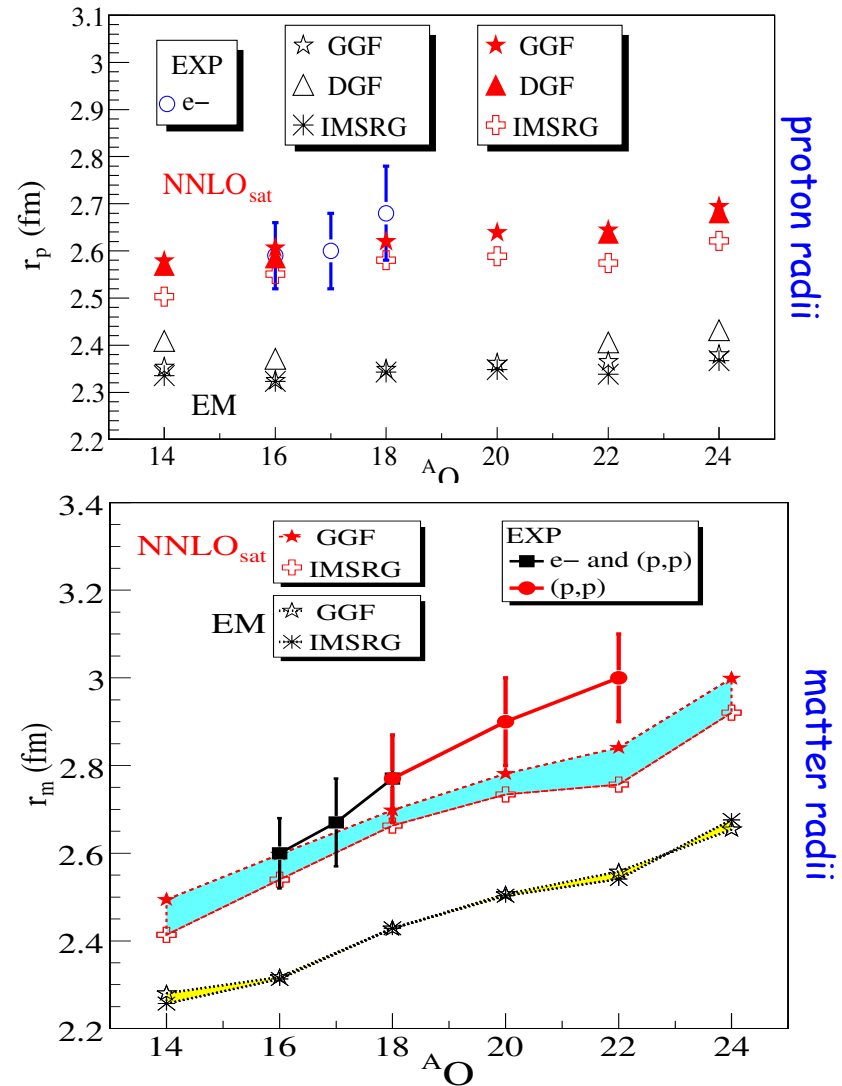


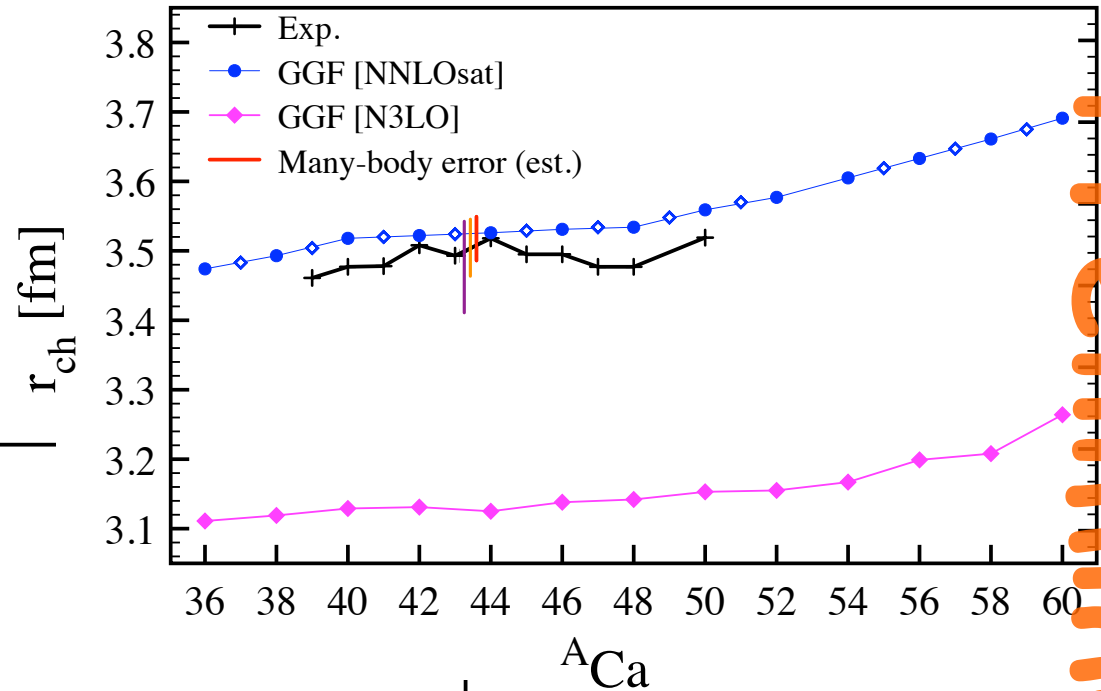
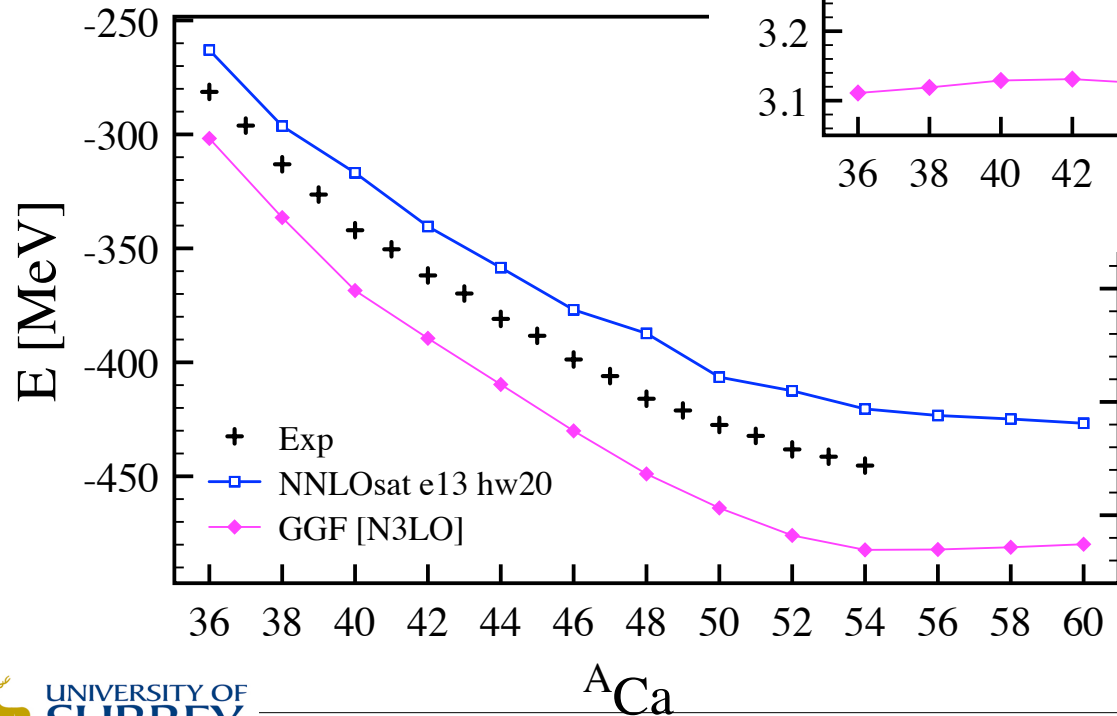
FIG. 1. Oxygen binding energies. Results from SCGF and IMSRG calculations performed with EM [20–22] and NNLO<sub>sat</sub> [26] interactions are displayed along with available experimental data.



# BE and charge radii in ${}^A\text{Ca}$

2<sup>nd</sup> order GGF 'correct'  
to give a slight under  
binding and larger radii

Radii of even-odd are  
possible

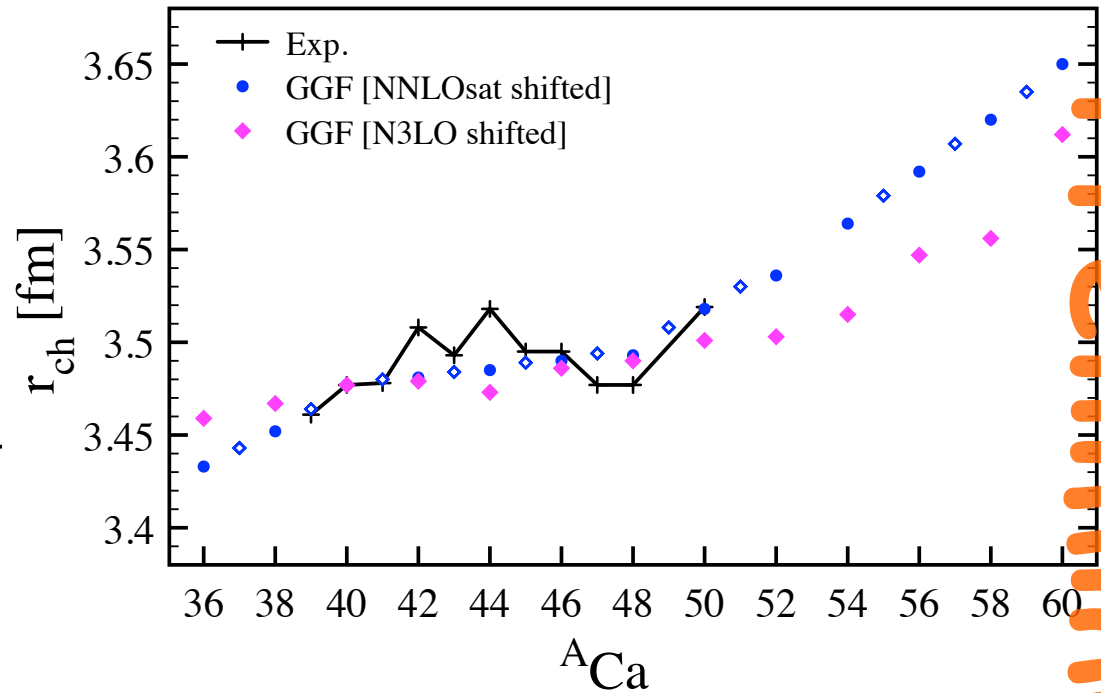
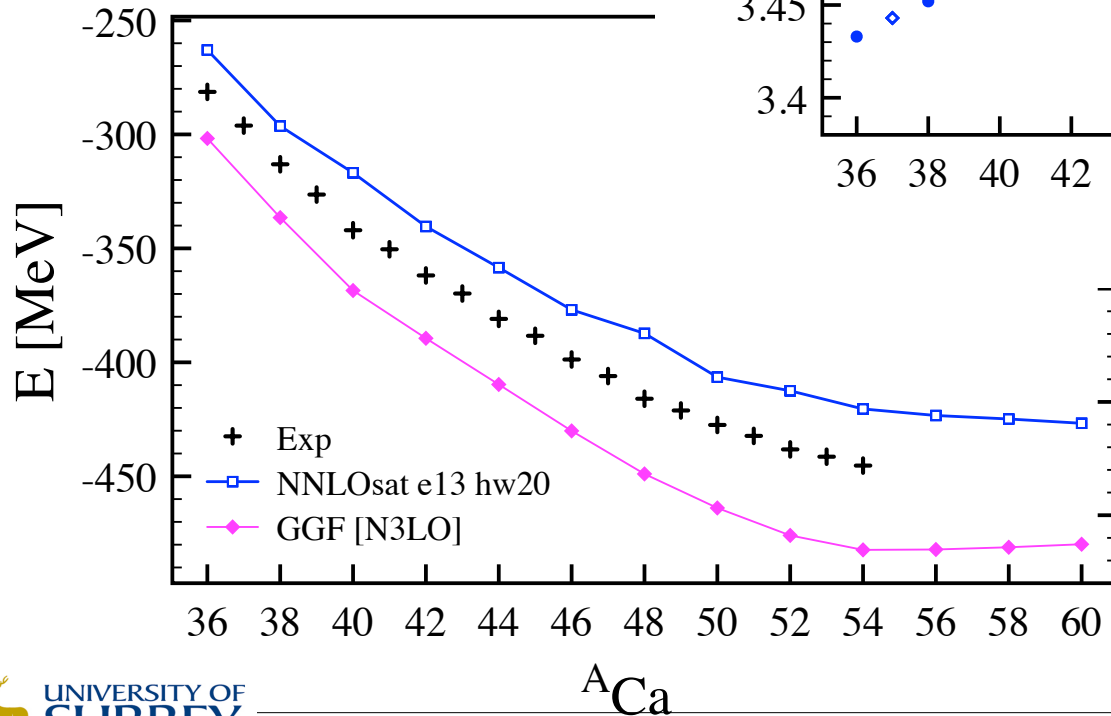


Preliminary

# BE and charge radii in ${}^A\text{Ca}$

2<sup>nd</sup> order GGF 'correct'  
to give a slight under  
binding and larger radii

Radii of even-odd are  
possible



NNLO sat improves  
trend of radii

radii of  ${}^{42-46}\text{Ca}$   
require shell model...

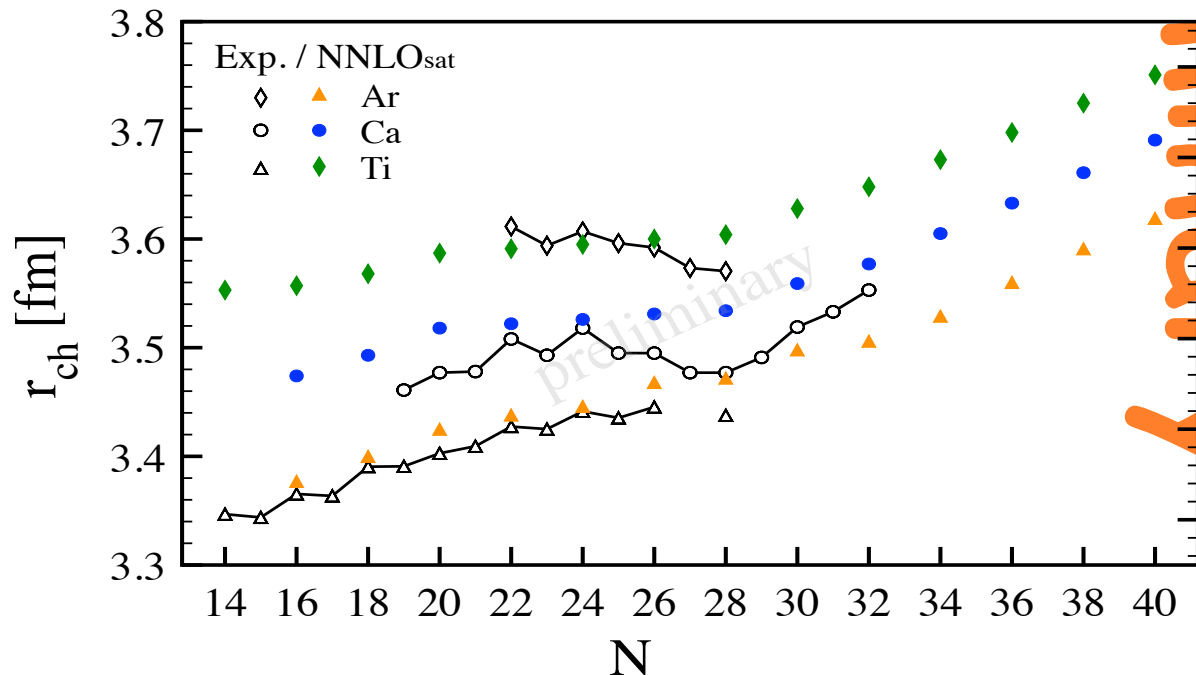
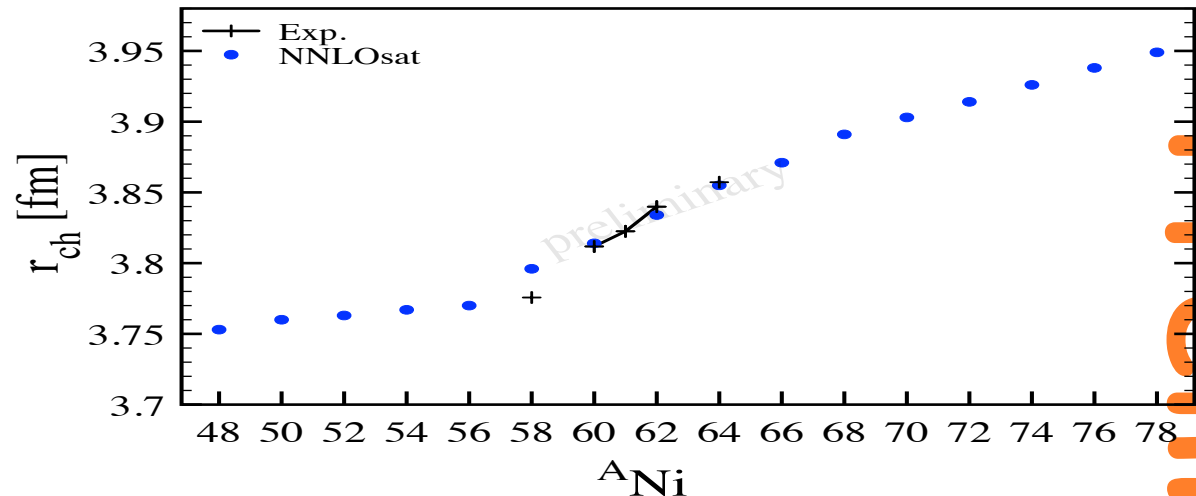
Preliminary

# charge radii in the pf shell

Size of radii not perfect but remains overall correct throughout the *pf* shell with NNLO-sat.

This suggests that saturation is indeed under control.

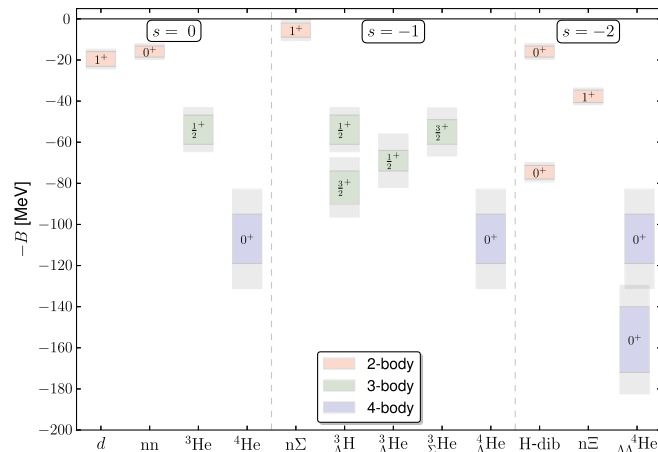
→ Improvements of many-body truncations beyond 2<sup>nd</sup> order Gorkov will also be relevant. (work in progress!)



Preliminary

# Study of nuclear interactions from Lattice QCD

Other paths in LQCD, see:



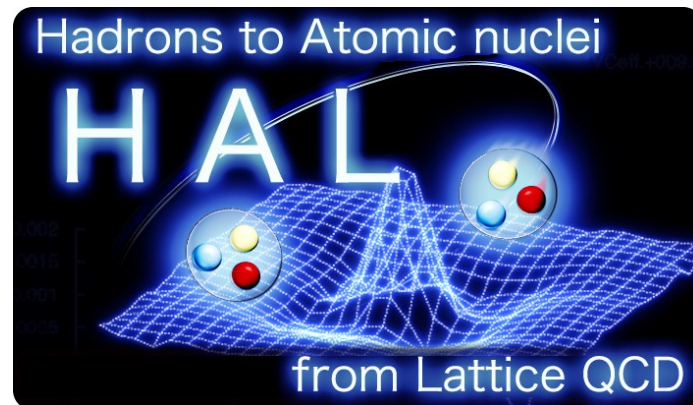
nuclei, the deuteron and the dineutron in  $2+1+1$  flavor QCD with  $m_\pi = 0.51$  GeV and  $m_N = 1.32$  GeV. The bound states are distinguished from the attractive scattering states by investigating the spatial volume dependence of the energy shift  $\Delta E_L$ . In the infinite spatial volume limit we obtain

$$-\Delta E_\infty = \begin{cases} 43(12)(8) & \text{MeV for } {}^4\text{He}, \\ 20.3(4.0)(2.0) & \text{MeV for } {}^3\text{He}, \\ 11.5(1.1)(0.6) & \text{MeV for } {}^3S_1, \\ 7.4(1.3)(0.6) & \text{MeV for } {}^1S_0. \end{cases} \quad (17)$$

PACS-CS PRD **86**, 074514 (2012)

# Study of nuclear interactions from Lattice QCD

*In collaboration with:*





## **Why should we investigate LQCD interactions?**

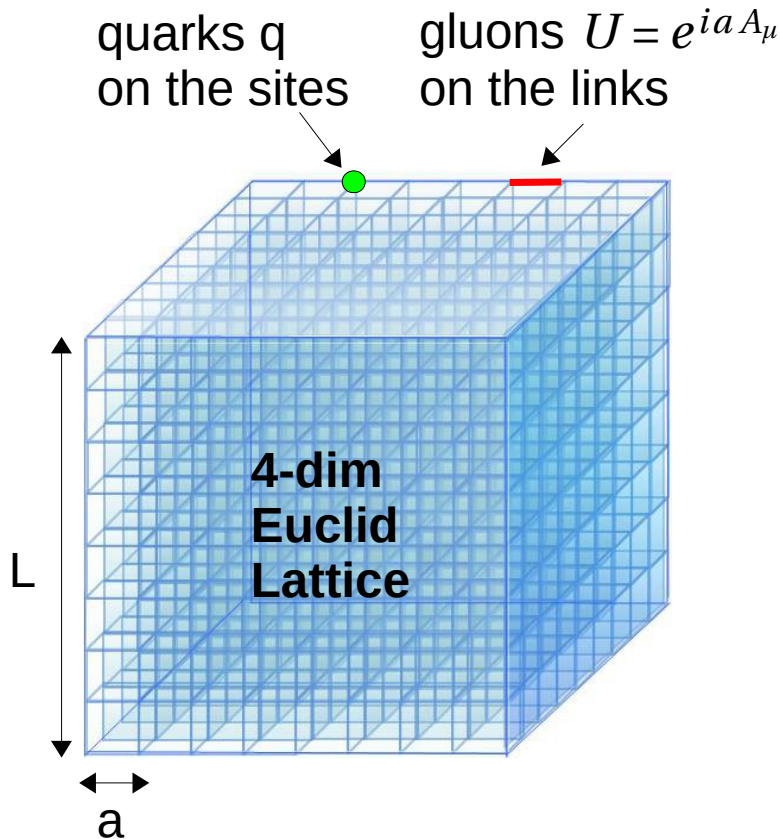
- It gives *complimentary insight to the EFT approach*:
  - *Allows to approach physical interaction from heavy quark masses (opposite direction than the chiral limit).*
  - *Can study implications of SU(3) limit.*
- *No need to fit to experiment. No LEC constants.*
- *Provides consistent interactions in the Hyperon sector.*
  
- *It is very fundamental approach (QCD), and an alternative to Chiral-EFT.*

## **Challenges and limitations:**

- *Mostly LO terms of the NN force exploited so far (but being improved).*
- *Physical pion mass limit requires efforts (but underway).*
- *NNN only barely addressed.*
- *Strong short-range repulsion is a challenge to ab-initio approaches.*

# Lattice QCD

$$L = -\frac{1}{4} G_{\mu\nu}^a G_a^{\mu\nu} + \bar{q} \gamma^\mu (i \partial_\mu - g t^a A_\mu^a) q - m \bar{q} q$$



Vacuum expectation value

$$\begin{aligned} & \langle O(\bar{q}, q, U) \rangle \\ &= \int dU d\bar{q} dq e^{-S(\bar{q}, q, U)} O(\bar{q}, q, U) \\ &= \int dU \det D(U) e^{-S_U(U)} O(D^{-1}(U)) \\ &= \lim_{N \rightarrow \infty} \frac{1}{N} \sum_{i=1}^N O(D^{-1}(U_i)) \end{aligned}$$

path integral

quark propagator

{ U<sub>i</sub> } : ensemble of gauge conf. U  
generated w/ probability  $\det D(U) e^{-S_U(U)}$

- ★ Well defined (regularized)
- ★ Manifest gauge invariance
- ★ Fully non-perturbative
- ★ Highly predictive

# The HAL-QCD Method

Define a general potential  $U(\mathbf{r}, \mathbf{r}')$  which is **non-local** but **energy independent** up to inelastic threshold, such that:

$$-\frac{\nabla^2}{2\mu} \varphi_{\vec{k}}(\vec{r}) + \int d\vec{r}' U(\vec{r}, \vec{r}') \varphi_{\vec{k}}(\vec{r}') = E_{\vec{k}} \varphi_{\vec{k}}(\vec{r})$$

for the **Nambu-Bethe-Salpeter (NBS)** wave function,

$$\varphi_{\vec{k}}(\vec{r}) = \sum \langle 0 | B_i(\vec{x} + \vec{r}, t) B_j(\vec{x}, t) | B = 2, \vec{k} \rangle$$

Operationally, measure the **4-pt function** on the QCD Lattice

$$\psi(\vec{r}, t) = \sum_{\vec{x}} \langle 0 | B_i(\vec{x} + \vec{r}, t) B_j(\vec{x}, t) J(t_0) | 0 \rangle = \sum_{\vec{k}} A_{\vec{k}} \varphi_{\vec{k}}(\vec{r}) e^{-W_{\vec{k}}(t-t_0)} + \dots$$

and extract  $U(\mathbf{r}, \mathbf{r}')$  from:

$$\left\{ 2M_B - \frac{\nabla^2}{2\mu} \right\} \psi(\vec{r}, t) + \int d\vec{r}' U(\vec{r}, \vec{r}') \psi(\vec{r}', t) = -\frac{\partial}{\partial t} \psi(\vec{r}, t)$$

A **local potential**  $V(\mathbf{r})$  is then obtained through a derivative expansion of  $U(\mathbf{r}, \mathbf{r}')$ , which **must give the same observables** of the LQCD simulation:

$$U(\vec{r}, \vec{r}') = \delta(\vec{r} - \vec{r}') V(\vec{r}, \nabla) = \delta(\vec{r} - \vec{r}') \{ V(\vec{r}) + \mathcal{O}(\nabla) + \mathcal{O}(\nabla^2) + \dots \}$$

$$\rightarrow V(\vec{r}) = \frac{1}{2\mu} \frac{\nabla^2 \psi(\vec{r}, t)}{\psi(\vec{r}, t)} - \frac{\frac{\partial}{\partial t} \psi(\vec{r}, t)}{\psi(\vec{r}, t)} - 2M_B$$

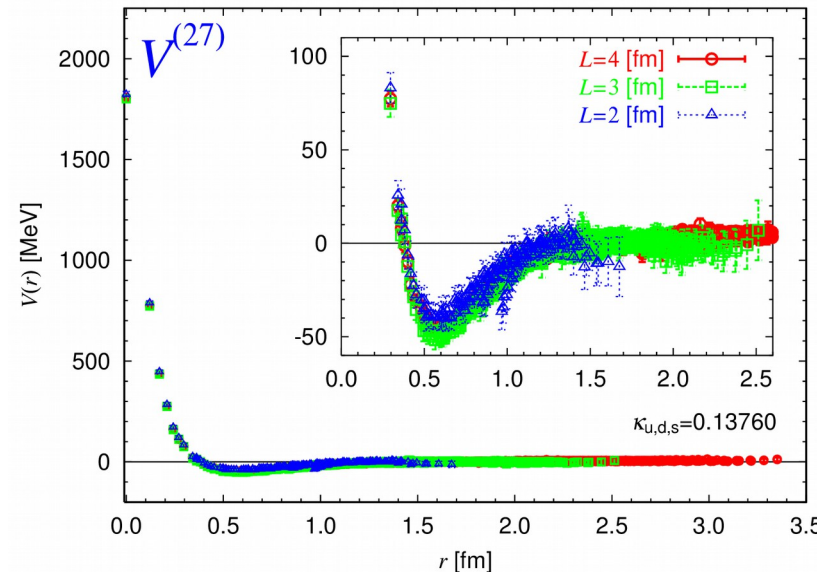
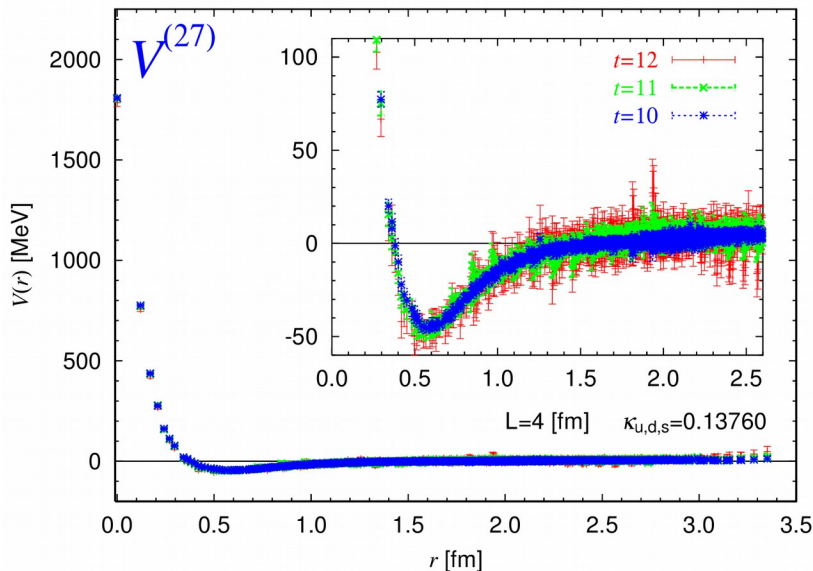
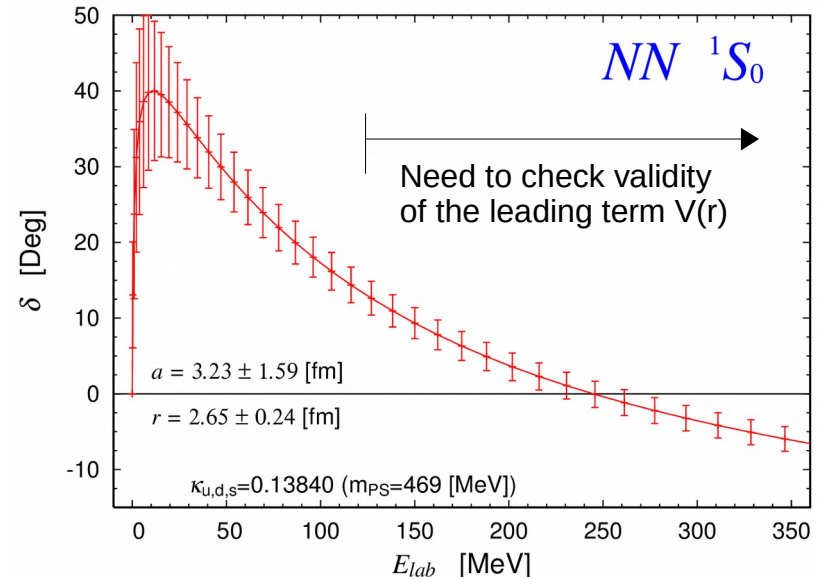
Tensor/Yukawa  
force in S-D

Spin-orbit  
force, P waves

# The HAL-QCD Method

## Advantages:

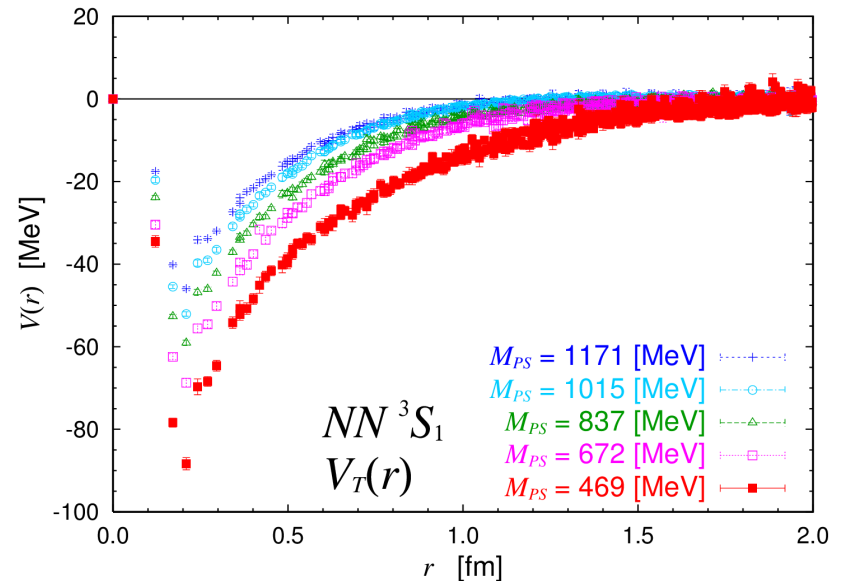
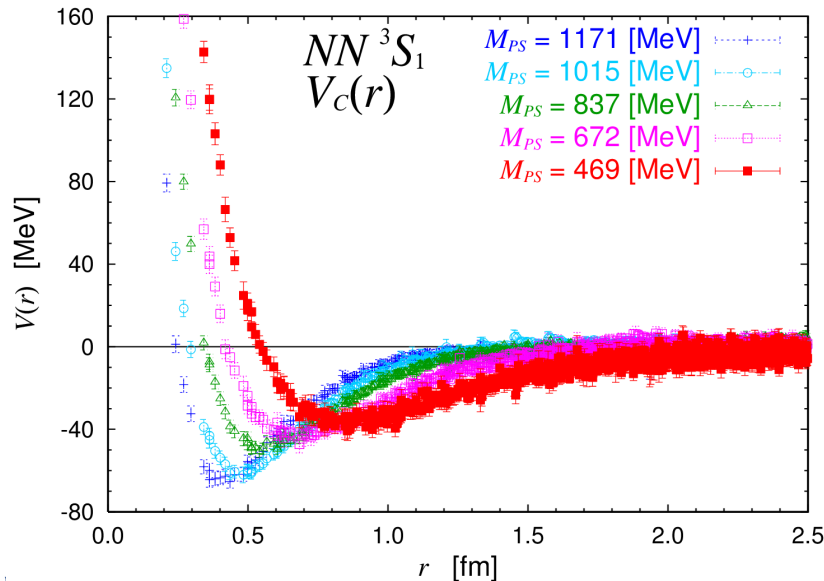
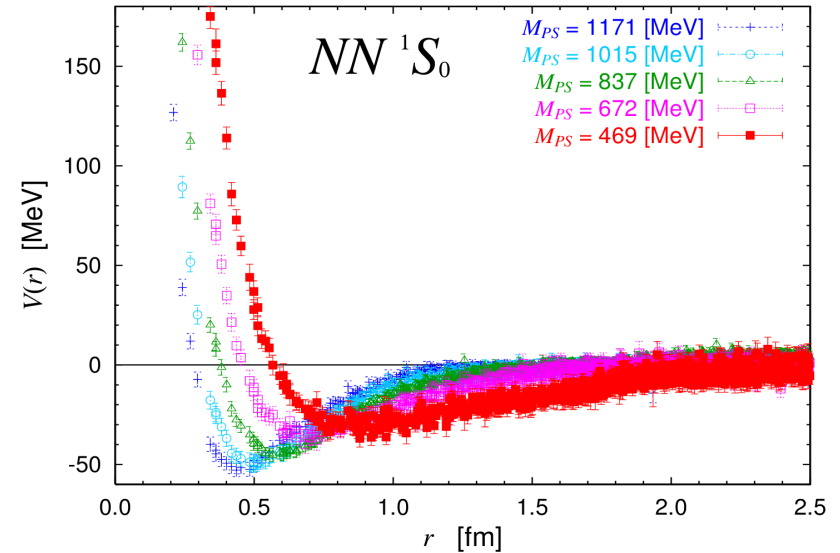
- ✓ No need to separate E eigenstate. Just need to measure  $\psi(\vec{r}, t)$
- ✓ Then, potential can be extracted.
- ✓ Demand a minimal lattice volume. No need to extrapolate to  $V=\infty$ .
- ✓ Can output more observables.
- ✓ One can address *large nuclei* too!!



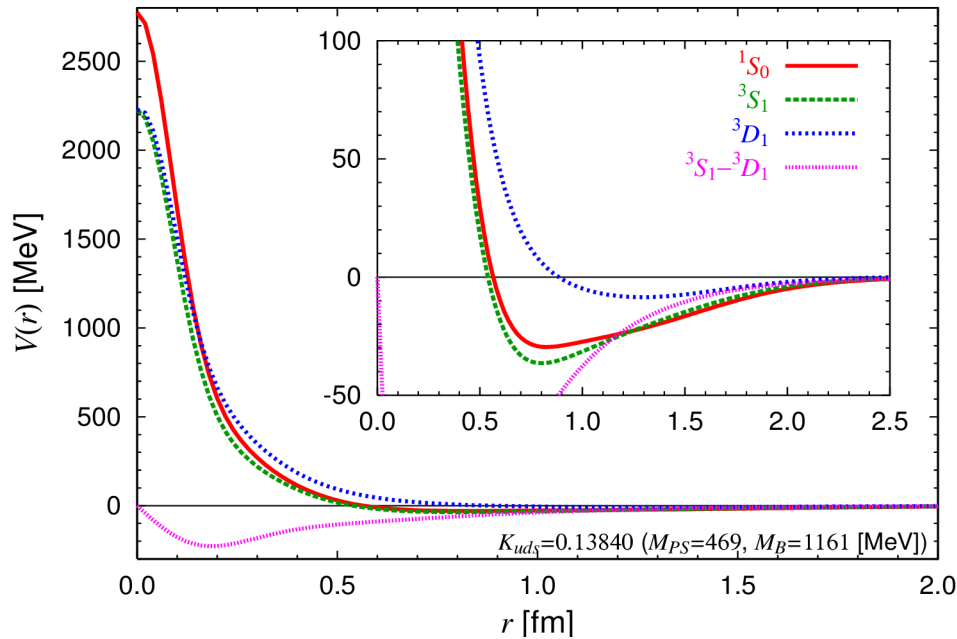
# Two-Nucleon HAL potentials

Quark mass dependence of  $V(r)$  for NN partial wave ( $^1S_0$ ,  $^3S_1$ ,  $^3S_1$ - $^3D_1$ )

→ Potentials become stronger  $m_{\text{q}}$  as decreases.



# Two-Nucleon HAL potentials

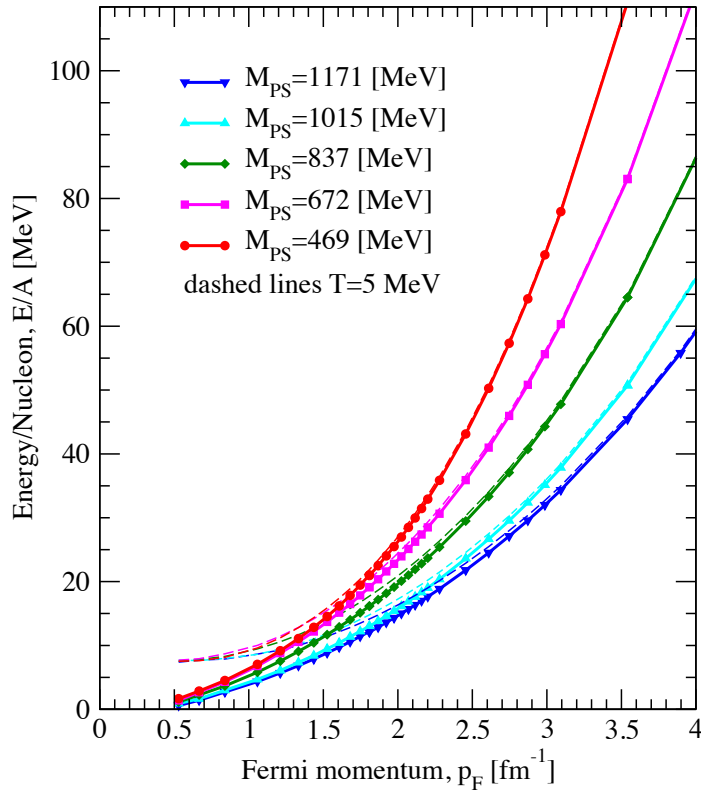


## Potential in partial waves at the lightest $m_\pi = 469$ MeV:

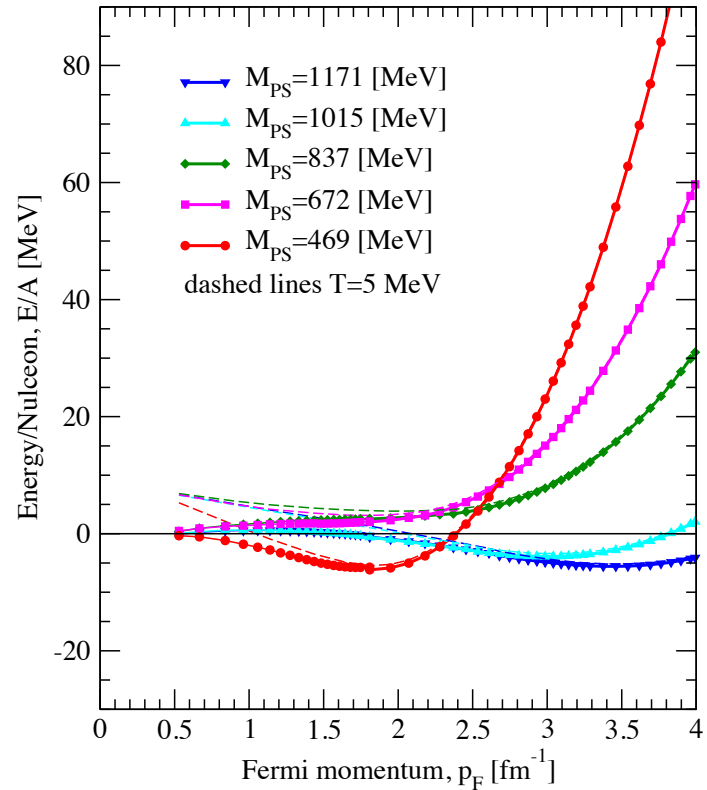
- ✓ Repulsive core, attractive pocket, and strong tensor components
- ✓ Similar to phenomenological potentials (e.g. AV18).
- ✓ Central value obtained from least  $\chi^2$  fit to data.
- ✓ Higher orders in the velocity expansion will also be available soon...

# Infinite matter

## Pure Neutron Matter



## Symmetric Nuclear Matter



*PNM unbound as usual, but less stiff*

*SNM saturates at  $m_{\pi}=469$  MeV but under bound and at higher densities that physical.*

T. Inoue *et al.*, Phys. Rev. Lett. **111** 112503 (2013).

*Finite-T results by A. Carbone, priv. comm.*



# Application of microscopic (Ab- Initio) SCGF to potentials with hard cores.

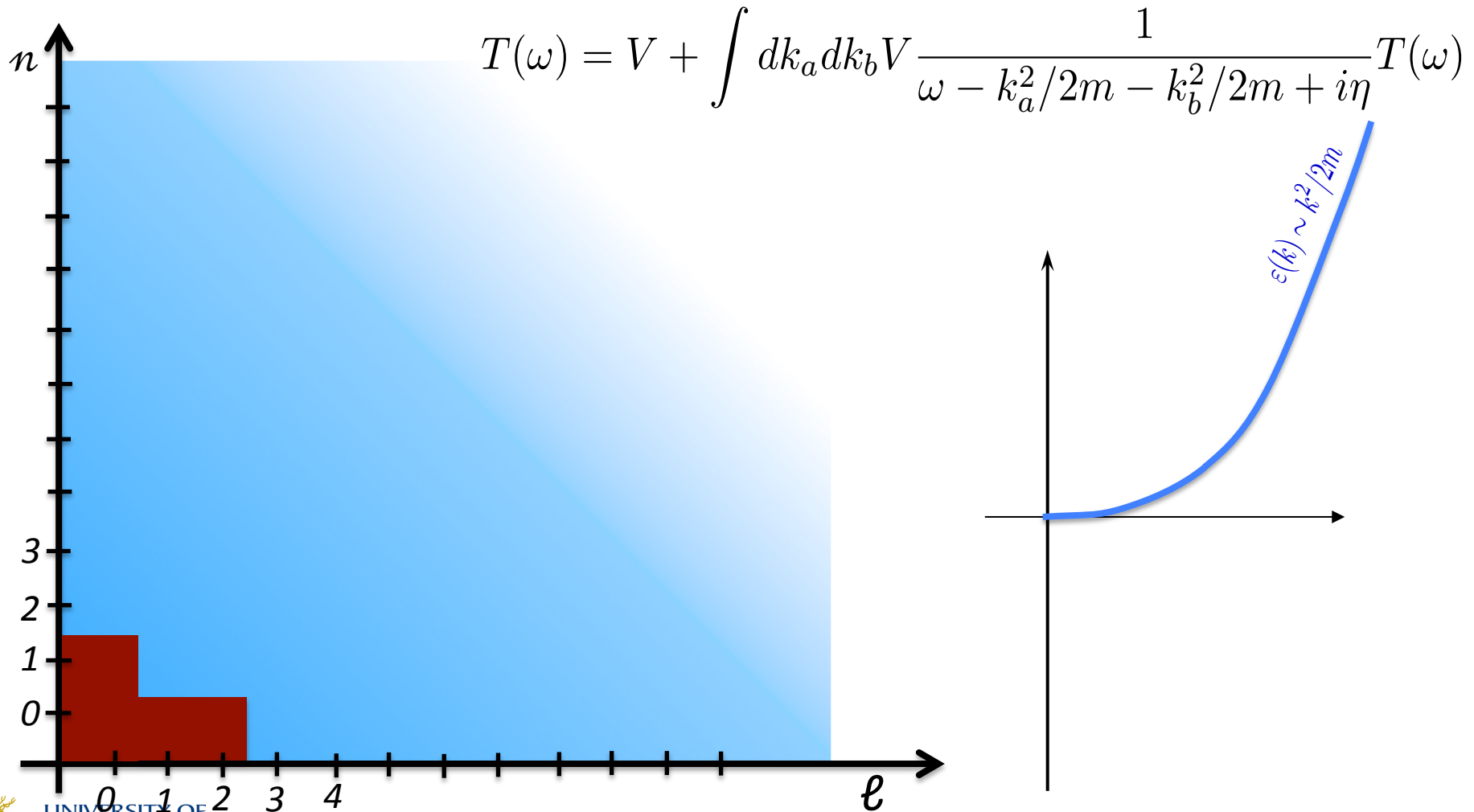
*How do we do it??*



*With a G-matrix!*

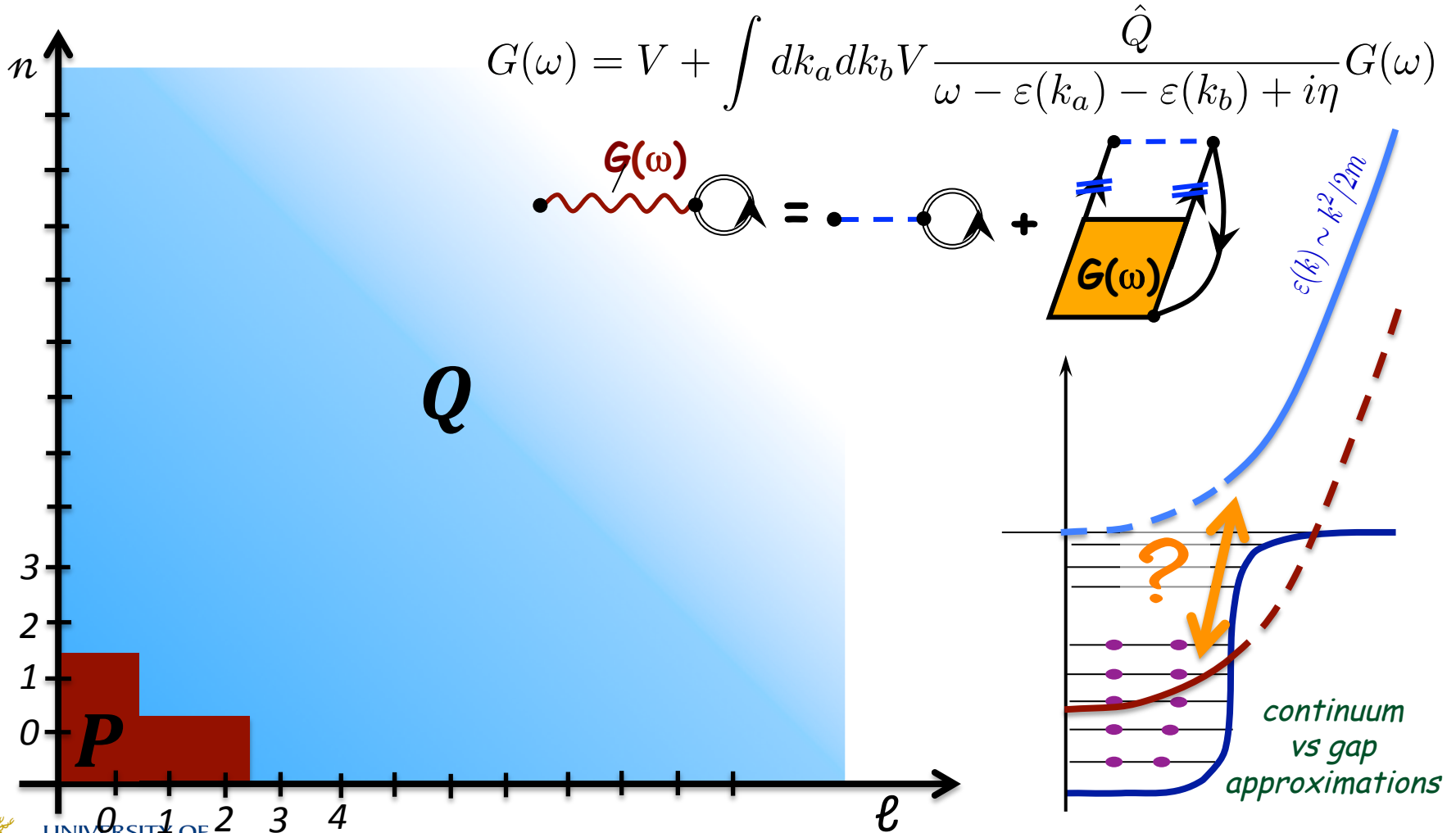
# Analysis of Brueckner HF

Scattering of two nucleon in free space:



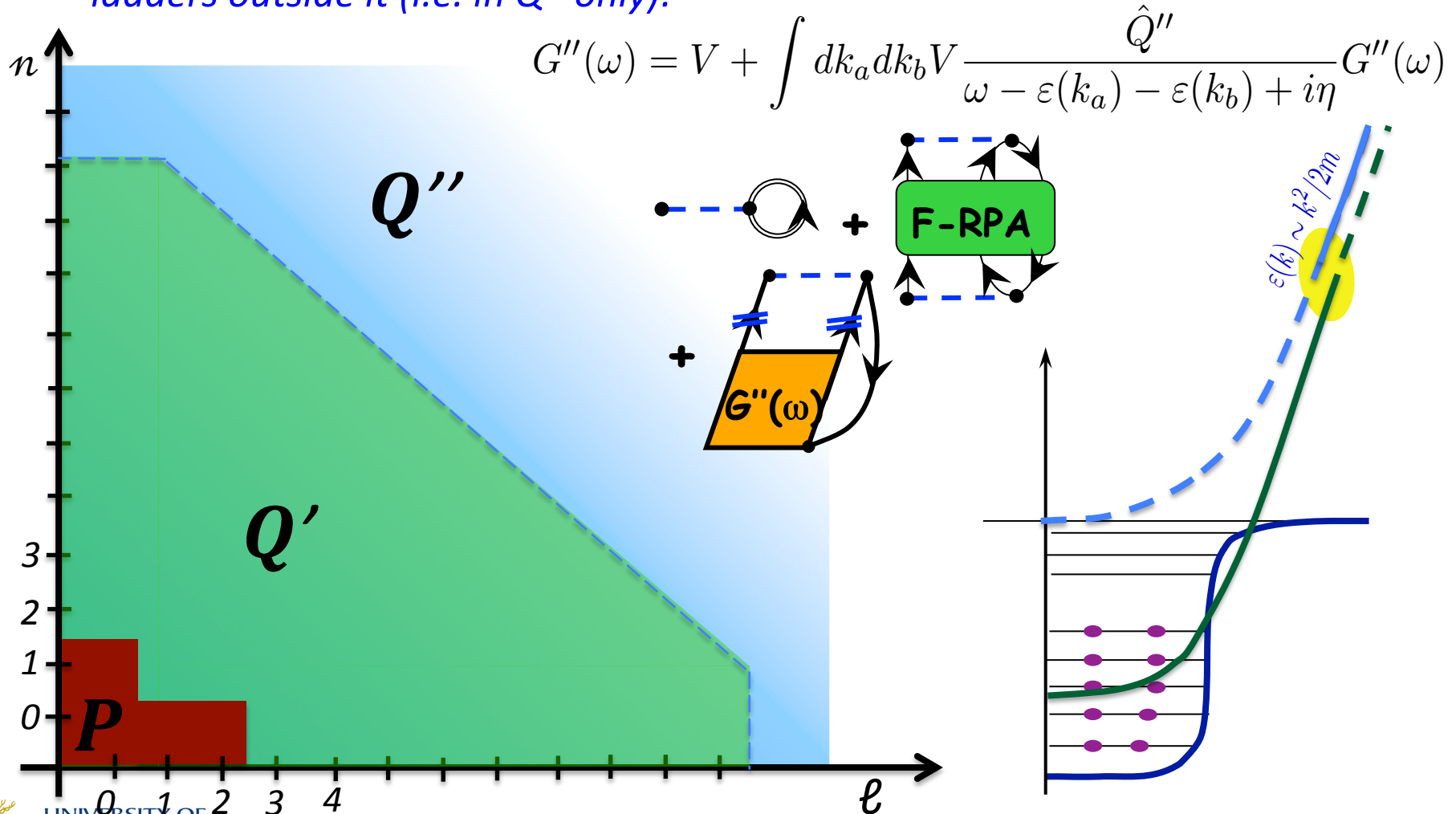
# Analysis of Brueckner HF

Scattering of two nucleons outside the Fermi sea ( $\rightarrow$ BHF):



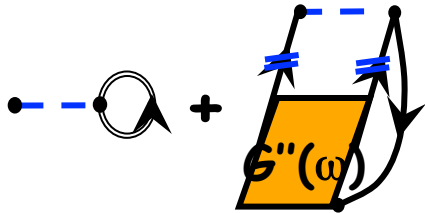
# Mixed SCGF-Brueckner approach

Solve full many-body dynamics in model space ( $P+Q'$ ) and the Goldstone's ladders outside it (i.e. in  $Q''$  only):

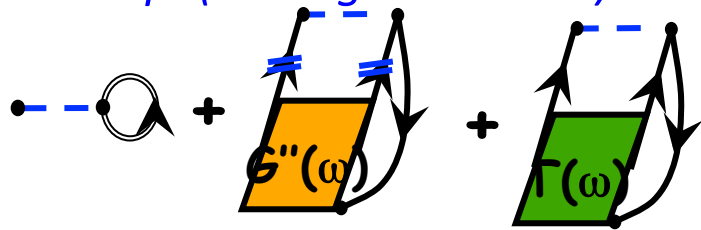


# Different levels of approximation:

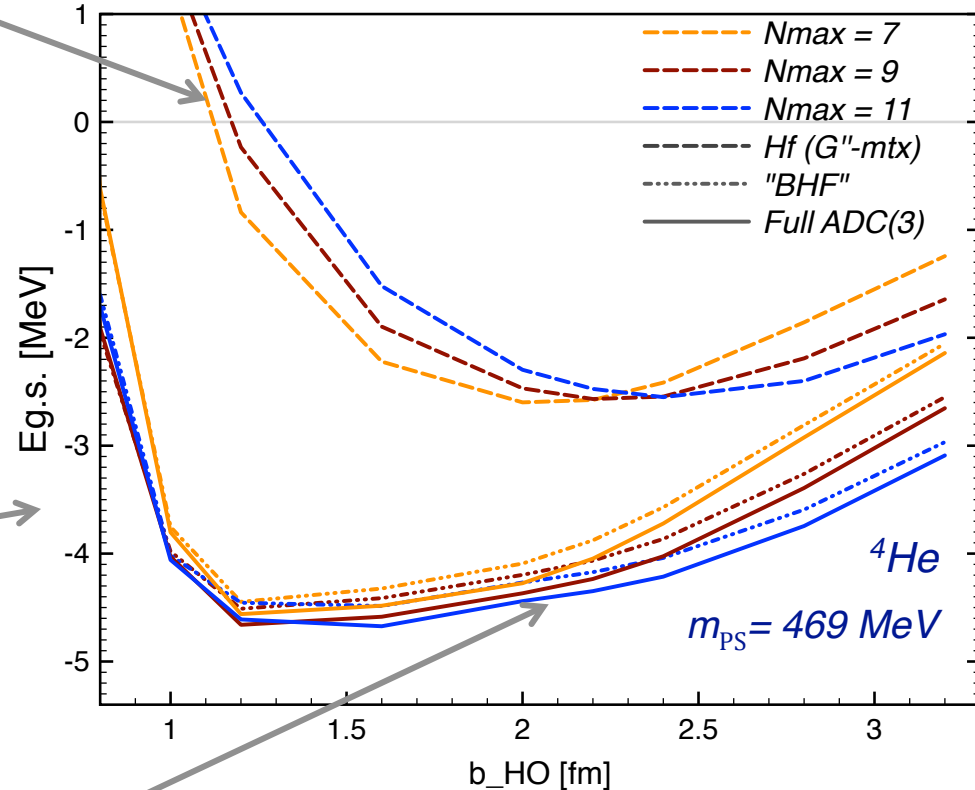
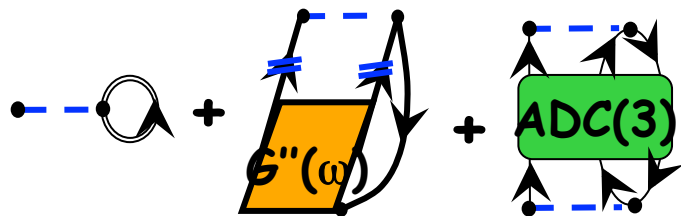
Goldstone's ladders outside the model space (i.e. in  $Q''$  only):



All ladders inside and outside the mod. sp. (analogous to BHF):

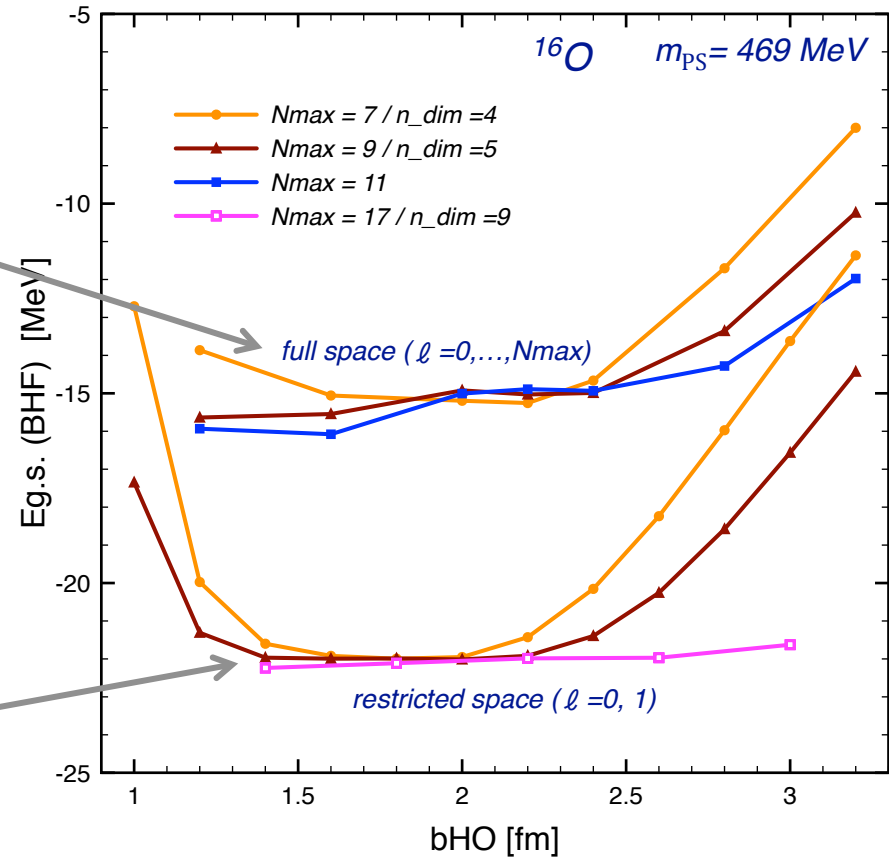
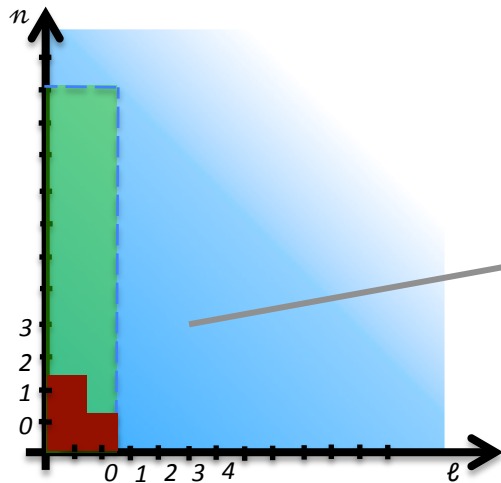
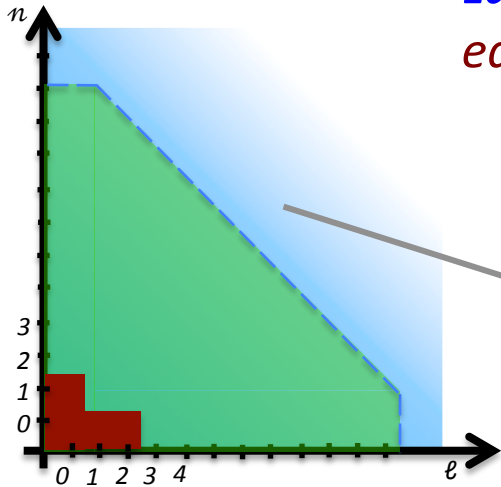


Full many-body dynamics [at ADC(3)]



# Sensitivity of BHF of the $\varepsilon(k)$ spectrum

Ladders calculated inside and outside the model are **NOT** equivalent because of the different  $\varepsilon(k)$  spectrum:



$$G''(\omega) = V + \int dk_a dk_b V \frac{\hat{Q}''}{\omega - \varepsilon(k_a) - \varepsilon(k_b) + i\eta} G''(\omega)$$

# Treating short-range corr. with a G-matrix

- The short-range core can be treated by summing ladders outside the model space:

$$\Sigma_{\alpha\beta}^{MF}(\omega) = i \sum_{\gamma\delta} \int \frac{d\omega'}{2\pi} G_{\alpha\gamma, \delta\beta}(\omega + \omega') g_{\delta\gamma}(\omega') = \text{Diagram}$$

The diagram shows a red wavy line labeled  $G(\omega)$  connecting two black dots. The right dot is part of a circular loop with an arrow, representing a self-energy correction.

$$\Sigma^*(\mathbf{r}, \mathbf{r}'; \omega) = \Sigma^{MF}(\mathbf{r}, \mathbf{r}'; \omega) + \tilde{\Sigma}(\mathbf{r}, \mathbf{r}'; \omega).$$

$$Z_\alpha = \int d\mathbf{r} |\psi_\alpha^{A\pm 1}(\mathbf{r})|^2 = \frac{1}{1 - \frac{\partial \Sigma_{\hat{a}\hat{a}}^*(\omega)}{\partial \omega}} \Bigg|_{\omega = \pm(E_\alpha^{A\pm 1} - E_0^A)}$$

An orange arrow points from the derivative term in the denominator to the text below.

Two contributions to the derivative:

- $\Sigma_{\alpha\beta}^{MF}(\omega)$  is due to scattering to (high-k) states in the Q space
- $\Sigma(\mathbf{r}, \mathbf{r}'; \omega)$  accounts for low-energy (long range) correlations



# (Galitskii-Migdal-Boffi-) Koltun sumrule

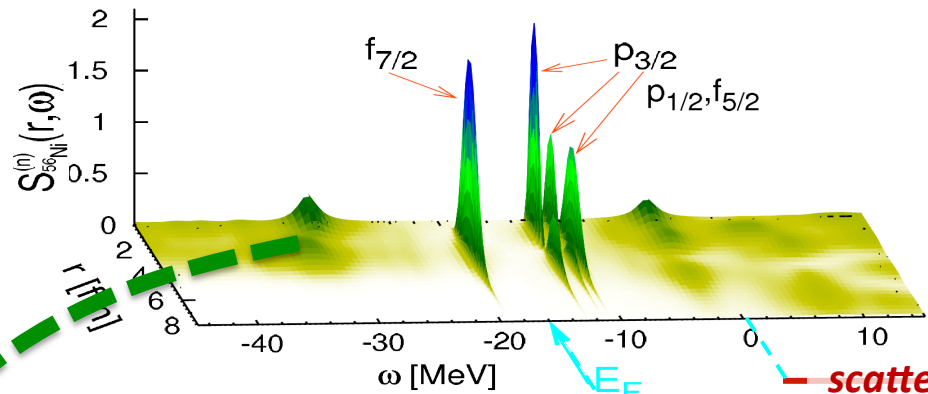
✱ Koltun sum rule (with NNN interactions):

$$\sum_{\alpha} \frac{1}{\pi} \int_{-\infty}^{\epsilon_F^-} d\omega \omega \text{Im} G_{\alpha\alpha}(\omega) = \langle \Psi_0^N | \hat{T} | \Psi_0^N \rangle + 2 \langle \Psi_0^N | \hat{V} | \Psi_0^N \rangle + 3 \langle \Psi_0^N | \hat{W} | \Psi_0^N \rangle$$

two-body

three-body

$$E_0^N = \frac{1}{2\pi} \int_{-\infty}^{\epsilon_F^-} d\omega \sum_{\alpha\beta} (T_{\alpha\beta} + \omega \delta_{\alpha\beta}) \text{Im} G_{\beta\alpha}(\omega) - \frac{1}{2} \langle \Psi_0^N | \hat{W} | \Psi_0^N \rangle$$



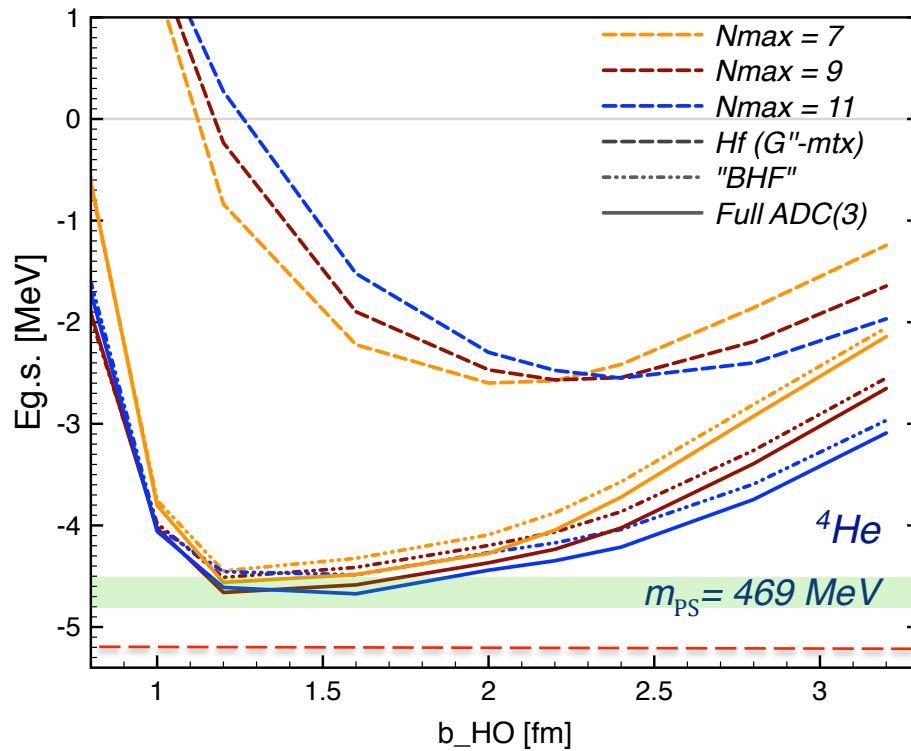
High-k and missing energy tail from SRC... (currently neglected in calculating Koltun SR)

← neutro n removal →

← scattering →

← neutro n addition →

# Benchmark on ${}^4\text{He}$



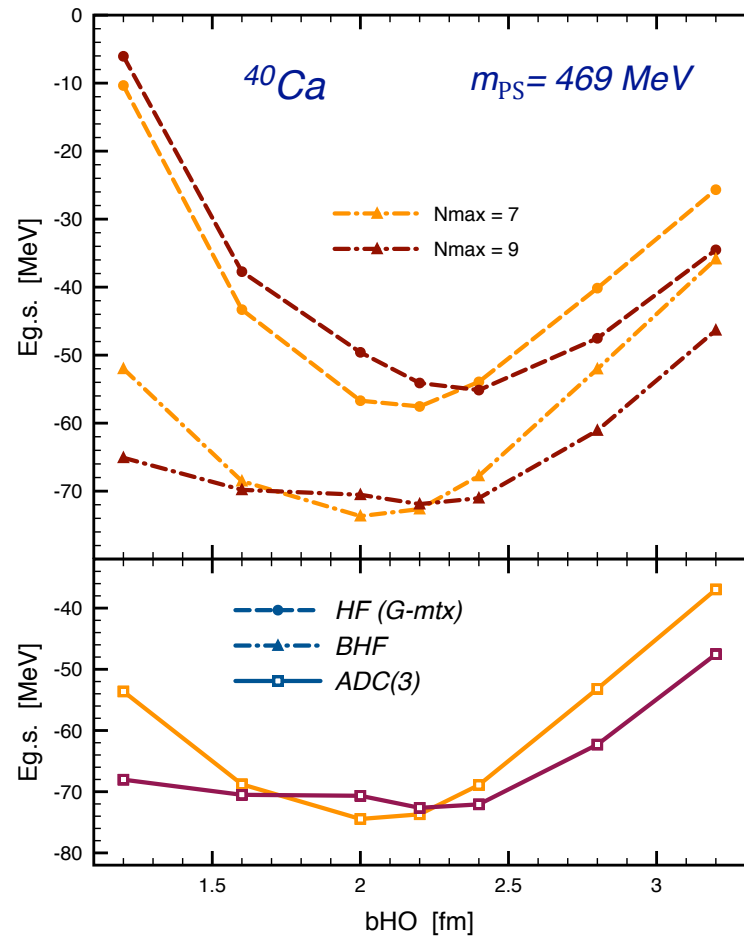
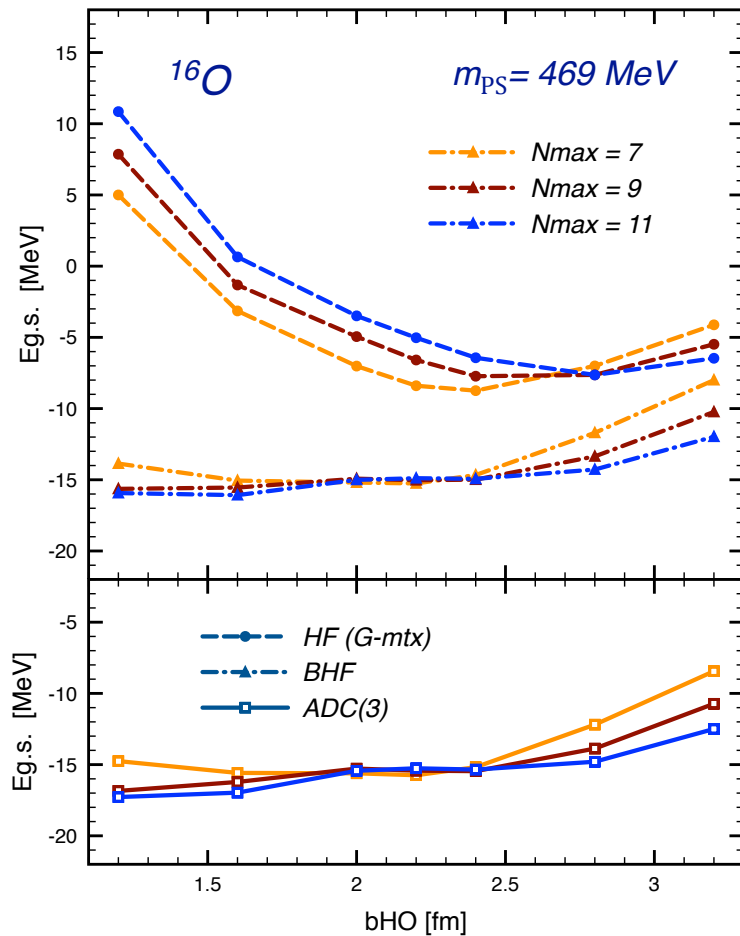
Can benchmark the  $G_{\text{mtx}} + \text{ADC}(3)$  method on light  ${}^4\text{He}$ , where exact solutions are possible:

	$G(\omega) + \text{ADC}(3)$	Exact
HALQCD @ $m_{\pi} = 469 \text{ MeV}$	4.7(2) MeV	5.09 MeV <sup>1</sup>

→ Can expect accuracy on binding energies at about 10%

<sup>1</sup>H. Nemura *et al.*, Int. J. Mod. Phys. E **23**, 1461006 (2014)

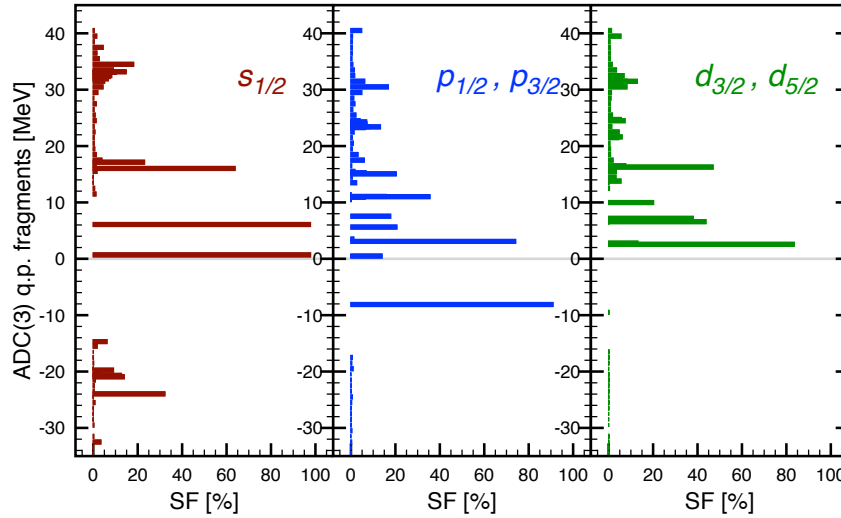
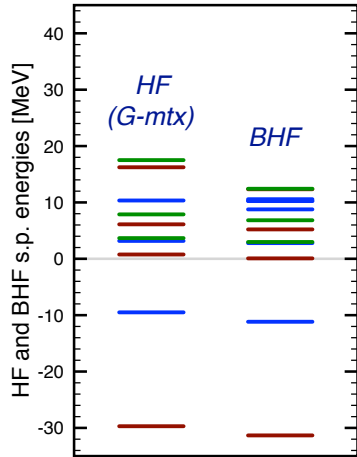
# Binding of $^{16}\text{O}$ and $^{40}\text{Ca}$ :



Binding energies are  $\sim 15 \text{ MeV}$   $^{16}\text{O}$  and  $70\text{-}75 \text{ MeV}$  for  $^{40}\text{Ca}$ . Possibly being underestimated by 10%

→  $^{16}\text{O}$  at  $m_{\pi} = 469 \text{ MeV}$  is unstable toward 4- $\alpha$  breakup!

# Spectral strength in $^{16}\text{O}$ and $^{40}\text{Ca}$ :



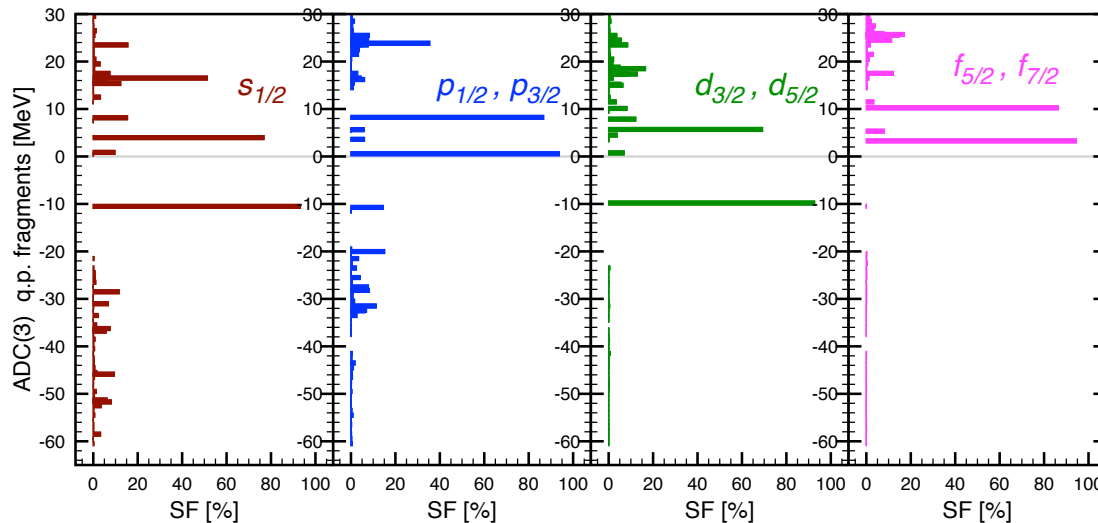
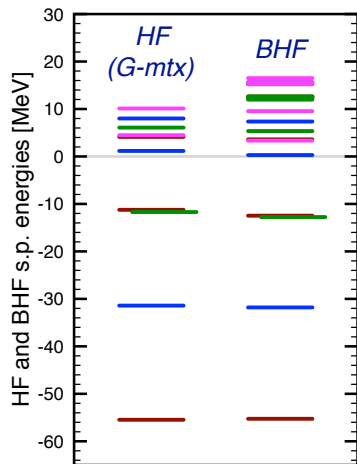
Particle-hole gaps

$^{16}\text{O}$

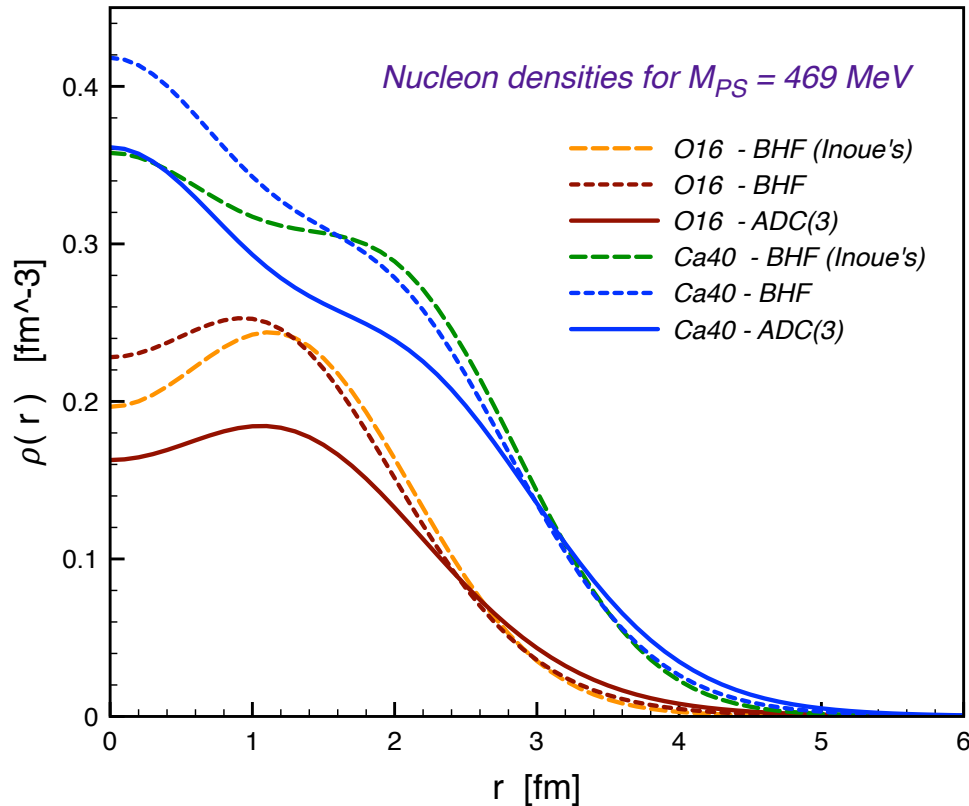
$m_{\pi} = 469$  MeV:  $\sim 8$  MeV  
 Expt (phys  $m_{\pi}$ ): 11.5 MeV

$^{40}\text{Ca}$

$m_{\pi} = 469$  MeV:  $\sim 10$  MeV  
 Expt (phys  $m_{\pi}$ ): 7.5 MeV



# Matter distribution of $^{16}\text{O}$ and $^{40}\text{Ca}$ :



Calculated matter radii at  $m_{\pi} = 469 \text{ MeV}$  are:

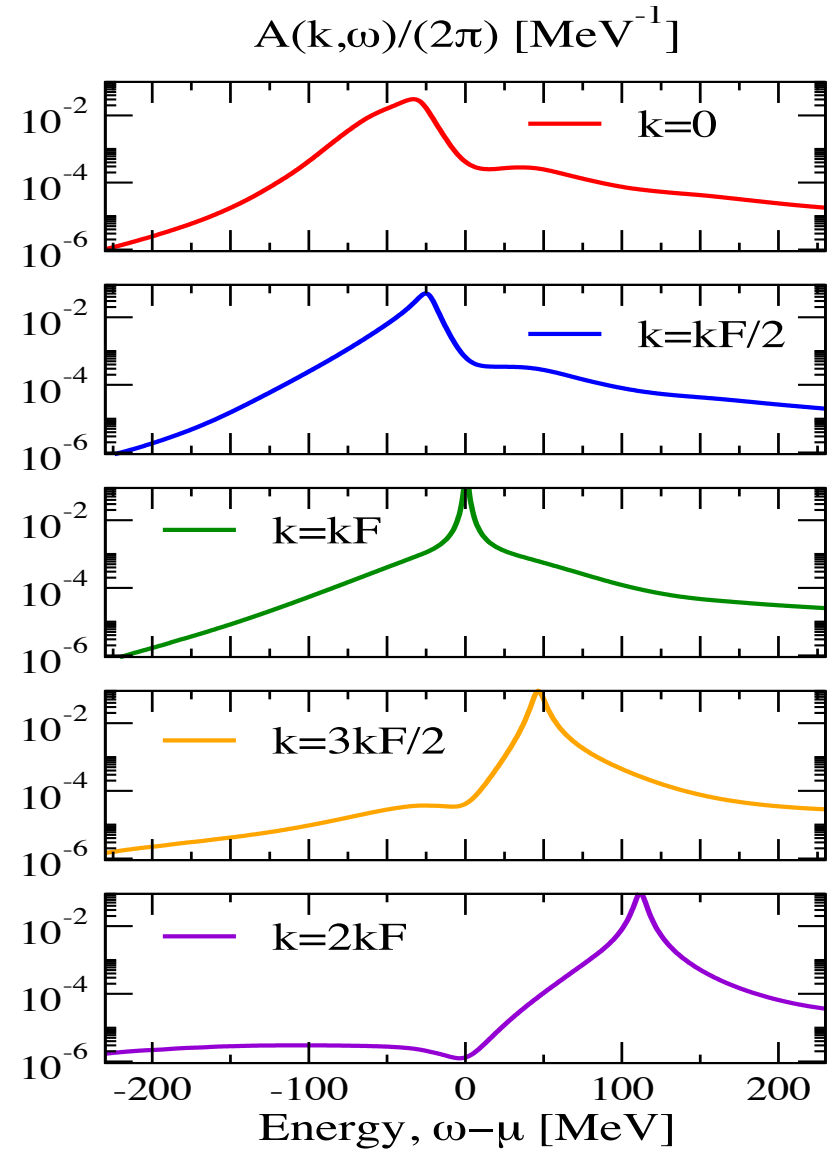
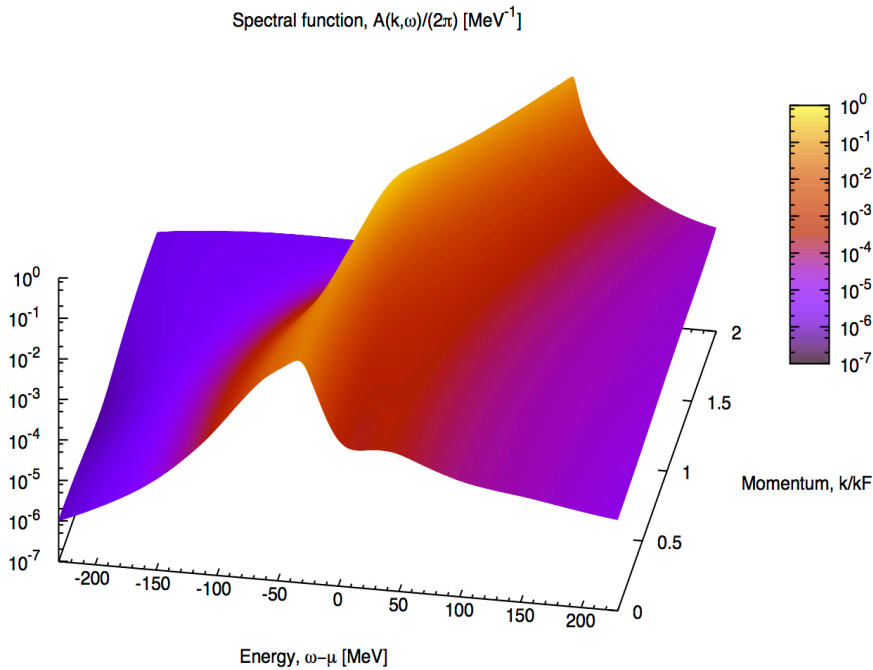
	$^{16}\text{O}$	$^{40}\text{Ca}$
BHF (Inoue)	2.35 fm	2.78 fm
"BHF"	2.33 fm	2.78 fm
ADC(3)	2.60 fm	2.97 fm
$r_{\text{charge}}$ (expt.)	2.73 fm	3.48 fm

→ Radii discrepancy worsens with increasing  $A$

# SCGF in infinite SNM @ $m_\pi=469\text{MeV}$

Single particle spectral distribution behaves as usual.

BHF results and binding remain confirmed in SCGF calculations.



Results by A. Carbone, priv. comm.

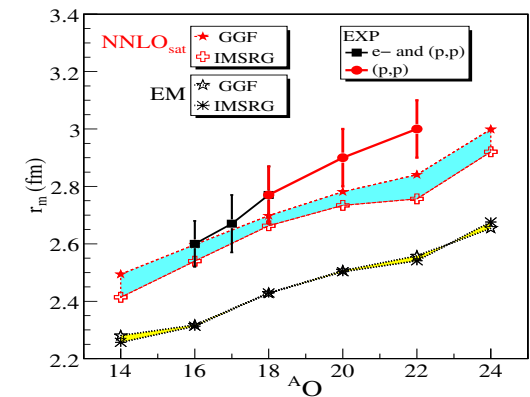
# Summary

## Mid-masses and chiral interactions:

- Leading order 3NF are crucial to predict many important features that are observed experimentally (drip lines, saturation, orbit evolution, etc...)
- Experimental binding is predicted accurately up to the lower *sd* shell ( $A \approx 30$ ) but deteriorates for medium mass isotopes (Ca and above) with roughly 1 MeV/A over binding.
- New fits of chiral interaction are promising for low-energy observables

## HALQCD Nuclear forces:

- Strong short range behavior calls for new ideas in *ab-initio* many-body methods. Diagram resummation through *G*-matrix is starting point (to be extended)
- At  $m_\pi = 469$  MeV, closed shell  $4\text{He}$ ,  $16\text{O}$  and  $40\text{Ca}$  are bound. But oxygen is unstable toward  $4\text{-}\alpha$  break up, calcium stays bound. Underestimation of radii increases with  $A$  do to large saturation density (as for  $\text{EM}(500) + \text{NLO}3\text{NF}$ ).



Thank you for your attention!!!

# Collaborators



**A. Cipollone, C. McIlroy**  
**A. Rios, A. Idini, F. Raimondi**



**A. Polls**



**V. Somà, T. Duguet**



**W.H. Dickhoff,**  
**S. Waldecker**

energie atomique • energies alternatives



**A. Carbone**



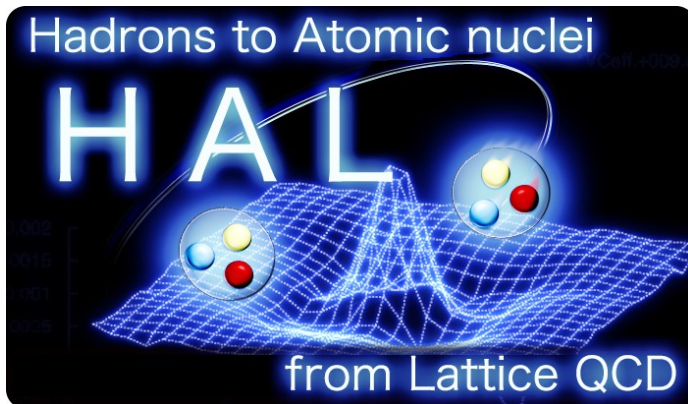
**D. Van Neck,**



**P. Navratil**



**M. Hjorth-Jensen**



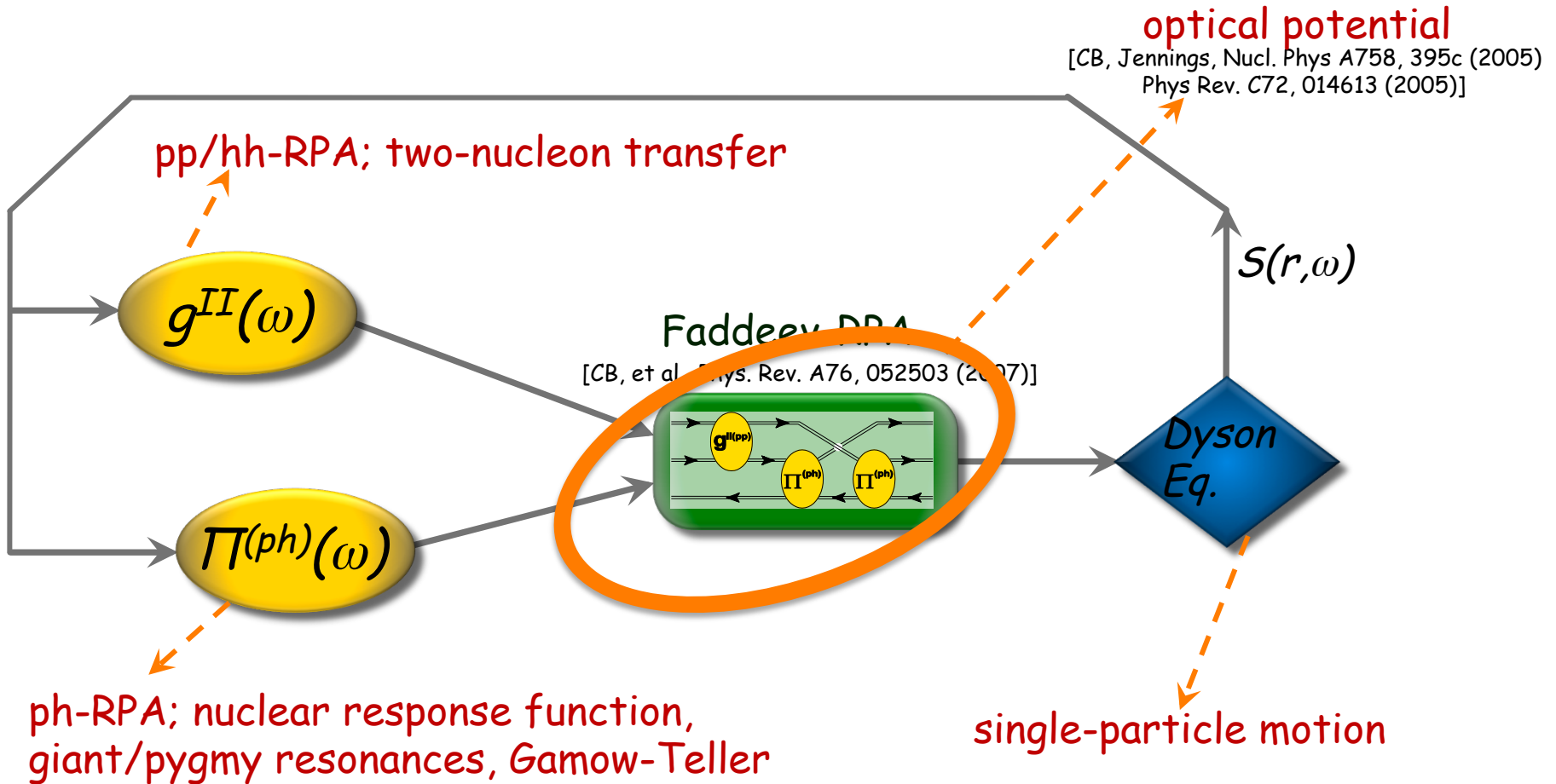
S. Aoki,  
**T. Doi, T. Hatsuda, Y. Ikeda,**  
**T. Inoue,**  
N. Ishii, K. Murano,  
**H. Nemura, K. Sasaki**  
F. Etminan  
T. Miyamoto,  
T. Iritani  
S. Gongyo

YITP Kyoto Univ.  
RIKEN Nishina  
Nihon Univ.  
RCNP Osaka Univ  
Univ. Tsukuba  
Univ. Birjand  
Univ. Tsukuba  
Stony Brook Univ.  
YITP Kyoto Univ.

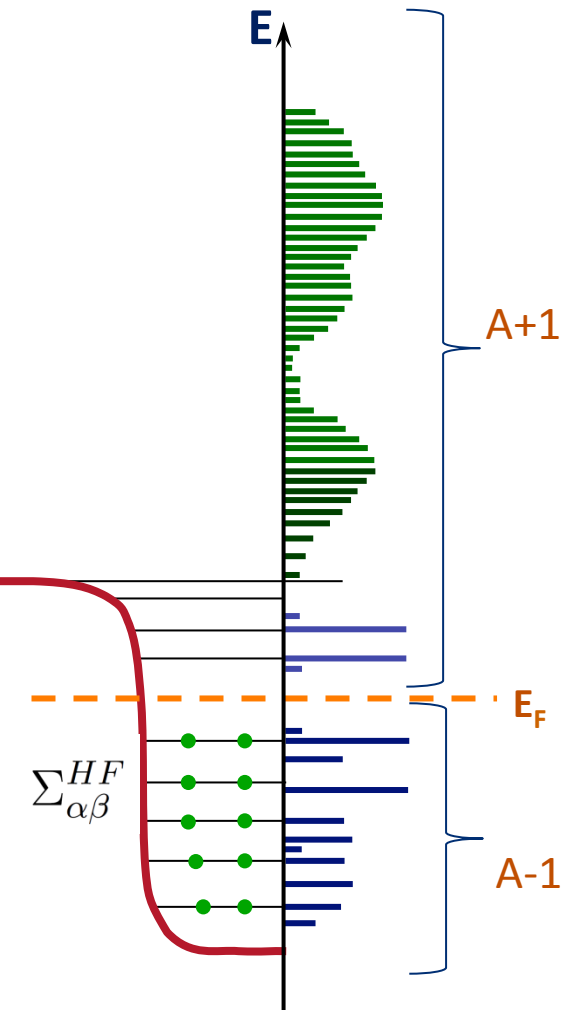


# Optical Potentials Based on the Nuclear Self-energy

# Self-Consistent Green's Function Approach



# Nucleon elastic scattering



The irreducible self-energy is a nucleon-nucleus optical potential [see e.g. Mahaux and Sartor, Adv. Nucl. Phys. 20, (1991)]

$$\Sigma^*(\mathbf{r}, \mathbf{r}'; \varepsilon) = \Sigma_{\alpha\beta}^{HF} - \frac{1}{\pi} \int_{\varepsilon_T^>}^{\infty} dE' \frac{\text{Im} \Sigma^*(\mathbf{r}, \mathbf{r}'; E')}{\varepsilon - E' + i\eta} + \frac{1}{\pi} \int_{-\infty}^{\varepsilon_T^<} dE' \frac{\text{Im} \Sigma^*(\mathbf{r}, \mathbf{r}'; E')}{\varepsilon - E' - i\eta}$$

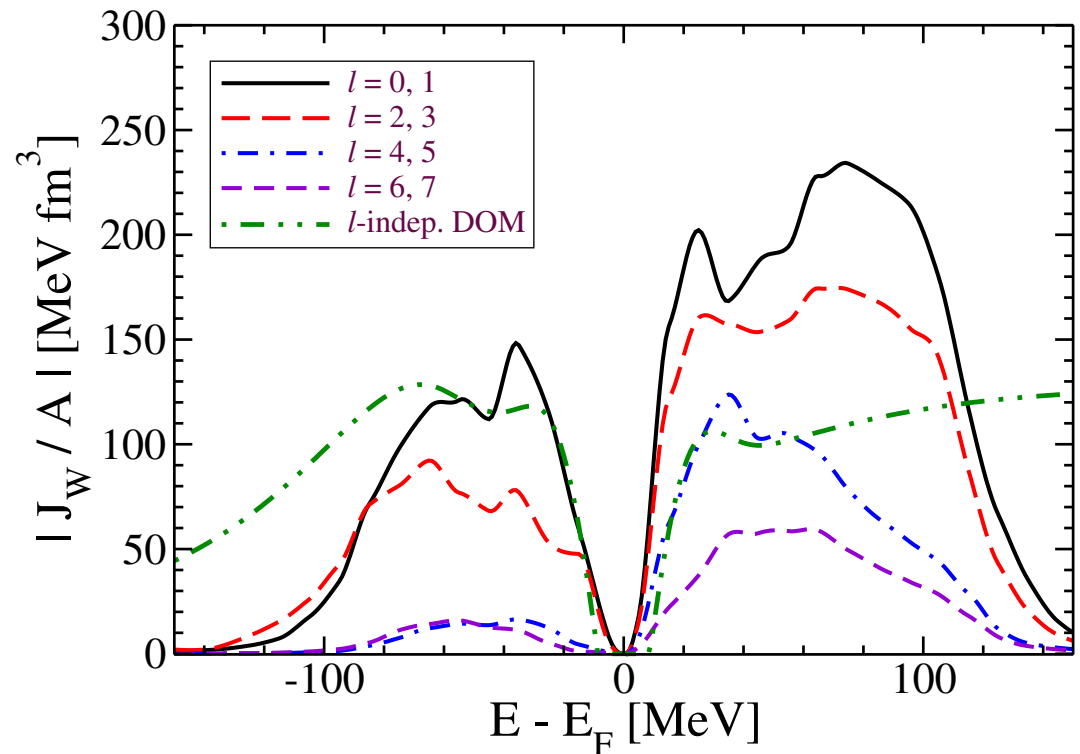
mean-field

resonances  
beyond mean-field

→ This provides *consistent* overlaps and scattering wave functions

# Convergence of Ab-Initio Calculated Optical Potentials

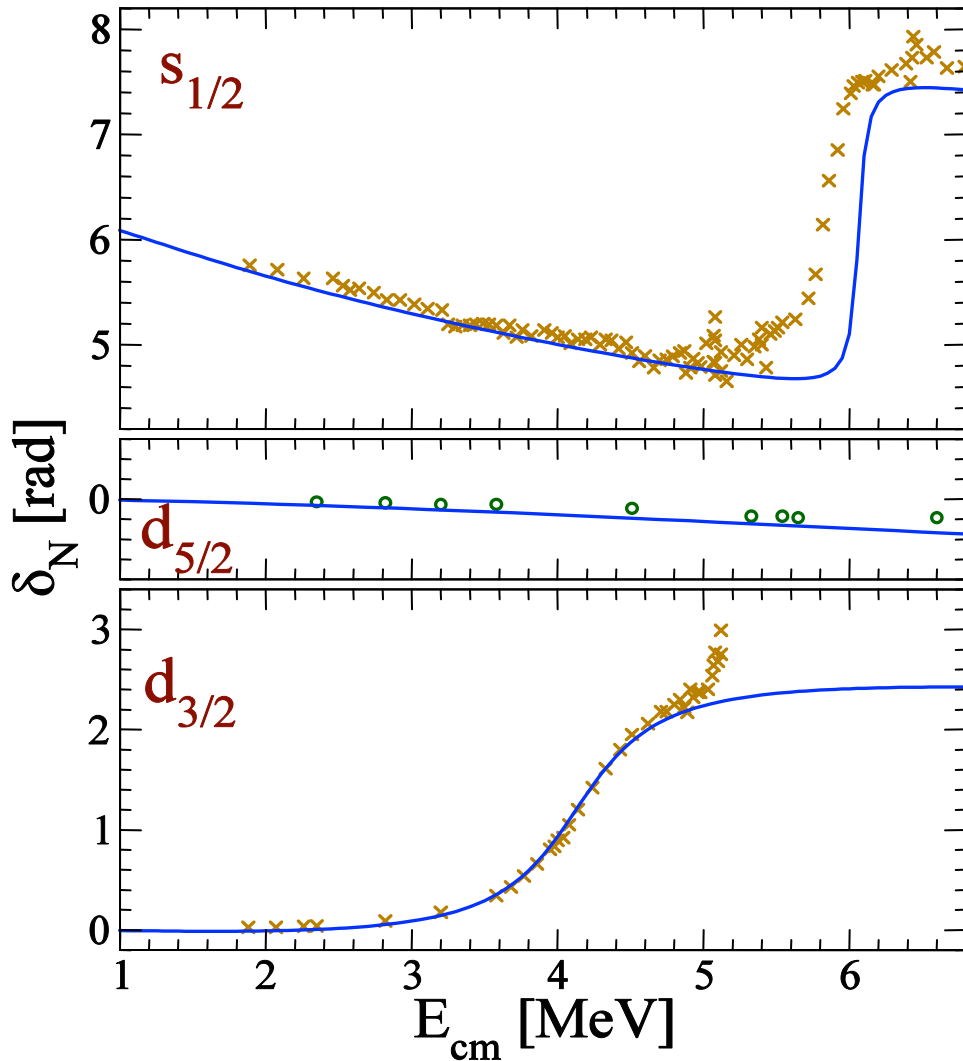
- $J_w$ : integral over the imaginary optical potential (overall absorption)
- angular momentum dependence (non locality) not negligible!  
→ in particular below  $E_F$



S. Waldecker, CB, W.Dickhoff – Phys. Rev. C84, 034616 (2011)

# $p\text{-}^{16}\text{O}$ phase shifts - positive parity waves

[C.B., B.Jennings,  
Phys. Rev. C72, 014613 (2005)]



• AV18 interaction

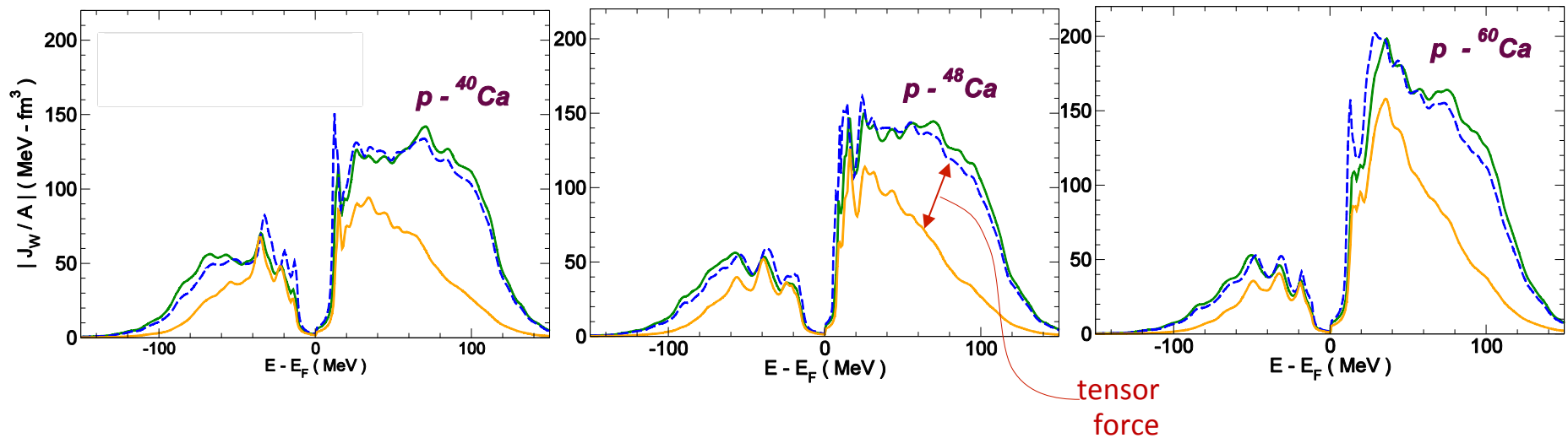
• The phase shifts are in agreement with the experiment!

• BUT does not reproduce phase shifts and bound state energies at the same time  
→ need for improved H / 3NF

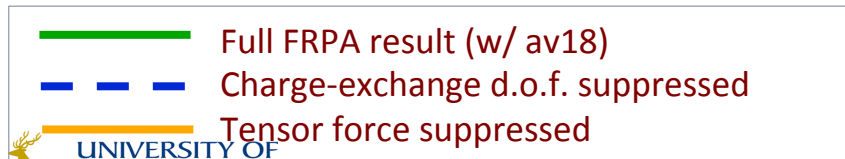
• Non-MF resonances "OK"

# Microscopic Optical Potential from FRPA

- absorption away from  $E_F$  is enhanced by the tensor force
- little effects from charge exchange (e.g.  $p\text{-}^{48}\text{Ca} \leftrightarrow n\text{-}^{48}\text{Sc}$ )



$J_W$ : integral over the imaginary opt. pot (overall absorption)



S. Waldecker, CB, W. Dickhoff – Phys. Rev. C84, 034616 (2011)

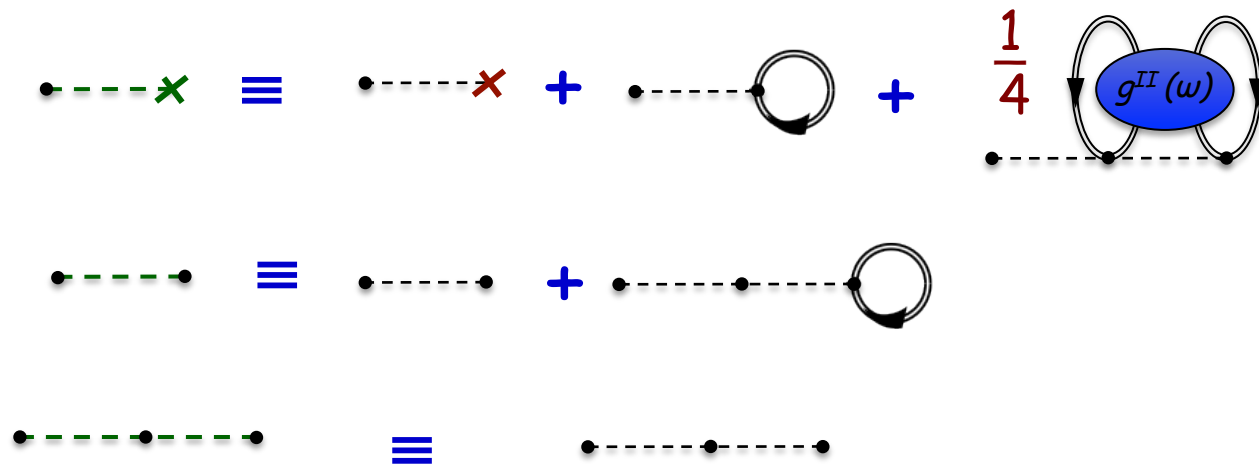
# Adding 3-nucleon forces

# Inclusion of NNN forces

A. Carbone, CB, et al., Phys. Rev. C88, 054326 (2013)

\* NNN forces can enter diagrams in three different ways:

→ Define new 1- and 2-body interactions and use only interaction-irreducible diagrams



- Contractions are with fully correlated density matrices (BEYOND a normal ordering...)



# Inclusion of NNN forces

A. Carbone, CB, et al., Phys. Rev. C88, 054326 (2013)

- Second order PT  
diagrams with 3BFs:

effectively:

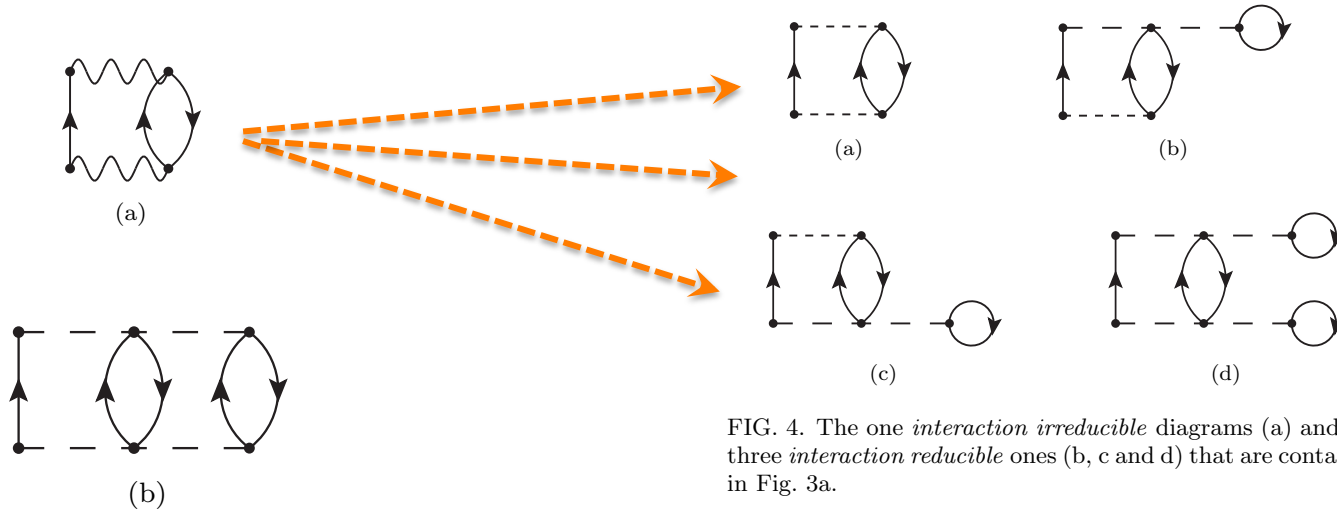
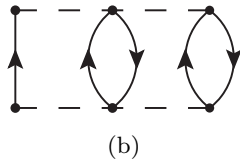
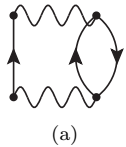


FIG. 4. The one *interaction irreducible* diagrams (a) and the three *interaction reducible* ones (b, c and d) that are contained in Fig. 3a.

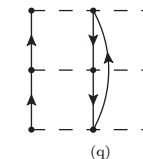
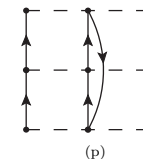
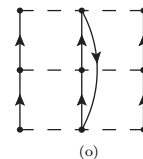
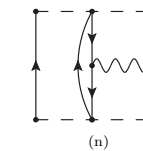
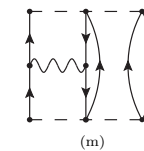
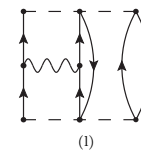
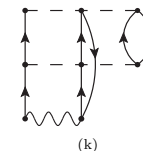
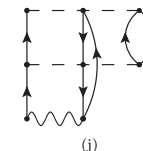
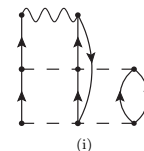
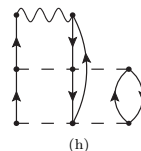
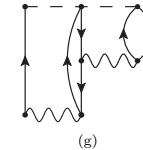
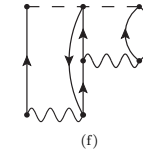
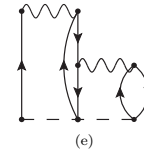
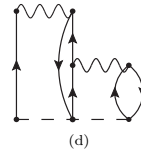
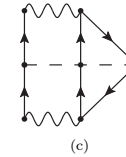
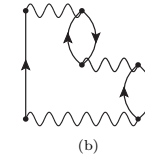
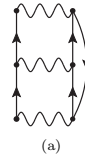
# Inclusion of NNN forces

A. Carbone, CB, et al., Phys. Rev. C88, 054326 (2013)

- Second order PT diagrams with 3BFs:



- Third order PT diagrams with 3BFs:



→ Use if effective interactions

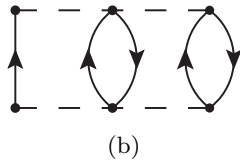
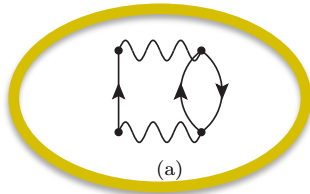
→ Need to correct the Koltun sum rule (for energy)

FIG. 5. 1PI, skeleton and interaction irreducible self-energy diagrams appearing at  $3^{\text{rd}}$ -order in perturbative expansion (7), making use of the effective hamiltonian of Eq. (9).

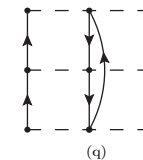
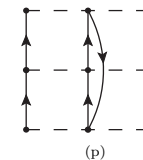
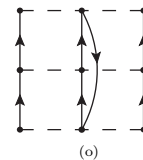
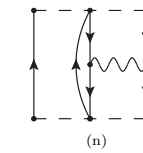
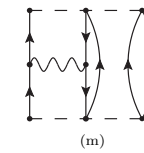
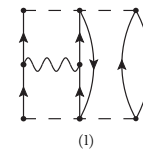
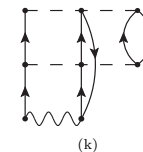
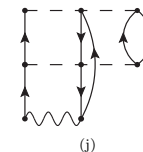
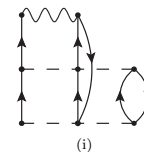
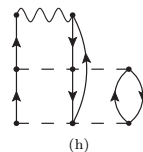
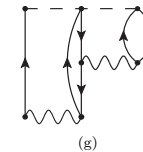
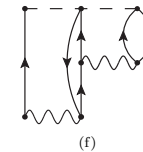
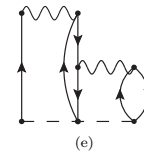
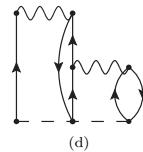
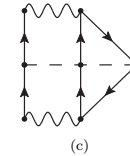
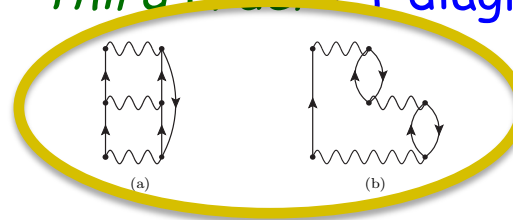
# Inclusion of NNN forces

A. Carbone, CB, et al., Phys. Rev. C88, 054326 (2013)

- Second order PT diagrams with 3BFs:



- Third order PT diagrams with 3BFs:



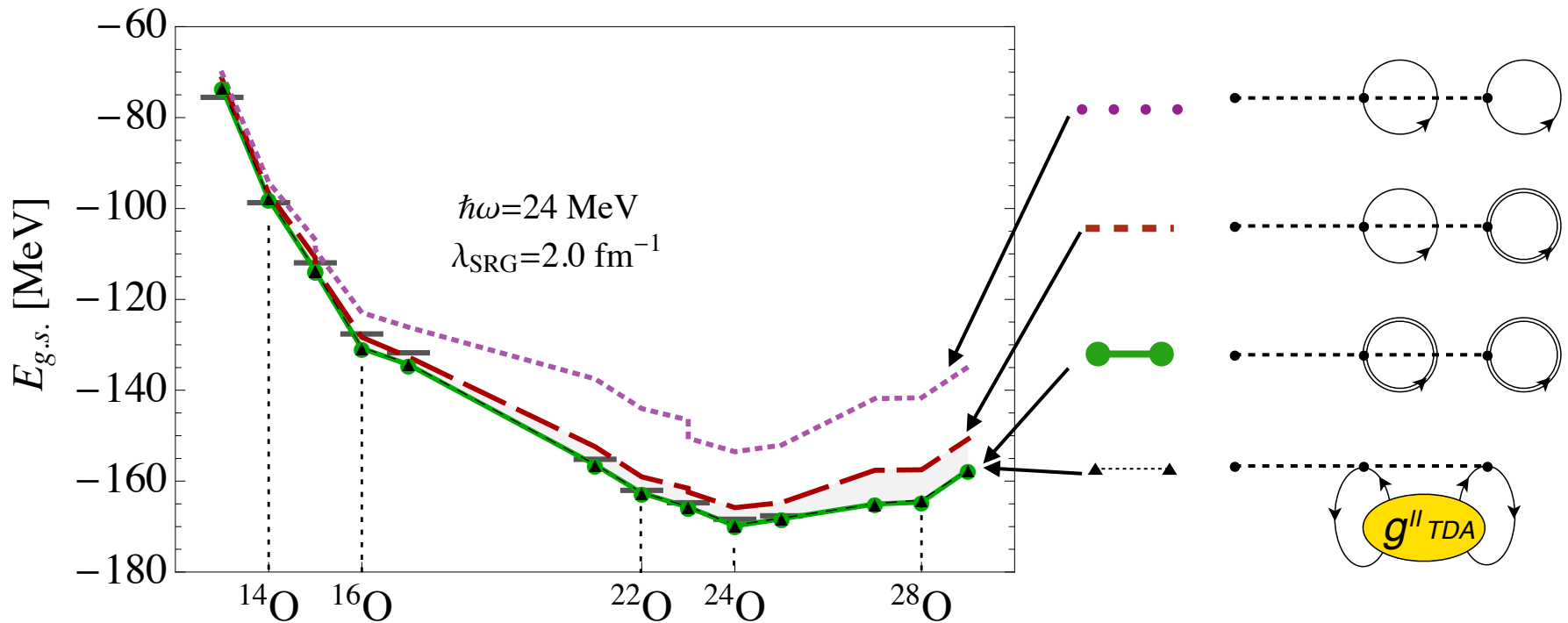
→ Use if effective interactions

→ Need to correct the Koltun sum rule (for energy)

FIG. 5. 1PI, skeleton and interaction irreducible self-energy diagrams appearing at  $3^{\text{rd}}$ -order in perturbative expansion (7), making use of the effective hamiltonian of Eq. (9).

# 3N forces in FRPA/FTDA formalism

→ Ladder contributions to static self-energy are negligible (in oxygen)



# 3N forces in FRPA/FTDA formalism

→ Ladder contributions to static self-energy are negligible (in oxygen)

